Quantifying the distributions and ecosystem services of oyster reefs within Virginia's coastal bays

Sara Hogan

Charlottesville, Virginia

B.S. Environmental Sciences, University of Notre Dame, 2016

A Dissertation presented to the Graduate Faculty of the University of Virginia in Candidacy for the Degree of Doctor of Philosophy

Department of Environmental Sciences

University of Virgnia

August 2021

Committee Members:
Matthew A. Reidenbach (Advisor)
Patricia L. Wiberg
John H. Porter
Jonathan L. Goodall
Max Castorani

TABLE OF CONTENTS

ABSTRACT

Within Virginia's coastal bays, the eastern oyster, *Crassostrea virginica*, is a native and primarily intertidal species. Although historically abundant, oyster populations sharply declined beginning in the mid-19th century from overharvesting and were further reduced in the 20th century with added pressures from disease and potentially poor water quality. Restoration efforts have enabled oysters to increase population size, although they still comprise only a few percent of what once existed. While restoring population size is the primary goal of most restoration initiatives, more recently efforts have aimed to enhance the health of the broader coastal bay system through ecosystem services attributed to oysters. These services include coastal protection by buffering wave energy, increasing habitat for flora and fauna, and altering sediment composition.

As restoration efforts continue within Virginia's bays, the focus of this research is to provide new methods for monitoring and quantifying where oyster populations exist and the ecosystem services they provide in order to guide successful restoration efforts. This research was composed of four distinct research projects. First, I utilized remotely-sensed airborne light detecting and ranging (LiDAR) data to develop a methodology to identify and map intertidal oyster reefs within the Virginia Coast Reserve (VCR). From this dataset of oyster locations, combined with the physical characteristics of elevation, wave fetch, and water residence time, I developed a physical habitat suitability model to determine suitable and unsuitable locations for oyster growth. Second, I used the LiDAR dataset to derive a method using slope statistics to locate marsh edges and quantify marsh edge morphology. This method was used to determine if oyster reef-adjacent edges experience protection from edge erosion by examining differences in morphology and retreat in reef-lined and control marsh edges. Third, utilizing a specific

restoration site constructed in 2017 composed of constructed reefs varying in elevation and width, I quantified which designs best enhance oyster populations and coastal protection. At this site I also determined differences in infauna communities and sediment composition before and after restoration across a 4-year time-period. Fourth, with an understanding of the effects that oyster reefs can have on intertidal communities, I used the mapped oyster reef dataset combined with field sampling to analyze if distance to oysters influences infauna and sediment distributions.

The results of these four studies are evidence that remotely-sensed airborne LiDAR data can be used in intertidal environments to monitor changes in oyster distributions. Data from mapped oyster patches indicate that oysters exist in a narrow band of elevation (-0.81 to -0.18 m NAVD88, the North American Vertical Datum of 1988) and approximately 12 % of the VCR bay and intertidal region is suitable for oyster habitat in terms of elevation, water residence time, and fetch. The results also advocate that LiDAR data can be a useful tool to remotely locate and quantify marsh edge morphology. Marsh edges adjacent to reefs were found to be more gently sloping, and this measurable difference in morphology is likely a precursor to changes in retreat. Measurements were analyzed from the top of marsh platforms and indicate no difference in retreat thus far, while it is likely that the lower toe edge, protected by the reef, is eroding more slowly. The long-term monitoring of constructed reefs provided evidence that reef elevation was important to design and reefs higher in elevation, relative to the neighboring marsh edge, better foster oyster growth and wave attenuation. Trends in increased infauna diversity and sediment organic matter were also observed after restoration. Additionally, data found that distance to oyster reefs is affects distributions of infauna taxa with large differences in presence apparent at approximately 40 m from reefs. Meanwhile local flow velocity is likely the primary driver of sediment distributions on intertidal mudflats.

Overall, these findings add to understanding of oysters as an important engineering estuarine species and contributes innovative methods to guide the success of continued monitoring and restoration efforts in Virginia’s coastal bays to support oyster populations, enhance community composition, and protect shorelines.

ACKNOWLEDGEMENTS

Thank you to the University of Virgnia, especially the Department of Environmental Sciences, for providing me an extraordinary educational experience. I would also like to thank the ABCRC coastal lab the VCR LTER for gifting me an amazing location to conduct research and becoming home for much of my summers over the past five years. My success is largely due to the supportive, collaborative environment provided by the professors, staff, and students I have been fortunate to work with during my time at UVA.

Specifically, I would like to thank my advisor, Professor Matthew Reidenbach, whose supportive mentorship fostered my growth as a scientist more than I thought possible. I would also like to extend thanks to my dissertation committee members including Professors Patricia Wiberg, John Porter, Jon Goodall, and Max Castorani. Each of you has helped me become a more well-rounded scientist and changed my ways of thinking- from GIS to ggplot to geomorphology.

I would like to thank the ABCRC staff, especially Cora Johnson, Donna Fauber, David Lee, and Buck Doughty, for helping coordinate my field experiences and making living and working on the Shore such a pleasant experience. I would also like to thank the Nature Conservancy for their collaboration, and particularly Bo Lusk for field expertise and guidance. Thank you to my Reidenbach and VCR lab mates for help with field and lab work, data analysis, and listening to my ramblings about oysters and LiDAR. Also, many thanks to all the REUs and volunteers that have helped me in my, sometimes less than pleasant, mudflat endeavors over the years. I would also like to acknowledge the other members of my cohort and Environmental

Sciences graduate students for friendship and bonding through the unique experience of graduate school.

And to those who may not understand my science but support me without hesitation regardless. Thank you to my parents who have always supported me in pursing my passions no matter the path. I am perpetually grateful for my mom, who continuously exemplifies how to be strong, loving, and full of life, and my dad, for being my adventure partner, who taught me how to listen, and shared his unfathomable breadth of knowledge from sports to literature. I am so lucky. And to my older sister, Catherine, my counterpart and contrast, who has always pushed me to best my best and is a reminder to be true to yourself, thank you.

The past five years have taught me to believe you never know what the day will hold, the people that will change your life, where you will go next, and what you are capable of.

Thank you.

CHAPTER 1: Introduction

The Eastern Oyster, *Crassostrea virginica*

Within the coastal bays of Virginia, the eastern oyster, *Crassostrea virginica*, is a native species found fringing marsh edges and in patch formations on mudflats. Oyster reefs accrete vertically from surrounding sediment, often acting as the necessary hard substrate for further oyster larvae to land in otherwise soft-sediment estuaries (Figure 1.1). In Virginia's coastal bays, they exist largely in the intertidal zone. There are trade-offs in being intertidal organisms, however. Oysters must balance submergence time necessary to feed while considering the risks of sedimentation and predation underwater and desiccation when emerged (Fodrie et al. 2014, Johnson & Smee 2014, Byers et al. 2015). Though historically abundant within the Virginia coastal region, which includes both the coastal bays and Chesapeake Bay, oyster populations experienced sharp declines from overharvesting in the mid-19th century and were further devastated in the 20th century from poor water quality and disease (Rothschild et al. 1994, Kemp et al. 2005). Therefore, over the past few decades management within this coastal system has placed a large focus on oyster restoration. Restoration goals initially concentrated on increasing oyster stock, however, more recently projects are taking a broader ecosystem-based approach with increased interest in the varied ecosystem services oysters can provide to estuarine communities (Coen & Luckenbach 2000, Ehrenfeld 2000, Grabowski et al. 2012).

Figure 1.1 Photos captured within the Virginia Coast Reserve (VCR) showing an (A) intertidal patch oyster reef in a soft-sediment mudflat and (B) the vertical elevation and accreting nature of oysters as they mature.

Through their structure and biophysical characteristics oyster reefs have been shown to provide beneficial ecosystem services to intertidal communities (Coen et al. 2007, Grabowski & Peterson 2007). The complex elevated structures provided by reefs alter hydrodynamic flows by increasing turbulence and drag (Whitman & Reidenbach 2012), and in turn attenuate waves as they pass over reefs (Wiberg et al. 2019) and promote sedimentation (Reidenbach et al. 2013). Since the main driver behind shoreline erosion can be attributed to incessant wave action and consequent shear stresses (Fagherazzi & Wiberg 2009), reefs have been found to decrease shoreline erosion and stabilize sediment (Meyer et al. 1997, Piazza et al. 2005, Scyphers et al. 2011). Combined with increased drag and physical trapping, filter feeding oysters remove suspended particles from the water column leading to deposition of fine particles (Reidenbach et al. 2013, Colden et al. 2016). Additionally, direct inputs from excrements deposited from filter feeding and the indirect facilitation of microphytobenthic species growth both work to increase sediment organic matter (Newell et al. 2002, Kellogg et al. 2013, Southwell et al. 2017). Furthermore, oyster reefs can enhance the biodiversity of species living in and around oysters, promoting biodiversity of fish, crab, and other infauna species seeking shelter and feeding grounds (Castel et al. 1989, Langlois et al 2006, Gregalis et al. 2009, Van der zee et al. 2015). Thereby restoring oyster reefs, not only are oyster populations enhanced, but the broader intertidal and coastal community can potentially benefit as well.

Restoration and Nature-Based Solutions

Increasing attention to ecosystem services has led coastal managers to revise their approaches to managing and restoring vulnerable coastal shorelines directly impacted by climate change and other anthropogenic causes. To protect coastal communities and eroding shorelines, coastal managers historically have largely relied on ‘grey’ infrastructure, primarily composed of concrete constructions such as sea walls and jetties, to lessen the impacts of wave action and coastal erosion (Duhring et al. 2006, Currin et al. 2010). However, these techniques are disadvantageous when considering needed maintenance and ecological drawbacks including the loss of biodiversity and alterations to sediment transport (Lee et al. 1999, Bozek & Burdick 2005, Bulleri & Chapman 2010, Sobocinski et al. 2010). To mitigate the negative impacts of 'grey' infrastructure, more recently a shift towards incorporating nature-based solutions, also known as 'green' infrastructure or 'living shorelines', has taken place. These management techniques use the natural ability of coastal organisms to buffer wave energy from reaching shorelines. These techniques may include the use of marsh plants, sea grasses, and oyster reefs. Living shorelines have proven to be comparatively effective in mitigating coastal erosion while also respecting local ecology (Davis et al. 2006, Swann 2008, Currin et al. 2010). It is known that oyster reefs have the potential to dissipate wave energy, however, research is still needed to understand how well oysters act as a nature-based solution to shoreline erosion and how managers can best implement them in restoration strategies. A portion of this dissertation will investigate if the hydrodynamic alterations caused by oyster reefs affect shorelines and how to design constructed reefs to foster ecosystem services including coastal protection.

Methods for Monitoring

With continuing restoration efforts, innovative techniques to monitor where oyster populations exist and what effects they have on their environments are crucial to guide successful management practices. Increasingly incorporated into research are remotely-sensed products that offer the benefits of broad scale, high resolution datasets with minimal to no need for in-situ sampling (Schenk & Csatho 2002, Morgan et al. 2010). Light detecting and ranging (LiDAR) data is one example of remotely-sensed data that can potentially benefit researchers to coastal systems. Airborne LiDAR elevation data are acquired by having an aircraft flown over a landscape and elevation is estimated at a location based on the return time of laser pulses sent towards the ground and the speed of light (Baltsavias 1999). Within coastal ecosystems, LiDAR has been used largely to map intertidal habitats (Garono et al. 2004, Morris et al. 2005, Marion et al. 2009, Halls & Costin 2016), however, less research exists on using LiDAR to quantify intertidal features such as marsh edges (Goodwin & Mudd 2020) and oyster reefs (Schill et al. 2006). This is due to airborne LiDAR's inability to penetrate water, and therefore depending on tidal ranges and time of data acquisition, LiDAR products can inadequately capture intertidal features. However, if a data set is collected at low tide, there is potential for LiDAR data products to be used in quantifying characteristics of vertically accreting oyster reefs and exposed marsh edges, data which can be beneficial to intertidal restoration initiatives.

Dissertation Objectives

The goals of this dissertation are guided by the need to understand oyster distributions in Virginia's coastal bays to promote successful restoration and determine oysters' efficacy as a nature-based solution to bolster populations while also enhancing the greater community. Specific objectives include developing new methods to quantify both oyster distributions to determine where they exist in the physical environment and the ecosystem services provided by natural and restored reefs. These objectives were achieved through four studies. The first study determines a methodology to map intertidal oyster reefs using LiDAR elevation data and use the resulting map of oyster distributions to create a habitat suitability map. The second study builds on the utility of LiDAR elevation to quantify marsh edge morphology and determine the role of oyster reefs in affecting marsh morphology and retreat to quantify oysters' role in coastal protection. In the third study, to determine best practices for designing restored reefs, ecosystem services are quantified over various constructed reefs with designs varying in elevation and width. Last, with an understanding of the services that oysters provide, in the fourth study I examine if the engineering effects of oysters influence infauna and sediment distributions within intertidal mudflats.

Literature Cited

Baltsavias EP (1999) Airborne laser scanning: basic relations and formulas. ISPRS J Photogramm Remote Sens 54:199-214

Bozek CM, Burdick DM (2005) Impacts of seawall on saltmarsh plant communities in the Great Bay Estuary, New Hampshire USA. Wetl Ecol Manag13:553-568

Bulleri F, Chapman MG (2009) The introduction of coastal infrastructure as a driver of change in marine environments. J Appl Ecol 47: 26-35

Byers, JE, Grabowski JH, Piehler MF, Hughes AR, Weiskel HW, Malek JC, and Kimbro DL (2015) Geographic variation in intertidal oyster reef properties and the influence of tidal prism. Limón Oceanogr 60:1051-1063

Castel J, Labourg PJ, Escaravage V, Auby I, Garcia ME (1989) Influence of seagrass beds and oyster parks on the abundance and biomass patterns of meio- and macrobenthos in tidal flats. Estuar Coast Shelf Sci 28: 71-85

Coen LD, Luckenbach MW (2000) Developing success criteria and goals for evaluating oyster reef restoration: ecological function or resource exploitation? Ecol Eng 15:323-343

Coen LD, Brumbaugh RD, Bushek D, Grizzle R, Luckenbach MW, Posey MH, Powers SP, and Tolley G (2007) Ecosystem services related to oyster restoration. Mar Ecol Prog Ser 341: 303-307

Colden A, Fall KA, Massey GM, Friedrichs C (2016) Sediment suspension and deposition across restored oyster reefs of varying orientation to flow: implications for restoration. Estuar Coast 39:1435-1448

Currin CA, Chappel WS, Deaton A (2010) Developing alternative shoreline armoring strategies: The living shoreline approach in North Carolina, in Shipman, H, MN Gelfenbaum, KL Fresh, and RS Dinicola, eds., Puget Sound Shorelines and the Impacts of Armoring-Proceedings of a State of the Science Workshop, May 2009: *U.S*. Geologic Survey Scientific Investigations Report 2010, 5254: 91-102

Davis JLD, Takacs RL, Schnabel R (2006) Evaluating ecological impacts of living shorelines and shoreline habitat elements: an example from the upper western Chesapeake Bay. Management, policy, science, and engineering of nonstructural control in the Chesapeake Bay, 55

Duhring, KA, TA Barnard Jr, S Hardaway Jr (2006) A survey of the effectiveness of existing marsh toe protection structures in Virginia. A final report to the Keith Campbell Foundation for the Environment, Inc. 25 p

Ehrenfeld JG (2000) Defining the limits of restoration: the need for realistic goals. Restor Ecol 8: 2-9

Fagherazzi S, Wiberg PL (2009) Importance of wind conditions, fetch, and water levels on wave-generated shear stresses in shallow intertidal basins. J Geophys Res 114 F03022, doi:10.1029/2008JF001139

Fodrie FJ, AB Rodriguez, CJ Baillie, MC Brodeur, SE Coleman, RK Gittman, DA Keller, MD Kenworthy, AK Poray, JT Ridge, EJ Theuerkauf, Lindquist NL (2014) Classic paradigms in a novel environment: inserting food web and productivity lessons from rocky shores and saltmarshes into biogenic reef restoration. J Appl Ecol 51:1314-1325

Garono RJ, Simenstad CA, Robinson R, Ripley H (2004) Using high spatial resolution hyperspectral imagery to map intertidal habitat structure in Hood Canal, Washington, USA. Can J Rem Sens 30:54-63

Goodwin CH, Mudd SM (2020) Detecting the morphology of prograding and retreating marsh margins- example of a mega-tidal bay. Remote Sens 12:13-39

Grabowski JH, Peterson CH (2007) Restoring oyster reefs to recover ecosystem services. In *Ecosystem engineers: concepts, theory and applications,* eds. K. Cuddington, J.E. Byers JE, W.G. Wilson, and A. Hastings, 281 – 298. Amsterdam: Elsevier-Academics Press

Grabowski JH, Brumbaugh RD, Conrad RF, Keeler, Opaluch JJ, Peterson CH, Piehler MF, Powers SP, Smyth AR (2012) Economic valuation of ecosystem services provided by oyster reefs. *BioScience* 621:900-909

Gregalis KC, Johnson MW, Powers SP (2009) Restored oyster reef location and design affect responses of resident and transient fish, crab, and shellfish species in Mobile Bay, Alabama. Trans Am Fish Soc 138: 314-327

Halls J, Costin K (2016) Submerged and emergent land cover and bathymetric mapping of estuarine habitats using WorldView-2 and LiDAR imagery. Remote Sens 8:718

Johnson KD, Smee D (2014) Predators influence the tidal distribution of oyster (Crassostrea virginica). Mar Biol 161: 557-1564

Kellogg ML, Cornwell JC, Owens MS, Kennedy PT (2013) Denitrification and nutrient assimilation on a restored oyster reef. Mar Eco Prog Ser 480: 1-19

Kemp WM, Boynton WR, Adolf JE, Boesch DF, Boicourt WC, Brush G, Cornwell JC, Fisher TR, Glibert PM, Hagy JD, Harding LD, Houde ED, Kimmel DG, Miller WD, Newell RIE, Roman MR, Smith EM, Stevenson JC (2005) Eutrophication of Chesapeake Bay: historical trends and ecological interactions. Mar Ecol Prog Ser 303:1-29

Langlois TJ, Anderson MJ, Babcock RC (2006) Inconsistent effects of reefs on different size classes of macrofauna in adjacent sand habitats. J Exp Mar Biol Ecol 334: 269-282

Lee, HJ, Chu YS, Park YA (1999) Sedimentary processes of fine-grained material and the effect of seawall construction in the Daeho macrotidal flat—nearshore area, northern west coast of Korea. Mar Geol 157:171-184

Marion C, Anthony EJ, Trentesaux A (2009) Short-term (<2yrs) estuarine mudflat and saltmarsh sedimentation: high-resolution data from ultrasonic altimetery, rod surface-elevation table, and filter traps. Estuar Coast Shelf Sci 83:475-484

Meyer DL, Townsend EC, Thayer GW (1997) Stabilization and erosion control value of oyster cultch for intertidal marsh. Restor Ecol 5:93-99

Morgan JL, Gergel SE, Coops NC (2010) Aerial Photography: a rapidly evolving tool for ecological management. BioScience 60:47-59

Morris JT, Porter D, Neet M, Nobel PA, Schmidt L (2005) Integrating LIDAR elevation data, multi-spectral imagery and neural network modelling for marsh characterization. Int J Remote Sens 26:5221-5234

Newell RIE, Cornwell JC, Owens MS (2002) Influence of simulated bivalve biodeposition and microphytobenthos on sediment nitrogen dynamics: A laboratory study. Limnol Oceanogr 47: https://doi.org/10.4319/lo.2002.47.5.1367

Piazza EP, Banks PD, La Peyre MK (2005) The potential for created oyster shell reefs as a sustainable shoreline protection strategy in Louisiana. Restor Ecol 13:499-506

Reidenbach MA, Berg P, Hume A, Hansen JCR, Whitman ER (2013) Hydrodynamics of intertidal oyster reefs: The influence of boundary layer flow processes on sediment and oxygen exchange. Limnol Oceanogr Fluids Environ 3: 225 -239

Rothschild BJ, Ault JS, Goulletquer P, Jensen WP, Heral M (1994) Decline of the Chesapeake Bay oyster population: a century of habitat destruction and overfishing. Mar Ecol Prog Ser 111:29-39

Schenk T, Csatho B (2002) Fusion of LiDAR data and aerial imagery for a more complete surface description. Int Arch Photogramm Remote Sense 34:310-317

Schill SR, Porter DE, Coen LD, Bushek D, Vincent J (2006) Development of an automated mapping Technique for monitoring and managing shellfish distributions. NOAA/UNH Cooperative Institute for Coastal and Estuarine Environmental Technology (CICEET)

Scyphers SB, Powers SP, Heck KL, Byron D (2011) Oyster reefs as natural breakwaters mitigate shoreline loss and facilitate fisheries. PLOS ONE 6(8): e22396

Sobocinski KL, Cordell JR, Simenstad CA (2010) Effects of shoreline modifications on supratidal macroinvertebrate fauna on Puget Sound, Washington beaches. Estuar Coast 33:699-711

Southwell MW, Veenstra JJ, Adams CD, Scarlett EV, Payne KB (2017) Changes in sediment characteristics upon oyster reef restoration, NE Florida, USA. J Coast Zone Manag 20 DOI: 10.4172/2473-3350.1000442

Swann L (2008) The use of living shorelines to mitigate the effects of storm events on Dauphin Island, Alabama USA. American Fisheries Society Symposium

Van der Zee EM, Tielens E, Holthuijsen S, Donadi S, Eriksson BK, Van der Veer HW, Piersma T, Olff H, Van der Heide T (2015) Habitat modification drives benthic trophic diversity in an intertidal soft-bottom ecosystem. J Exp Mar Biol Ecol 465:41-48

Whitman ER, Reidenbach MA (2012) Benthic flow environments affect recruitment of *Crassostrea virginica* larvae to an intertidal oyster reef. Mar Eco Prog Ser 463: 117-191

Wiberg PL, Taube SR, Ferguson AE, Kremer MR, Reidenbach MA (2019) Wave attenuation by oyster reefs in shallow coastal bays. Estuar and Coast 42: 331-347

Zhao Y, Wang Q, Wang D, Wang YP (2017) Rapid formation of marsh-edge cliffs, Jiangsu coast, China. Mar Geol 385:260-273

CHAPTER 2: Quantifying and mapping intertidal oyster reefs utilizing LiDAR-based remote sensing

Published in *Marine Ecology Progress Series* as:

Hogan S, Reidenbach MA (2019) Quantifying and mapping intertidal oyster reefs utilizing LiDAR-based remote sensing, Mar Ecol Prog Ser 630:83-99

ABSTRACT

Restoration and conservation of the eastern oyster, *Crassostrea virginica*, requires information on its distribution and abundance, which is logistically difficult to obtain. We demonstrate how Light Detecting and Ranging (LiDAR) can be used to obtain this information in a model intertidal system within the Virginia Coast Reserve (VCR) on the Eastern Shore of Virginia, USA. Specifically, we determined how LiDAR derived data can be used to classify land cover and identify intertidal oyster reefs. We used the locations of existing reefs to determine the physical characteristics of oyster habitat through the use of elevation, fetch, and water residence time data for the region. Trained with elevation, intensity, surface slope, and curvature data, the land cover classification identified oyster land cover with an accuracy of 81 %. Ground-truth patches were small, with the 50th percentile for area and perimeter being 11.6 m^2 and 14.5 m. Reef crests occurred in a narrow range of elevation (-0.81 to -0.18 m relative NAVD88) and patches had an average vertical relief of 0.14 m. The habitat suitability analysis located 52.4 km^2 of total oyster suitable habitat, or 12.03 % of the mapped area with similar elevation, fetch, and residence time characteristics of existing reef area. This suggests there is ample viable intertidal area for future oyster population restoration. Results also indicate that LiDAR data, coupled with physical attributes of existing reefs, can be used to target and prioritize locations for future restoration efforts in intertidal habitats.

Keywords: oyster, LiDAR, remote sensing, ecosystem restoration

INTRODUCTION

The native eastern oyster, *Crassostrea virginica,* is a dominant species in the intertidal zone of coastal bays on the Eastern Shore of Virginia, USA. Eastern oysters were historically abundant in Chesapeake Bay and the bordering coastal bays; however, due to overharvesting compounded by poor water quality and disease, the population rapidly declined in the latter half of the twentieth century, collapsing commercial harvest (Rothschild et al. 1994, Kemp et al. 2005). Largely due to partnerships including federal and state agencies, universities and non-profits, oyster populations have begun to recover in Chesapeake Bay (Schulte et al. 2009, Lipcius et al. 2017) and on the Eastern Shore (Wesson et al. 1999, Ross & Luckenbach 2009). On the Eastern Shore, over 20 ha of reefs have been successfully created and populated by oysters in the past decades largely by introducing hard substrate as habitat that creates suitable settlement locations for oyster larvae and ultimately, oyster growth. The recovery of the eastern oyster is important because the species is economically significant as a fishery and provides many ecological services, including water filtration (Coen et al. 2007, Van der Zee et al. 2012, Reidenbach et al. 2013) and mitigation of wave energy that erodes shorelines (Piazza et al. 2005, Scyphers et al. 2011, Wiberg et al. 2019).

To understand the progress of restoration and current populations of oysters on Virginia's Eastern Shore, it is imperative to have accurate information regarding oyster stock and location. Remote sensing is a way to acquire environmental data from a distance and can be beneficial to visualize landscape cover and environmental change on different temporal and spatial scales (Morgan et al. 2010). Airborne-based LiDAR data is a recent form of remote sensing that can be used to estimate elevation based on the return time of laser lights emitted from the aircraft and reflected from the land below. Advantages of LiDAR include robust data with high data density and vertical elevation accuracy (Schenk & Csatho 2002).

Due to these advantages, LiDAR elevation datasets have been used in coastal and estuarine environments to understand inundation (Gesch 2009), marsh classification and sedimentation (Morris et al. 2005, Marion et al. 2009), and classification of seagrass beds (Ishiguro et al. 2016) and intertidal habitat (Garono et al. 2004, Halls & Costin 2016).

While orthoimagery, geometrically corrected imagery, has been used previously to aid in oyster mapping, in itself, it presents the disadvantages of low spatial extent, and in many instances produces inconsistencies that cause intertidal land classification to change depending on when imagery was collected with respect to the tides. This is an important consideration because the majority of oysters found Virginia's Eastern Shore are intertidal (Ross & Luckenbach 2009).

One characteristic of oyster reefs that makes the use of LiDAR especially attractive is that oysters accrete vertically and differ in elevation from surrounding land area. Many studies have relied largely on orthoimagery (Grizzle et al. 2002, Ross & Luckenbach 2009) and hyperspectral data (Garono et al. 2004, Le Bris et al. 2016) to identify and survey reefs. The greater inaccuracies of earlier image interpretation are attributed to pixel size, and with greater pixel resolution came improved analysis (Grizzle et al. 2002, Schill et al. 2006, Halls & Costin 2016, Le Bris et al. 2016). With high resolution satellite imagery, intertidal landscapes for oysters have been classified with accuracies greater than 70 % (Green & Lopez 2007, Le Bris et al. 2016). Moreover, pairing LiDAR elevation data with aerial imagery and other terrain data, intertidal land classification can be improved (Smith et al. 2015, Halls & Costin 2016), with oyster classification accuracies reaching 85 %. In the past, few researchers have investigated the use of

LiDAR derived data alone to classify intertidal land cover, and those that have experienced limited success (Schill et al. 2006). With greater availability and knowledge on how to acquire accurate LiDAR data by mitigating error propagation from sensors, flight missions, and processing (Baltsavias 1999, Ahokas et al. 2003, Hodgson & Bresnahan 2004, May & Toth 2007, Cekada et al. 2009), it remained to be determined if LiDAR derived data alone can successfully classify intertidal oyster reefs.

Given previous success in other habitats, LiDAR data may provide an alternative technique to estimate distributions and abundances of intertidal oyster reefs. Marked difficulties in mapping oyster reefs include differences in size, location, origin (restored, natural, public, private), and overlap with habitats including mudflats and coarse beaches (Garono et al. 2004, Schill et al. 2006, Halls & Costin 2016). In addition, airborne-based LiDAR data has limitations in land classification (i.e., oyster vs. marsh) since LiDAR returns do not provide scene information (Schenk & Csatho 2002). Similarly, LiDAR has limited ability to penetrate dense vegetation and water surfaces (Schmid et al. 2011), such that oyster reefs below the water surface cannot be identified using LiDAR. Because airborne-based LiDAR vertical elevation accuracy is typically on the order of 10s of centimeters, it is unable to detect all differences in land covers that are similar in elevation. Similarly, if the horizontal spatial resolution of the airborne-based LiDAR data is too large (typically 0.5 to 1 m), small oyster patches may go undetected.

To continue successful restoration efforts, in addition to identifying suitable oyster elevation habitat, it is also necessary to understand the physical environments that foster successful larval recruitment and oyster growth (Fodrie et al. 2014). Successful larval recruitment and survival of oysters to maturity along the Eastern Shore of Virginia rely upon hard substrate for attachment

(Whitman & Reidenbach 2012). In addition, oysters depend upon currents to transport larvae, and locations with higher tidal energy and flow speed have been associated with greater oyster growth (Lenihan 1999, Byers et al. 2015). High flow velocities and turbulence act to transport and increase the supply of larvae, increase incidence of larvae encountering substrate, and reduce mortality from sedimentation (Lenihan 1999, Hendriks et al. 2006, Fuchs et al. 2013, Hubbard & Reidenbach 2015). However, if velocities adjacent to benthic surfaces are too high, this can prevent successful settlement (Crimaldi et al. 2002, Reidenbach et al. 2009). Often high energy environments that include significant wave activity limit successful recruitment of oysters (Ortega 1981, Bushek 1988, O'Beirn et al. 1995).

By understanding where and under what physical conditions oyster reefs exist, we can gain an understanding of suitable habitat to better manage and restore oyster populations (Schulte et al. 2009, Fodrie et al. 2014, Colden & Lipcius 2015, Lipcius et al. 2015, Theuerkauf & Lipcius 2016, Colden et al. 2017). Because reef elevation controls the amount of time oysters are exposed, it can also be considered the primary variable in determining the fate of oysters (Fodrie et al. 2014). In addition to elevation, the local hydrodynamic environment determines oyster growth and larval recruitment (Bartol et al. 1999, Lenihan 1999, Schulte et al. 2009, Colden et al. 2017). Therefore, the three main objectives of this study were to:

1) Determine if LiDAR elevation data can be used to identify and map oyster reefs within intertidal regions.
2) Describe the physical environment where oysters are found in relation to elevation, and the hydrodynamic factors of fetch and water residence time.
3) Identify existing intertidal regions within the VCR with similar physical environments that can be used as target regions for future restoration efforts.

MATERIALS & METHODS

Study Site and Areas of Interest

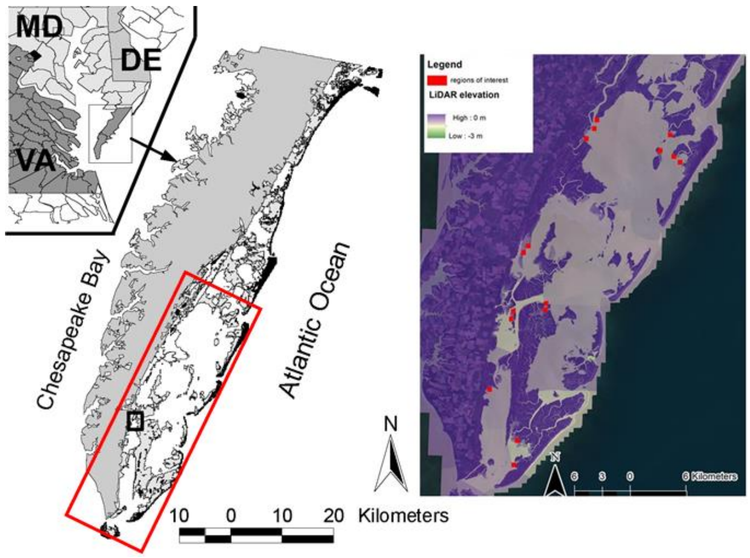

Figure 2.1. Left) The Delmarva Peninsula, VA, with land shown in grey and water in white is a land mass between the Chesapeake Bay and Atlantic Ocean. The Virginia Coast Reserve (VCR) is comprised of the marshes, coastal bays, and barrier islands on the Atlantic Ocean side of this peninsula. The black box on the peninsula shows the location of Hillcrest oyster reefs, a site of healthy natural and restored reefs. The red box is extent of the image on the right. Right) The 16, 0.25 km^2 regions (red) of interest chosen throughout the VCR for oyster reef mapping. LiDAR data (purple) was flown for the extent of the peninsula.

This study focused on oysters within the intertidal region of the Virginia Coast Reserve (VCR), located on the Atlantic Ocean side of the Delmarva Peninsula, on the Eastern Shore of Virginia. Within the coastal habitat of the VCR, which extends along approximately 100 km of coastline and contains coastal bays and barrier islands that extend towards the open ocean, 16 areas (500 m x 500 m, 0.25 km^2) were analyzed for oyster land cover (Figure 2.1). These areas were chosen because they contained intertidal reef patches that represented some of the more densely populated areas. They also provided spatial distribution across the VCR. The areas were used to ground-truth, train, and test a supervised classification for oyster and non-oyster land cover. The patchy and vertical accretion of oysters in the VCR are shown in Figure 2. To determine suitable habitat, a total area of 436.4 km^2 encompassing intertidal and coastal bay area was analyzed.

LiDAR Data Sources and Derived Spatial Layers

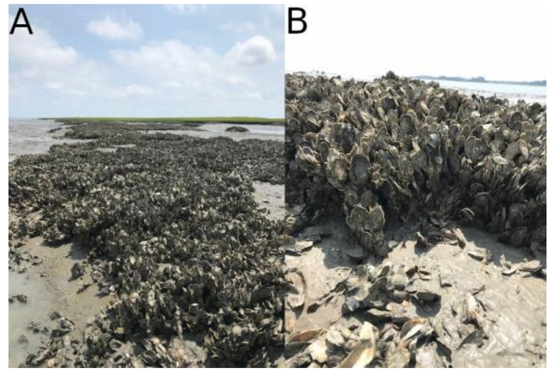

Figure 2.2. Intertidal oysters photographed within the VCR showing their A) patchy distributions and B) vertical growth.

An airborne-based LiDAR data set accessed through the VCR data portal (USGS LiDAR 2015) was collected for the project area. LiDAR data acquisition was completed by Leading Edge Geomatics while classification, products, and quality assurances were completed by Dewberry, the primary contractor. Data were acquired between April 11 to April 24, 2015 (Dewberry 2016). Flights were conducted within 2 hours of the lowest low tide for the two weeks that flights were completed. System specifications included a flight altitude of 1000 m, speed of 100 knots, and a pulse rate of 200 kHz. The vertical accuracy reported for non-vegetated had a 95 % confidence level RMSE of 12.5 cm. Though not statistically significant (only based on 17 of 113 checkpoints) the horizontal accuracy was 64.9 cm (Dewberry 2016). Ground surface returns were filtered and breaklines made to distinguish land and water. Editing corrected misclassified land cover and artifacts and uneven water surfaces due to tidal and wave action were flattened. The LiDAR point data were used to create an elevation model layer with square pixels sized 0.76 m^2 and an aggregate nominal point density of 3.45 points per m^2. The original layer was then projected with horizontal (WGS84 UTM 18N) and vertical datums (NAVD88) in meters. All elevations in this study are relative to NAVD88 unless specified. Some reefs were located below sea level during the time of flight when LiDAR data were collected, and therefore were not visible in the dataset, preventing a complete oyster population survey. For many intertidal locations, reefs were easily distinguishable within LiDAR elevation maps and appeared different than surrounding land cover due to their distinct elevation change.

The LiDAR elevation data also included intensity data, measure of the strength of return, from the flight paths. Mosaic raster layers of intensity values were created for the area covering the 16 regions of interest. Additionally, a slope layer was derived from the elevation layer using the neighborhood of immediate cells (3x3) for the same regions. A final slope of the slope layer was computed forming the curvature layer which measures the convexity or concavity of a surface and can account for additional textural differences between land covers (Pittman et al. 2009). ArcMap 10.5 GIS software was used to analyze and map the LiDAR data.

Ground-Truth and Surveyed Oyster Data

ArcMap 10.5 GIS software was also used to create ground-truth data. To create a ground-truth map of oyster land cover in the areas of interest, the 16 regions were delineated on the elevation layer. Satellite imagery and GPS tracks were used to determine the appearance of oyster reef patches on the elevation layer and validate the patches seen. The basemap provided by ESRI via ArcMap (DigitalGlobe 2017) was used as the source of the satellite imagery. The imagery was used to validate the patches of reef mapped on the elevation layer, but primarily served to determine the appearance of oyster reefs on the elevation layer, where oyster patches were only visualized in terms of elevation. Specifically, images from DigitalGlobe with up to 0.3 m resolution satellite images during low tide for September 24, April 27, and April 16, 2017 were used based on availability for individual locations. As an additional check to determine if mapped patches were in the same locations of intertidal reefs, GPS tracks were made *in-situ* using a handheld Garmin GPSMAP 64s (maximum accuracy of 3 m) during the summer of 2017 for portions of 8 of the 16 regions of interest (Red Bank (3 areas), Hillcrest, Narrows, Ramshorn

(2 areas)) which were easily accessible and known for healthy, dense patches of oyster reef. These GPS tracks were imported into GIS as line features and manually edited to make closed polygons. Polygons with area less than 10 m^2 were discarded, while those greater than 10 m^2 in area but less than 1m apart were aggregated. The resulting polygons were then imported on to the elevation layer. Because imagery was from 2017, while LiDAR elevation data was from 2015, only one data set, the elevation layer, was used to map reef patches. An oyster reef layer was created by drawing polygons around the perimeter of visible patches. As a check on digitally mapped reef accuracy, the GPS tracks served to determine if LiDAR mapped reefs were present within the GPS tracks. Although ground-truth oysters covered only 0.07 km^2, or 1.8% of the 4 km^2 of total intertidal land cover within the 16 regions, greater than 86% of GPS tracks contained LiDAR elevation mapped patches. Hence, the digitized reefs served as a good proxy for ground-truth data and were used instead of *in-situ* tracks for ground-truth oyster land cover in this study.

Supervised Classification of Oyster Reefs in the VCR

Creating an oyster reef signature for maximum likelihood classification

Spatial data on elevation, intensity, slope, and curvature were used to provide training data to complete a maximum likelihood image classification in GIS. In total, 4 layers were made to create signatures for oyster patches. Multi-band rasters were created with the different data types as different bands which were then used to determine which of the variables are most useful in identifying oysters. First, analysis from signatures using individual elevation, intensity, and slope layers were completed, followed by 2-layer composites of all combinations of elevation, intensity, and slope, then a 3- layer composite of elevation, intensity, and slope. Finally, a 4-layer composite was computed with curvature added. Adding layers to a multi-band composite adds a dimension of data for each location in space and therefore, with more data a greater amount of descriptive information can be used to create signatures from the input data.

Training samples were created from 8 oyster regions, (half of the 16 total regions), by manually drawing polygons on the elevation layer identifying different land cover types, including water, marsh, and mud of differing elevations and appearances. Oyster reef polygons previously described were used identify oyster land cover. Reefs for each of the 8 oyster regions were grouped as separate land covers to represent 8 potential types of oysters to account for regional differences in the signature. Because we were interested in classifying land for oyster land cover, this was done to make the signature more robust to identify oysters of varying size, shape, age, and appearance. Only reefs that covered areas equivalent to at least 50 pixels (11.6 m^2) or greater were included to provide enough of a signature to be able to classify the data as an oyster patch. In total 13 classes of land cover were discriminated, including the 8 representing oysters, high, medium, and low elevated muds, marsh, and water. Average elevation, intensity, slope, and curvature for training samples of oyster land cover within each of the 8 training regions are stated in Table 2.1. Data from the multi-band rasters (ranging from 1-4 bands of

Table 2.1. Summary of the means and standard deviations for elevation, intensity, slope, and curvature data within oyster patches for each training region.

Location	Elevation (m relative NAVD88)		Intensity		Slope (degree)		Curvature	
	Mean	Standard deviation	Mean	Standard deviation	Mean	Standard deviation	Mean	Standard deviation
Hillcrest	-0.23	0.14	66.46	27.39	3.67	2.85	51.45	19.85
Mockhorn	-0.51	0.22	146.58	67.63	4.24	2.66	51.83	18.93
North1	-0.22	0.10	133.22	46.56	2.15	2.15	52.90	17.26
North2	-0.39	0.08	176.06	57.41	3.40	2.19	50.38	17.83
Ramshorn	-0.26	0.10	80.91	30.44	4.28	2.58	56.01	17.29
RedBank1	-0.32	0.2	92.25	38.38	6.70	5.09	64.46	17.58
RedBank2	-0.27	0.11	129.04	44.32	4.21	2.81	56.10	18.84
South1	-0.21	0.12	197.92	61.58	4.43	2.34	51.51	20.87

elevation, intensity, slope, and curvature) were extracted to the shapefile made from the training samples for all land cover types to produce the respective signature files. The signature for each land cover category was based on the mean and covariance of the data in training samples so that for each land cover, a statistical representation of what each land cover type looks like in terms of elevation, slope, intensity, and curvature was formulated. A sensitivity analysis was conducted to determine the best combination of LiDAR derived data to use in a supervised classification to identify oyster reefs.

Maximum Likelihood Classification in ArcMap 10.5 and interpretation of output

The maximum likelihood classification tool in ArcMap 10.5 was used to produce a classified raster on the remaining 8 oyster regions, referred to as test regions, using the created signature files. This is a pixel-based classification method that classifies images by putting pixels into different classes based on statistical probability using class means and covariances informed by the sample-based signature. The pixels classified to be similar to samples of oyster reefs from the training regions were reclassified to create one larger oyster class. The remaining classes of pixels for different land covers were reclassified to represent one class of non-oyster land cover. Although this data could be used to classify land cover, such as marsh and mud, in this study we were concerned only with success in identifying oyster reefs and generated ground-truth data for just this land cover.

Accuracy Assessment: comparing classified and ground-truth oyster land cover

To validate the classification and determine which combined data layers created the best signature for oyster reefs, accuracy assessments were completed for classified test regions. In a similar way to reclassifying the classified outputs to have two categories, oyster and non-oyster land cover, a ground-truth raster layer was made where digitized (ground-truth) oysters comprised the oyster class and all other land was classified as non-oyster. The raster matched the projection and resolution of the classified layers (WGS 1984 UTM Zone 18N, 0.76 x 0.76 m resolution). A total of 500 points spread across the regions were generated, using an equalized stratified random sampling technique, such that the 500 points were distributed randomly for the total area, but an equal number of points were randomly assigned to oyster and non-oyster classes based on the ground-truth data layer. Stratified sampling has the advantage of including categories of data that are rarer and less likely to appear with simple random sampling and has proven to work accurately with habitat and remotely sensed data (Congalton 1991, Hirzel & Guisan 2002). The ground-truth land cover type for each point was compared to the land cover type on the classified layer assessed, and a confusion matrix was generated to determine the accuracy of the classified layer in identifying oyster and non-oyster land covers. In addition to overall accuracy, the confusion matrices determined user and producer accuracies for oyster and kappa coefficients.

Confusion matrices, also known as error matrices, provide a means to determine what portion of classified data is correctly classified based on reference data (Story & Congalton 1986). Reference and classified data are organized in columns and rows, respectively, and separated into categories, in this case whether the points were found in pixels categorized as oyster and non-oyster. Agreement between the reference and the classified data is along the matrix's major diagonal. This is used to determine the overall accuracy by adding all the correctly classified data points for both categories and dividing by the sum of all random points. To assess individual category accuracy, the correctly classified data points are divided by the total ground-truth data points for that category. In this scenario, this is all the random points correctly classified as oyster divided by the total number of ground-truth oyster points. This measures the producer accuracy, which is suggestive of errors of omission (omission error = 1-

producer accuracy), which can be defined as the percent of ground-truth oysters not correctly classified (i.e., oyster area omitted from the produced map). User accuracy for a category is calculated by dividing the number of correctly classified points by the total number of points classified as that category (Story & Congalton 1986). This is a measure of error of commission (commission error = 1- user accuracy), a determinant of the rate of false positives. It explains the chance of discovering a location classified on the map as oyster to be a different land cover in reality. A kappa value takes the classifier as a whole and compares the observed agreement between the classified and reference data and the agreement that is likely to occur by chance if observations were independent. In this way, it is the proportional agreement between data that has been corrected for chance. A value of 1 would indicate complete agreement between the observed and classified data, a value of 0 is indicative of no difference with what is expected by chance, and a value of -1 would indicate complete disagreement after considering corrections for chance (Agyemang et al. 2011).

To compare how the classification differed by test region, individual accuracy assessments for oyster and non-oyster land cover for each region were also performed in a similar way, by generating 500 random points, equally stratified for oyster and non-oyster land covers for each of the 8 test regions. This analysis was completed using the classified raster produced from the most successful composite determined through the sensitivity analysis. The mean of the difference between elevation of oyster patch crests and the buffered 2 m of adjoining land, mean oyster patch area, and mean patch perimeter per region were quantified. To calculate mean elevations for patches and surrounding land, all points within each polygon were averaged, where elevation points were spaced 0.75 m apart set by the LiDAR point density. Regression analyses were performed to determine if differences in local accuracies were explained by these variables. The elevation was also made relative to local mean sea level (lmsl) by adding a conversion factor layer to the LiDAR elevation layer available through the VCR (Richardson 2013) to determine the local position of reefs. It was hypothesized that with 1) greater difference in elevation between reef crests and surrounding land and 2) larger oyster patches, the classification and identification of oysters would be more successful.

Using Digitized Reefs to Determine Suitable Habitat within the VCR

In addition to the LiDAR dataset, water residence time and fetch data layers were created in GIS using model output from Safak et al. (2015) and Wiberg et al. (2019) to characterize intertidal lands suitable for oysters. Water residence time was modeled with a three-dimensional coastal ocean model utilizing particle tracking and validated with field observations, while fetch was weighted by wind direction. In this study, water residence time and fetch serve as proxies for water mean velocity and wave energy from winds, respectively. Residence time data can also predict the exchange of water masses, which is likely an important factor in not only providing reefs with food, but also enhancing larval exchange. These layers were projected and resampled using the nearest neighbor method to match the datum and resolution of the LiDAR elevation data (WGS 84 UTM Zone18N, resolution of 0.762 x 0.76 m). The data were then extracted to overlapping ground-truth oyster reef polygons from all 16 regions to find the mean for each oyster patch using zonal statistics, where mean values for each variable were calculated per reef. Suitable habitat analysis for the VCR was restricted to the area where data were available for all three variables, eliminating land features which had no water residence time or fetch data. The range for elevation of land surrounding oyster patches within 2 m was computed, and the middle 99 % of oyster patch elevation (range from the 0.5 to 99.5 percentiles) was set as suitable elevation. The surrounding land rather than the elevation of patches (reef crests) was used for suitable elevation because this is more representative of the elevation of land oysters are recruited to and more useful to target land for restoration. However, an examination using the same method but with reef crest elevation was also completed for comparison. Using the elevation range from the middle 99 % of the sample excluded some extreme data that may have been wrongly identified as oyster habitat. This range also excluded much of the subtidal areas that would not be visible on the LiDAR dataset. Next, the area of suitable habitat was further restricted by eliminating areas where fetch was not suitable, and finally reduced by excluding area with unsuitable water residence time. Fetch and water residence time were not affected by errors in the modeled elevation, so the full range of data (maximum to minimum average values found in the oyster sample) were used to categorize areas suitable and less suitable for these variables. The combination of elevation and water residence time was also examined to help determine which variable, water residence time or fetch, was a more useful criterion in determining suitable oyster habitat.

The results of suitable habitat using elevation defined by land surrounding oyster patches were then compared to the most recent oyster survey conducted within the VCR completed in 2007 by Ross and Luckenbach (2009). This survey combined ground-truth data with aerial images from 2007 to determine oyster area. This survey was input as a GIS layer and then the polygon layer was converted to a raster with resolution matching the LiDAR data. Then the suitable land cover product was extracted to the reefs for the 16, 0.25 km^2 regions used to create ground-truth oysters.

RESULTS

LiDAR classification

Satellite orthoimagery and GPS tracks were useful in helping to determine how oyster patches appear on an elevation layer. Greater than 86 % (151/175) of GPS tracks intersected digitally mapped reefs based on LiDAR elevation (Figure 2.3), 90.3 % of the GPS tracks were within 3 m of digitized reefs. There were apparent differences in the overlap for the different areas surveyed. Most of the unaccounted tracks were in the regions near Red Bank (three regions), which accounted for 15 of the total 24 tracks that did not overlap digitized reefs.

Figure 2.3. A) A birds-eye view of the Narrows region visualized with satellite imagery (DigitalGlobe 7/27/18) and B) the LiDAR mapped oyster patches (red) and GPS tracks completed (black outline) for this region.

In the sensitivity analysis, the classified raster became more accurate as more layers were used to create signatures (Table 2.2). Confusion matrices using information from random points showed that overall accuracy of land classification increased when composites of multiple layers were formed to provide signatures for land cover (Table 2.2).

Of the analyses performed on the individual layers of elevation, slope, and intensity, slope performed the best with a high overall accuracy (0.77). When data from elevation, intensity, and slope layers were combined, the overall accuracy and kappa value increased to 0.76 and 0.58, values similar to slope alone. However, with the signature informed by three

Table 2.2. Accuracy assessment results for classified land cover produced from signatures created using different combinations of elevation, intensity, slope, and curvature data. User and producer accuracy for oyster classes, in addition to overall accuracy and kappa coefficients were computed for land cover classified as oyster or non-oyster. Accuracies range from 0 to 1 and the kappa coefficients range from -1 to 1.

No. of layers	Combination of data	Oyster user accuracy	Oyster producer accuracy	Overall accuracy	Kappa coefficient
1	Elevation	0.62	0.48	0.59	0.19
	Slope	0.83	0.68	0.77	0.54
	Intensity	0.66	0.66	0.66	0.32
2	Elevation & Slope	0.66	0.78	0.72	0.48
	Elevation & Intensity	0.73	0.72	0.73	0.46
	Intensity & Slope	0.87	0.6	0.76	0.51
3	Elevation, Intensity, & Slope	0.83	0.74	0.79	0.58
4	Elevation, Intensity, Slope, & Curvature	0.81	0.80	0.81	0.62

layers, the kappa value increased while also creating more balanced errors of omission (26%) and commission (17%). Additionally, with more layers added, the resulting land cover result more accurately reflected the training data, where all 13 categories were represented, whereas only a few categories were produced with single layers. When the additional layer of curvature was added to provide greater textural information for the signature, the accuracies again increased and this 4-layer composite was analyzed further and used to investigate regional differences.

In the accuracy assessment for the classification trained using all data layers (Table 2.3), the error of commission (19 %) was almost balanced with the error of omission (20 %) for oyster land cover, given the user accuracy of 0.81 and the producer accuracy of 0.80. This suggests there was a 20 % chance that true oyster cover at a

Table 2.3. Confusion matrix created for the classification produced by signature with the 4-layer composite for land classified as oyster and non-oyster. For each of the 500 random points, the table lists whether they are categorized as oyster or non-oyster according to ground-truth and classified data. Accuracies range from 0 to1 and the kappa coefficient ranges from -1 to 1.

		GROUND-TRUTH LAND COVER				
		Non-oyster	Oyster	Total	User Accuracy	Kappa
CLASSIFIED LAND COVER	Non-oyster	204	49	253	0.81	
	Oyster	46	201	247	0.81	
	Total	250	250	500		
	Producer Accuracy	0.82	0.80		0.81	
	Kappa					0.62

location was omitted from the map, and a 19 % chance that a pixel classified as oyster was a false positive. This balance of omission and commission was improved compared to the 3-layer results, where omission error was reduced from 26 to 20 %. The overall accuracy in classifying land as oyster or non-oyster was 0.81 and the kappa coefficient was 0.62. The high kappa coefficient supports the conclusion that there was a reduced chance that the similarity between the classified and ground-truth data layers was due to chance alone (Table 2.3).

In total, 80.8% of the area of ground-truth reefs were correctly classified as oyster. Additionally, ground-truth reef polygons were analyzed to determine if they contained pixels that

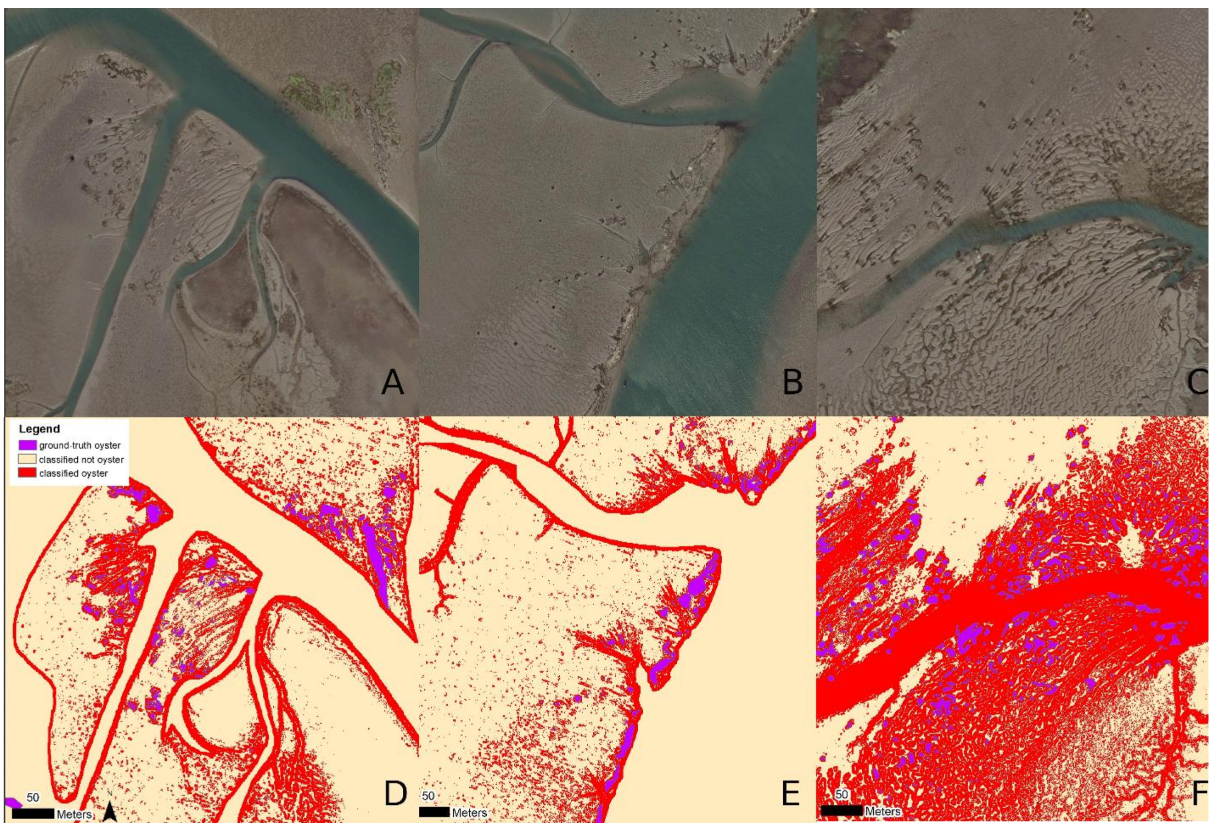

Figure 2.4. Aerial images of three test regions named A) Narrows, B) Ramshorn, and C) Mockhorn are shown. The classified rasters (D, E, F) are shown below their respective regions. Red indicates areas classified as raster, yellow indicates area classified as non-oyster land cover, and purple represents ground-truth polygons. Overall accuracy and kappa values for Narrows, Ramshorn, and Mockhorn regions were 0.71, 0.81, 0.67 and 0.43, 0.63, 0.34, respectively. Image layer credits: DigitalGlobe A and B) April 27, 2017 C) September 24, 2017.

were classified as oysters. This measured the classified raster's ability to detect oyster patches, if not their entire area. Of the 1259 ground-truth oyster reef polygons located in the test regions, 1218, or 97 % contained at least one pixel that was classified oyster. Therefore, almost all ground-truth reefs were at least partly represented in the classified map.

A visual comparison for a sample of classified test regions compared with ground-truth oyster reefs is seen in Figure 4. The overall accuracy for individual test regions ranged from 0.65 to 0.92, while kappa values were lower and had a greater range from 0.30 to 0.83 (Table 2.4). The average patch elevation (reef crest) for oysters within the test regions was -0.31 m relative NAVD88. The difference between mean oyster elevation and surrounding land elevation provides an estimate of the average vertical relief of oysters in each region, which ranged from 0.103-0.225 m for the different test regions (Table 2.4), supporting that reef patches were positioned higher than the surrounding land cover. The overall average for oyster relief in test regions was 0.14 m. For the VCR, local mean sea level was below NAVD88 ranging in

Table 2.4. Quantified characteristics for each of the classified test regions describing region overall accuracy, mean elevation (m), mean oyster elevation (m), the mean difference in elevation between oyster patch crests and surrounding land (m), mean oyster patch area (m^2), and mean oyster patch perimeter (m) for the patches located in each region.

Region Name	overall accuracy	Kappa	oyster elevation (m lmsl)	oyster elevation (m NAVD88)	Difference between crest and land elevation (m NAVD88)	patch area (m^2)	patch perimeter (m)
Narrows	0.71	0.43	-0.308	-0.408	0.103	33.1	22.0
Mockhorn	0.67	0.34	-0.213	-0.322	0.169	24.9	19.5
Ramshorn	0.81	0.63	-0.161	-0.268	0.143	41.6	25.0
Red Bank	0.72	0.45	-0.145	-0.247	0.126	48.0	32.8
North1	0.92	0.83	-0.420	-0.522	0.130	91.7	44.4
North2	0.85	0.71	-0.201	-0.306	0.135	8.5	11.0
South1	0.65	0.30	-0.071	-0.179	0.116	13.9	15.2
South2	0.91	0.81	-0.065	-0.183	0.225	159.4	68.5

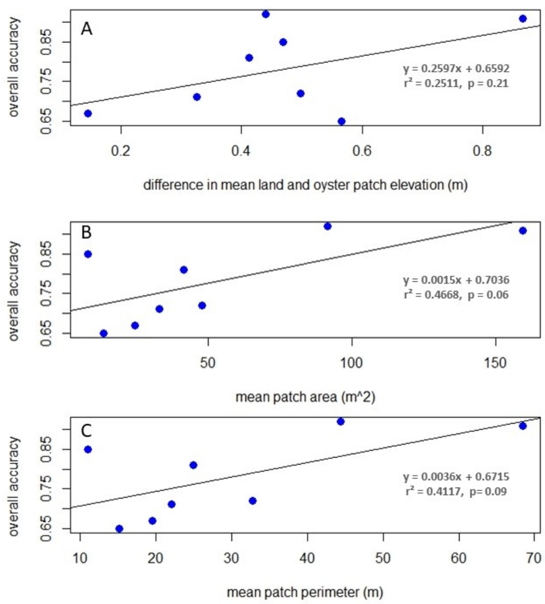

Figure 2.5. Linear regressions plotted to determine relationships between region accuracy and A) difference in mean surrounding land and oyster elevation, B) mean patch area, and C) mean patch perimeter.

magnitude from 0.039-0.149 m. The mean patch elevation was at -0.207 m lmsl and the average patch elevation for each region ranged from -0.308 to -0.065 m lmsl (Table 2.4).

There was no significant relationship between region overall accuracy and vertical relief ($r^2 = 0.25$, $p = 0.21$) (Figure 2.5A). There were positive relationships between region accuracy and mean patch area with 94 % confidence ($r^2 = 0.47$, $p = 0.06$) and mean patch perimeter with 91 % confidence ($r^2 = 0.41$, $p = 0.09$). These strong positive relationships may indicate that with larger reefs there is increased accuracy (Figures 2.5B and 2.5C).

Physical environment and habitat suitability

The elevation range found for the middle 99 % of land surrounding oysters was -0.92 to -0.13 m for oyster reefs (n = 2089). For the intertidal and coastal bay region analyzed within the VCR, 83.2 km^2, or 19.1% of the total 436.4 km^2, fell within the range of suitable elevation (Figure 2.6A). Suitable elevation, when instead defined by reef crests, led to a suitable elevation range (middle 99 %) of -0.81 to -0.18 m and covered 32.3 km^2 or 7.3 % of the study area (Figure 2.6B). Water residence time for 2026 oyster patches ranged from 23.2 to 2000 h, while fetch data for 1498 patches ranged from 40.0 to 4643.0 m. Area of suitable water residence time and fetch were much less restrictive, covering 294.2 and 295.2 km^2, respectively (Figures 6C and

6D). Areas having both suitable fetch and residence time totaled 226.5 km^2, so that areas suitable for both these variables were often coincident. When the study area was subjected to

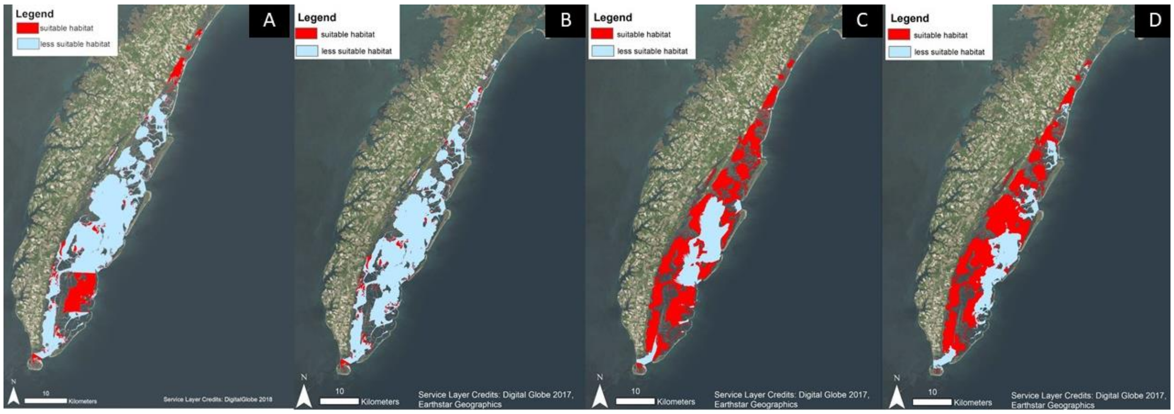

Figure 2.6. Areas of suitable (red) and less suitable (blue) A) elevation defined by land surrounding reefs, B) elevation defined by reef crests C) fetch, and D) water residence time for VCR. Service layer credits: DigitalGlobe 2017, Earthstar Geographics.

meet suitable criteria for elevation, water residence time, and fetch, a total of 52.4 km^2, or 12.0 % of the study area, remained (Figure 2.7). Areas of suitable habitat were distributed throughout the study area but were often near higher areas of mud and marsh land covers. Using reef crest elevation led to a similar but more restrictive overall suitable habitat of 23.1 km^2 or 5.3 % of the study area, though areas further from land and toward more open water were reduced. Greater than 83 % of the ground-truth reefs area fell within suitable habitat with elevation set by surrounding land, after reefs were converted to raster. Some disagreement existed because the model was computed on a pixel basis, whereas the average values for elevation, fetch, and residence time, were calculated for each oyster patch to set criteria (Figure 2.8A).

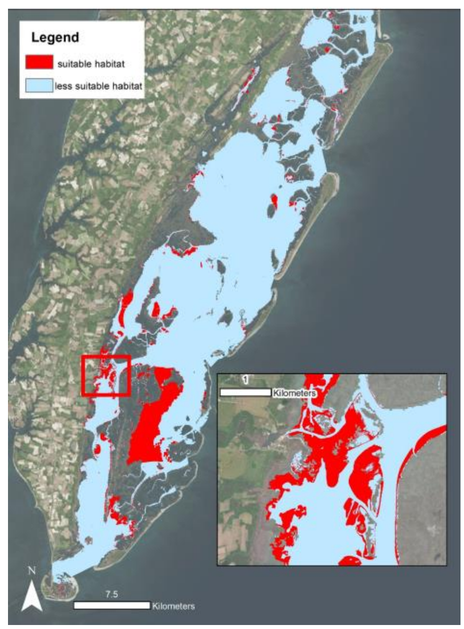

Figure 2.7. Area of suitable elevation (red) remaining after areas with less suitable elevation, fetch, and water residence time were removed. Service layer credits: USA FSA 2016, DigitalGlobe 2018.

Also, some ground-truth reefs did not have modeled data because either fetch or water residence time was absent for areas of higher elevations.

Comparison to Ross and Luckenbach (2009) oyster survey

In the comparison between the suitable area within the 16, 0.25 km^{2}regions and the Ross and Luckenbach (2009) survey, most surveyed area overlapped with modeled suitable habitat that met all three criteria of elevation, fetch, and water residence time (Figure 2.8B). Of the 0.21 km^2 of surveyed reef within these 16 regions for which suitable habitat was modeled, 0.138 km^2 or 66.3 % was described as suitable. Total suitable land in the regions was 1.44 km^2 so that overlapping surveyed reefs accounted for about 10% of suitable area. While there was good agreement between the survey and suitable land for these regions, the comparison between the two data sets should be used with caution because many of the areas surveyed by Ross and Luckenbach were in hydroflattened areas of the LiDAR elevation data.

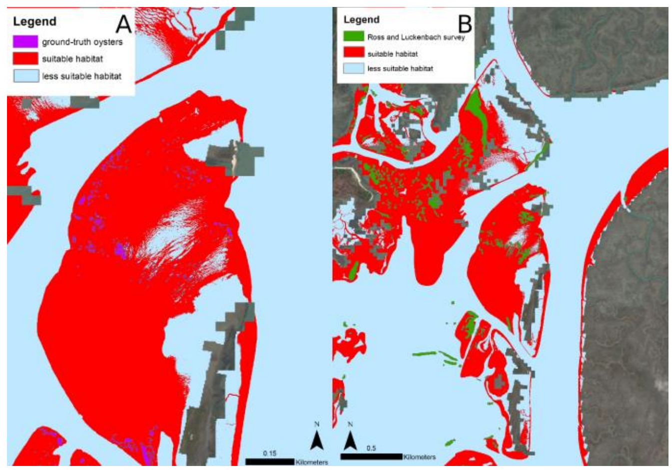

Figure 2.8. A) Ground-truth oysters (purple) and B) Ross and Luckenbach reef polygons layered on the suitable habitat map, where suitable land is seen in red and less suitable habitat in blue. Both ground-truth and surveyed reef polygons greatly overlap with suitable habitat. Service layer credits: DigitalGlobe 2018.

DISCUSSION

This study found that LiDAR data can be used to identify intertidal oyster reefs along the Virginia, USA coastline and the locations of existing reefs can be used to identify the physical environments in which they are most often found. While producing a complete population survey is unachievable using this data due to the lack of subtidal and at some locations low-intertidal LiDAR information, the study was successful in determining methods for automatic classification. By successfully quantifying elevation, fetch, and water residence time data over areas of existing reefs, the study also determined target regions within the VCR where oyster restoration is likely to be successful.

Oyster Land Cover Classification

A multi-band raster including elevation, intensity, slope, and curvature data increased the accuracy in identifying reefs (Table 2.3). This combination of data provided a signature that distinguished oysters from other land covers with high accuracy. This study took a simplified approach and used only layers derived from LiDAR. In this way, we tested the utility of LiDAR for classification of intertidal oysters. Other land classification studies included additional roughness parameters, such as surface rugosity, plan curvature (concavity perpendicular to the maximum slope), and fractal dimension, to characterize landscapes (Pittman et al. 2009), which may prove more beneficial in other environments and particular land covers. The accuracy was not greatly improved by adding curvature to our analysis and did not warrant further additions. Different kernel (3x3 cells) statistics including maximum, minimum, standard deviation, and range for elevation, intensity, and slope were examined, but did not benefit the classification and were colinear with the other data. These layers were therefore excluded.

Our method of using data only derived from LiDAR, supported the idea that LiDAR data can distinguish between land that is oyster and non-oyster with 81 % accuracy, based on the confusion matrix created using 500 equally stratified random points. The kappa coefficient, 0.62, supported agreement between the classified and ground-truth land cover layers at 62 %. This value may be more reflective of the accuracy, due to the small amount of land cover that is truly oyster reef. Oysters covered approximately 2 %, 0.04 km^2, of the total 2 km^2 of land within the test regions, and therefore there may have been some chance agreement involved in classifying non-oyster cover because it covered vast majority of the land. In creating a method to classify oysters, it was important to not only identify reefs correctly, but also minimize the extent to which false positives were produced. This study successfully balanced the error of omission (20 %) with error of commission, or false positive rate (19 %). One common error in the classified output was that the edges of mudflats were often denoted as being oyster cover. While this is an error of commission in many areas, oysters are commonly found fringing mudflats and marshes, and therefore are areas that are also likely to have similar elevations to ground-truth oyster samples. Additionally, while the overall accuracy was 81 % in identifying oyster from non-oyster land cover, 80.8 % of ground-truth reef area was classified as reef and 97% of ground-truth patches had at least one pixel classified as oyster. Therefore, the classification was successful in identifying almost all of the true reef patches, albeit lacking in identifying the total area. This suggests that portions of reef patches are more representative of the training data than others.

The classification scheme may be useful to define areas where oysters are located, although the results of this study support that ground truthing or manual digitization using LiDAR is necessary to identify full cover. Certainly, using LiDAR to train classification tools to identify oyster reefs can narrow the area with potential reef cover from remote locations. Therefore, this study supports that if LiDAR data is available for a different geography, elevation can be used to create ground-truth training data informed with derived layers (including elevation, intensity, slope, and curvature) to automatically classify land for oysters with a high accuracy. While the study has shown that obtaining full oyster coverage using LiDAR is unlikely, LiDAR can be used to manually map known locations of oyster with greater patch definition compared to ground surveys. More precise patches can foster the ability to monitor change over time. Both growth and mortality might be quantified based on measurable changes in horizontal and vertical dimensions. For the VCR, past LiDAR surveys over the region were not conducted during low tide, preventing comparisons with the data used in this study. However, now knowing that patches can be mapped with LiDAR, monitoring can take place with future LiDAR surveys.

Mapping with LiDAR elevation, with the user trained with imagery and *in-situ* data as described here, presents a more precise method to delineate area. Surveying on foot can cause larger tracks to be taken due to accessibility and effort. The GPS tracks in this study were not collected with the intention to assess accurate area or population size, but for a more qualitative comparison to learn how terrain is visualized on an elevation layer. Therefore, the accuracy was less meaningful and comparison with digitized reefs utilized a presence-absence method which showed that reefs seen on LiDAR elevation were also present with *in-situ* reef tracks, though areal comparison should be viewed with caution. In addition to error introduced by the handheld GPS accuracy, the LiDAR data also has errors in horizontal accuracy and can only discriminate patches with discernable vertical relief. The regional differences seen in overlap between LiDAR digitized reefs and GPS tracks indicates that differences in geographic position such as elevation or patch size may affect digitization, and it is difficult to resolve whether error is in the GPS or LiDAR data.

Past studies using various methodologies have reported similar results for accuracy and kappa coefficients for estuarine land covers including oyster reefs, which were difficult to distinguish remotely within coastal habitats (Halls & Costin 2006, Le Bris et al. 2016).

Obstacles include misrepresentation of oyster patches with other land covers such as mud or gravel. These errors have been attributed to lower proportion of cover and sample data, similar textures and elevations between land covers, and the ephemeral exposure within intertidal landscapes (Garono et al. 2004, Schill et al. 2006, Halls & Costin 2016). Studies successful in classifying coastal habitats often rely on combining different sources of data including high resolution and hyperspectral imagery (Grizzle et al. 2002, Schill et al. 2006, Chust et al. 2008, Dumbauld et al. 2011, Le Bris et al. 2016), and hydrodynamic (Smith et al. 2015), radar (Choe et al. 2012), and acoustic sonar (Smith et al. 2001, Allen et al. 2005) data. Even when high degrees of accuracy (greater than 80 %) were achieved in intertidal habitat classifications, oysters were one of the least successful categories of cover (Halls & Costin 2016).

While most of the surveys completed in the past have relied on high resolution imagery, the 2 % of oyster cover found in the of the largely intertidal regions investigated in this study is similar to other accounts for the VCR and along intertidal oyster habitats on the mid-Atlantic coast (Bahr 1976, Bahr & Lanier 1981, Ross & Luckenbach 2009). Notwithstanding recent successful restoration efforts (Schulte et al. 2009, Lipcius et al. 2015), the eastern oyster remains only a small percentage, about 1%, of historical population size in Chesapeake Bay (Rothschild et al. 1994, Kemp et al. 2005), though the intertidal populations in the coastal lagoons adjacent to Chesapeake Bay (e.g. VCR) are somewhat higher (Ross & Luckenbach 2009). In the most recent stock survey, oyster reef land cover in the VCR area represented 0.4 % of habitat mapped (Ross & Luckenbach 2009). This low percentage of cover appears to be common along the mid-Atlantic for the last few decades (Bahr 1976, Bahr & Lanier 1981). The percentage quantified from this study, however, is likely inflated due to the concentrated mapping on areas chosen to be dense with oyster reefs.

The idea that mapping oysters with elevation data would be successful is based on the understanding that oysters grow vertically above surrounding land cover. Contrary to the hypothesis that differences in elevation between oyster and adjoining mudflat would be related to the ability to detect oysters, there was no significant relationship. The mean elevation difference between patches and surrounding land (2 m buffer), 0.14 m, likely represents the difference in elevation needed for reef recognition from LiDAR elevation data and may account for discrepancies in what was visible on LiDAR vs *in-situ* mapping. This value can serve as a benchmark in deciding whether or not LiDAR data can be used to map reefs in different regions. In our regional analysis the average oyster patch for each region fell within a narrow range of elevation relative to NAVD88 from -0.52 to -0.17 m. Therefore, it is likely that within this approximately half meter of elevation, virtually all intertidal oysters exist. The spatial variation in local mean sea level (lmsl) could account for the range of average patch elevations relative to NAVD88. For all digitized oysters the average crest elevation in terms of lmsl was -0.207 m. With the top of the oyster patches falling below local mean sea level, oysters are likely underwater for at least half the tidal cycle.

The regressions relating oyster identification with area and perimeter had positive trendlines indicating that regions with larger patches were more accurate. The accuracy for individual test regions varied over a narrow range from 0.65 to 0.92, suggesting that areas with smaller average patch sizes still had a relatively high accuracy in identifying reefs. This is important for oysters in the VCR because the distribution of patch size from the sample of ground-truth oysters indicated that most oyster patches were small, with the 50th percentile being 11.6 m^2 and 14.5 m for area and perimeter, respectively. Knowing the size distribution of reefs in this area can help indicate the accuracy likely to be attained via LiDAR classification and lead to further understanding of spatial distributions.

Suitable Habitat

The digitized reefs provided a large sample size that was spatially diverse, and therefore likely representative of oyster patches within the VCR. The suitability map created using three environmental variables (elevation, fetch, and water residence time) was successful in identifying areas that are likely to be highly suitable oyster habitat. Suitable water residence time and fetch covered much greater areas than suitable elevation. Individually, suitable elevation defined by land surrounding reefs, reef crests, fetch, and residence time covered approximately 83.2, 32.3, 294.2, and 295.2 km^2 of the total study area, which was 436.4 km^2. The low land cover for suitable habitat when all three variables are considered, 52.4 km^2 or 12.03 % of the area, is therefore limited by suitable elevation, the most restrictive variable. When reef crests are used to determine suitable habitat, the model was even more restrictive describing only 23.1 km^2 as suitable habitat. While it is likely that managers are more interested in the suitability of land without oysters that can be used to further restoration, represented here by the elevation of land surrounding reefs, reef crests also represent substrate which attracts larvae and could be used to consider a more conservative examination of suitable habitat.

Although most ground-truth reefs overlapping with the suitability model were in suitable habitat, a small percent was modeled as less suitable habitat. Unless additional unquantified variables play a significant role in preventing recruitment and growth, this suggests oysters can survive beyond the boundaries set by the model for suitable habitat. The elevation criteria presented here are then likely to be conservative and represents areas that would be most suitable, or prime habitat for oyster restoration. Most of the suitable habitat was located near higher intertidal areas adjacent to mudflats and marshes, and more towards the mainland. In these locations, oysters are likely to experience a greater amount of protection from harsh wave action, explaining why the bays and areas near inlets were less suitable, where high wave energy was likely incompatible with oyster growth (Crimaldi et al. 2002, Reidenbach et al. 2009).

The area of suitable habitat was also compared with a past survey completed by Ross and Luckenbach (2009). This comparison was restricted to the 16 test regions because these represented locations where the LiDAR data was capable of accurately identifying oyster reefs. Comparing the total model area with the survey would not accurately reflect the agreement between the two datasets. For reefs within the entire modeled area, there was a significant difference in the elevation of the reefs with those surveyed by Ross and Luckenbach, which typically were much lower in elevation than those in this study, where mean patch elevations were -0.85 and -0.31 m NAVD88, respectively. These lower reefs were likely located in areas that are subtidal or under water during the majority of the tidal cycle. While some of the reefs included in the survey by Ross and Luckenbach (2009) may not have been visible on our dataset, others may no longer exist. When ground-truth tracks were taken for this study, some areas indicated as reef on their map no longer existed. There may have been oyster cover at these locations in the past, but our analysis suggests that these regions are not the most suitable for oyster growth and survival. Nonetheless, the comparisons drawn between the two data sets should be viewed with caution. Differences between the data sets show the challenges in surveying intertidal environments and how differing surveying techniques and sources of remotely sensed data can cause deviations in the ephemerally exposed areas, such as intertidal oyster reefs.

The VCR is a dynamic environment where the landscape is continuously changing due to external drivers and internal feedbacks (McGlathery et al. 2013). Areas that may have been suitable environment for oysters in the past, may have been transformed between the time that data were collected for this study and that by Ross and Luckenbach (2009). Historic documentation described that oysters covered a much greater area (Schulte 2017), supporting that a greater land area was favorable for habitat.

Many current restoration projects in coastal lagoons primarily seek to restore intertidal oyster reefs at higher elevations because they promote greater recruitment and growth (Schulte et al. 2009) while also adding coastal protection (Piazza et al. 2005, Borsje et al. 2011, Scyphers et al. 2011, Wiberg et al. 2019). Our results should prove useful in choosing locations for future projects with these goals. While the majority of the surveyed reefs were within suitable land area, the model also showed that total suitable habitat within the 16 test areas was 1.44 km^2, and within this habitat the total surveyed reef area was only 0.14 km^2. Therefore, the surveyed reefs only comprised about 10% of potential suitable habitat for oysters. Across the entire VCR region, spanning approximately 100 km of coastline, there may be various locations suitable for future oyster restoration.

ACKNLOWLEDGEMENTS

We would like to thank the staff of the Anheuser-Busch Coastal Research Center for field assistance and local expertise. This research was funded by the National Science Foundation to the Virginia Coast Reserve Long Term Ecological Research program (Grant #1832221).

LITERATURE CITED

Agyemang TK, Heblinski J, Schmieder K, Sajadyan H, Vardanyan L (2011) Accuracy assessment of supervised classification of submersed macrophytes: the case of the Gavaraget region of Lake Sevan, Armenia. Hydrobiologia 661:85-96

Ahokas E, Kaartinen H, Hyyppa J (2003) A quality assessment of airborne scanner data. Int Arch Photogramm Remote Sens 34: 1-7

Allen YC, Wilson CA, Roberts HH, Supan J (2005) High resolution mapping and classification of oyster habitat in nearshore Louisiana using sidescan sonar. Estuaries 28:435-446

Bahr LM (1976) Energetic aspects of the intertidal oyster reef community at Sapelo Island Georgia USA. Ecology 57: 121-131

Bahr LM, Lanier WP (1981) The ecology of intertidal oyster reefs of the South Atlantic coast: a community profile. U.S. Fish and Wildlife Service, Office of Biological Services, Washington, D.C. FWS/OBS-81/15 105 pp.

Baltsavias EP (1999) Airborne laser scanning: basic relations and formulas. ISPRS J Photogramm Remote Sens 54: 199-214

Bartol IK, Mann R, Luckenbach M (1999) Growth and mortality of oysters (*Crassostrea virginica*) on constructed intertidal reefs: effects of tidal height and substrate level. J Exp Mar Bio Eco 237:157-184

Borsje BW, van Wesenbeeck BK, Dekker F, Paalvast P, Bouma TJ, van Katwijk MM, De Vries MB (2010) How ecological engineering can serve in coastal protection. Ecol Eng 37: 113-122

Bushek D (1988) Settlement as a major determinant of intertidal oyster and barnacle distributions along a horizontal gradient. J Exp Mar Bio Ecol 122: 1-18

Byers JE, Grabowski JH, Piehler MF, Hughes A, Weiskel HW, Malek JC, Kimbro DL (2015) Geographic variation in intertidal oyster reef properties and the influence of tidal prism. Limnol Oceanogr 60:1051-1063

Cekada MT, Crosilla F, Josmatin-Fras M (2009) A simplified analytical model for a-priori Lidar point-positioning error estimation and a review of Lidar error sources. Photogramm Eng Remote Sensing 75: 1425-1439

Choe BH, Kim D, Hwang JH, Oh Y, Moon WM (2012) Detection of oyster habitat in tidal flats using multi-frequency polarimetric SAR data. Estuar Coast Shelf Sci 97:28-37

Chust G, Galparsoro I, Borja A, Franco J, Uriarte A (2008) Costal and estuarine habitat mapping, using LiDAR height and intensity and multi-spectral imagery Estuar Coast Shelf Sci 78:633-643

Coen LD, Brumbaugh RD, Bushek D, Grizzle R, Luckenbach MW, Posey MH, Powers SP, Tolley SG (2007) Ecosystem services related to oyster restoration. Mar Ecol Prog Ser 341: 303-307

Colden AM, Lipcius RN (2015) Lethal and sublethal effects of sediment burial on the eastern oyster *Crassostrea virginica*. Mar Ecol Prog Ser 527: 105-117

Colden AM, Latour RJ, Lipcius RN (2017) Reef height drives threshold dynamics of restored oyster reefs. Mar Ecol Prog Ser 582: 1-17

Congalton RG (1991) A review of assessing the accuracy of classifications of remotely sensed data. Remote Sens Environ 37:35-46

Crimaldi JP, Thompson JHR, Lowe RJ, Koseff JR (2002) Hydrodynamics of larval settlement: The influence of turbulent stress events at potential recruitment sites. Limnol and Oceanogr 47: 1137-1151

Dewberry (2016) Eastern shore Virginia QL2 LiDAR BAA. Report Produced for US Geological Survey. USGS Contract:G10PC00013. Task Order G15PD00284. https://coast.noaa.gov/htdata/lidar2_z/geoid18/data/8445/supplemental/va2015_usgs_eastern_shore_m8445_project_report.pdf

Dumbauld BR, Kauffman BE, Trimble AC, Ruesink JL (2011) The Willapa Bay oyster reserves in Washington State: fishery collapse, creating a sustainable replacement, and the potential for habitat conservation and restoration. J Shellfish Res 30(1):71-83

Fodrie FJ, AB Rodriguez, CJ Baillie, MC Brodeur, SE Coleman, RK Gittman, DA Keller, MD Kenworthy, AK Poray, JT Ridge, EJ Theuerkauf, Lindquist NL (2014) Classic paradigms in a novel environment: inserting food web and productivity lessons from rocky shores and saltmarshes into biogenic reef restoration. J Appl Ecol 51:1314-1325

Fuchs HL, Hunter EJ, Schmitt EL, Guazzo RA (2013) Active downward propulsion by oyster larvae in turbulence. J Exp Bio 216:1458-1469

Garono RJ, Simenstad CA, Robinson R, Ripley H (2004) Using high spatial resolution hyperspectral imagery to map intertidal habitat structure in Hood Canal, Washington, USA. Can J Rem Sens 30:54-63

Gesch, DB (2009) Analysis of lidar elevation data for improved identification and delineation of lands vulnerable to sea-level rise. Journal of Coastal Research: Special Edition. 53:49-58

Green K, Lopez C (2007) Using object-oriented classification of ADS40 data to map the benthic habitats of the state of Texas. Photogramm Eng Remote Sensing 73: 861-865

Grizzle RE, Adams JR, Walters LJ (2002) Historical changes in intertidal oyster (*Crassostrea virginica*) reefs in a Florida lagoon potentially related to boating activities. J Shellfish Res 21:749-756

Halls J, Costin K (2016) Submerged and emergent land cover and bathymetric mapping of estuarine habitats using WorldView-2 and LiDAR imagery. Remote Sens 8:718

Hendriks IE, van Duren LA, Herman PMJ (2006) Turbulence levels in a flume compared to the field: Implications for larval settlement studies. J Sea Res 55:15-29

Hirzel A, Guisan A (2002) Which is the optimal sampling strategy for habitat suitability modelling. Ecol Modell 157:331-341

Hodgson ME, Bresnahan P (2004) Accuracy of airborne Lidar-derived elevation: empirical assessment and error budget. Photogramm Eng Remote Sensing 70: 331-339

Hubbard AB, Reidenbach MA (2015) Effects of larval swimming behavior on the dispersal and settlement of the eastern oyster *Crassostrea virginica*. Mar Ecol Prog Ser 535:161-176

Ishiguro S, Yamada K, Yamakita T, Yamano H, Oguma H, Matsunaga T (2016) Classification of seagrass beds by coupling airborne LiDAR bathymetry data and digital aerial photographs. In: Nakano S, Yahara T, Nakashiuka T (eds) Aquatic Biodiversity Conservation and Ecosystem Services. Ecol Res Monogr Springer, Singapore

Kemp WM, Boynton WR, Adolf JE, Boesch DF, Boicourt WC, Brush G, Cornwell JC, Fisher TR, Glibert PM, Hagy JD, Harding LW, Houde ED, Kimmel DG, Miller WD, Newell RIE, Roman MR, Smith EM, Stevenson JC (2005) Eutrophication of Chesapeake Bay: historical trends and ecological interactions. Mar Ecol Prog Ser 303:1-29

Le Bris A, Rosa P, Lerouxel A, Cognie B, Gernez P, Launeau P, Robin M, Barille L (2016) Hyperspectral remote sensing of wild oyster reefs. Estuar Coast Shelf Sci 172:1-12

Lenihan HS (1999) Physical-biological coupling on oyster reefs: how habitat structure influences individual performance. Ecol Monogr 69:251-275

Lipcius RN, Burke RP, McCulloch DN, Schreiber SJ, Schulte DM, Seitz RD, Shen J (2017) Overcoming restoration paradigms: value of the historical record and metapopulation dynamics in native oyster restoration. Front Mar Sci 2:65 doi.org/10.3389/fmars.2015.00065

Marion C, Anthony EJ, Trentesaux A (2009) Short-term (<2yrs) estuarine mudflat and saltmarsh sedimentation: high-resolution data from ultrasonic altimetery, rod surface-elevation table, and filter traps. Estuar Coast Shelf Sci 83:475-484

May NC, Toth CK (2007) Point positioning accuracy of airborne LiDAR systems: a rigorous analysis. Int Arch Photogramm Remote Sens 36 (3/W49B)

McGlathery KJ, Reidenbach MA, D’Odorico P, Fagherazzi S, Pace ML, Porter JH (2013) Nonlinear dynamics and alternative stable states in shallow coastal systems. Oceanography 26:220-231

Morgan JL, Gergel SE, Coops NC (2010) Aerial Photography: a rapidly evolving tool for ecological management. BioScience 60:47-59

Morris JT, Porter D, Neet M, Noble PA, Schmidt L, Lapine LA, Jensen JR (2005) Integrating LiDAR elevation data, multi-spectral imagery and neural network modeling for marsh characterization. Int J Remote Sens 26:5221-5234

O’Beirn FX, Heffernan PB, Walker RL (1995) Preliminary recruitment studies of the eastern oyster, *Crassostrea virginica*, and their potential applications, in coastal Georgia. Aquaculture 136:231-242

Ortega S (1981) Environmental stress, competition, and dominance of *Crassostrea virginica* near Beaufort, North Carolina, USA. Mar Bio 62:47-56

Piazza BP, Banks PD, La Peyre MK (2005) The potential for created oyster shell reefs as a sustainable shoreline protection strategy in Louisiana. Restor Ecol 13:499-506

Pittman SJ, Costa BM, Battista TA (2009) Using LiDAR bathymetry and boosted regression trees to predict the diversity and abundance of fish and corals. J Coast Res SI 53:27-38

Reidenbach MA, Koseff JR, Koehl MAR (2009) Hydrodynamic forces on larvae affect their settlement on coral reefs in turbulent, wave-driven flow. Limnol Oceanogr 54:318-330

Reidenbach MA, Berg P, Hume A, Hansen JCR, Whitman ER (2013) Hydrodynamics of intertidal oyster reefs: the influence of boundary layer flow processes on sediment and oxygen exchange. Limnol Oceanogr 3:225-239

Richardson, D (oysters2013) Tidal datum conversion grids for the Eastern Shore of Virginia and surrounding waters (2013). Virginia Coast Reserve Long-Term Ecological Research Project Data Publication knb-lter-vcr.219.5 (doi:10.6073/pasta/aeb2fe3192348fe201bd6252b64a3af7)

Ross PG, Luckenbach MW (2009) Population assessment of eastern oysters (Crassostrea virginica*)* in the seaside coastal bays. Virginia Coastal Zone Management Program, Virginia Department of Environmental Quality, Richmond Virginia

Rothschild BJ, Ault JS, Goulletquer P, Jensen WP, Heral M (1994) Decline of the Chesapeake Bay oyster population: a century of habitat destruction and overfishing. Mar Ecol Prog Ser 111:29-39

Safak I, Wiberg PI, Richardson DL, Kurum MO (2015) Controls on residence time and exchange in a system of shallow coastal bays. Cont Shelf Res 97:7-20.

Schenk T, Csatho B (2002) Fusion of LiDAR data and aerial imagery for a more complete surface description. Int Arch Photogramm Remote Sense 34:310-317

Schill SR, Porter DE, Coen LD, Bushek D, Vincent J (2006) Development of an automated mapping Technique for monitoring and managing shellfish distributions. NOAA/UNH Cooperative Institute for Coastal and Estuarine Environmental Technology (CICEET*)*

Schmid KA, Hadley BC, Wijekoon N (2011) Vertical accuracy and use of topographic LiDAR data in coastal marshes. J of Coast Res 27:116-132

Schulte DM (2017) History of the Virginia oyster fishery, Chesapeake Bay, USA. Front Mar Sci https://doi.org/10.3389/fmars.2017.Schule

Schulte DM, Burke RP, Lipcius RN (2009) Unprecedented restoration of a native oyster metapopulation. Science 325:1124-1128

Scyphers SB, Powers SP, Heck KL, Byron D (2011) Oyster reefs as natural breakwaters mitigate shoreline loss and facilitate fisheries. PLOS ONE 6(8): e22396

Smith GF, Bruce DG, Roach EB (2001) Remote acoustic habitat assessment techniques used to characterize the quality and extent of oyster bottom in the Chesapeake Bay. Mar Geod 24:171-189

Smith G, Yesilnacar E, Jiang J, Taylor C (2015) Marine habitat mapping incorporating both derivatives of LiDAR data and hydrodynamic conditions. J Mar Sci Eng 3:492-508

Story M, Congalton G (1986) Accuracy assessment: A user's perspective. Photogramm Eng Remote Sensing 52:397-399

Theuerkauf SJ, Lipcius RN (2016) Quantitative validation of a habitat suitability index for oyster restoration. Front Mar Sci 3: 63 doi: 10.3389/fmars.2016.00064

Van der Zee EM, van der Heide T, Donadi S, Eklof JS, Eriksson BK, Olff H, van der Veer HW, Piersma T (2012) Spatially extended habitat modification by intertidal reef-building bivalves has implications for consumer-resource interactions. Ecosystems 15(4):664-673

Wesson J, Mann R, Luckenbach M (1999) Oyster restoration efforts in Virginia. In: Luckenbach MW, Mann R, Wesson JA (eds) Oyster Reef Habitat Restoration: A Synopsis and synthesis of Approaches. Virginia Institute of Marine Science Press, Gloucester Point, VA, 117-129.

Whitman ER, Reidenbach MA (2012) Benthic flow environments affect recruitment of *Crassostrea virginica* larvae to an intertidal oyster reef. Mar Ecol Prog Ser 463:177-191

Wiberg P, Taube SR, Ferguson AE, Kremer MR, Reidenbach MA (2019) Wave attenuation by oyster reefs in shallow coastal bays. Estuar Coasts 42:331-347

CHAPTER 3: Utilizing airborne LiDAR data to quantify marsh edge morphology and the role of oyster reefs in mitigating marsh erosion

In Press at *Marine Ecology Progress Series* as:
Hogan S, Wiberg PL, Reidenbach MA (2021) Utilizing airborne LiDAR data to quantify marsh edge morphology and the role of oyster reefs in mitigating marsh erosion, Mar Ecol Prog Ser, in press.

ABSTRACT

Marsh habitats, experiencing accelerated change, require accurate monitoring techniques. Therefore, we developed methods to quantify marsh edge morphology using airborne LiDAR data. We then apply these methods within the context of oyster reef restoration within the shallow coastal bays of Virginia, USA by comparing retreat and morphology quantified at paired reef-lined and control marsh edges at ten different marsh sites. Retreat metrics were analyzed between 2002 and 2015, utilizing a LiDAR derived edge for the year 2015 from points of maximum slope and aerial imagery pre-2015. Retreat was also compared before and after oyster reef restoration to determine if reefs slow erosion. We found that slope statistics from airborne LiDAR elevation data can accurately capture marsh edge morphology. Retreat rate, measured at edges typically found near the vegetation line, was not significantly different between reef-lined and control marshes and ranged from 0.14 to 0.79 m yr^{-1}. Both retreat rate (ρ = -0.90) and net movement (ρ = -0.88) were strongly correlated to marsh edge elevation. Exposed control marshes had significantly greater mean and maximum slope values compared to reef-lined marshes. The mean edge slope for exposed marshes was 11.4^{o} and for reef-lined marshes was 6.0^{o}. We hypothesize that oyster reefs are causing an elongation of the marsh edge by reducing retreat at lower elevations of the marsh edge. Therefore, changes in marsh edge morphology

may be a precursor to changes in marsh retreat rates over longer timescales and emphasizes the need for repeated LiDAR measurements to capture processes driving marsh edge dynamics.

Keywords: marsh edge, morphology, LIDAR, oyster reefs, retreat

INTRODUCTION

Remote Sensing of Marshes

Conservatively, 1-2% of marshes are lost per year (Duarte et al. 2008), with loss accelerating over the last two centuries (Davidson 2014). Although it has been found that marshes may be able to keep pace with sea level rise in the vertical dimension (Blum et al. 2021), marsh edge erosion in the lateral dimension reduces areal marsh platform habitat (Kirwan et al. 2010, Mariotti & Fagherazzi 2013). For marshes found along coastal bays, lateral migration that is associated with eroding edges has been recorded at rates greater than 1 m yr^{-1} (Kastler & Wiberg 1996, Day et al. 1998, McLoughlin et al. 2015). These rates are likely affected by edge morphology, where different erosional processes are responsible for transporting sediment (Van de Koppel et al. 2005, Leonardi et al. 2016a).

To determine marsh edge characteristics and their rates of change, it is necessary to have an accurate means for measuring and monitoring spatial morphology. Remote sensing is increasingly being utilized for topographic analyses of marshes and proves advantageous over other surveying techniques by providing a method for non-invasive data collection that also produces robust, accurate datasets (Schenk & Csatho 2002). Specifically, the creation of digital elevation models (DEMs) through Light Detecting and Ranging (LiDAR) surveys has been useful for characterizing marshes at broader scales than surface elevation tables and erosion markers can capture (Mattheus et al. 2010). Other derivatives of elevation, such as slope, aspect, and curvature, have been fundamental in remotely sensing the characteristics of various landscapes (Glenn et al. 2006). Because change in ocean shorelines using LiDAR has been largely successful (Stockdon et al. 2002), this technology is likely to be useful in analyzing marsh edges as well. While previous studies have largely relied on aerial imagery to capture horizontal change in marsh edge location (e.g. Kastler & Wiberg 1996, McLoughlin et al. 2015, Leonardi et al. 2016a), this imagery cannot readily provide information about marsh edge elevation and steepness. LiDAR elevation mapping of salt marshes has been largely successful at classifying vegetation types (Morris et al. 2005, Hladik et al. 2013) and geomorphic features (Millette et al. 2010, Chassereau et al. 2011, Chirol et al. 2018), although there can be elevation errors in regions of dense vegetation owing to reduced laser penetration (Schmid et al. 2011, Medieros et al. 2015). LiDAR has also been used to monitor marsh edge retreat and volumetric accretion rates (Mattheus et al. 2010, Zhao et al. 2017). However, few studies have utilized remote sensing to describe marsh margins compared to those describing platform elevations and vegetation (Goodwin & Mudd 2020). Within marsh margin studies, both in-situ and remote sensing methods have been developed to locate marsh edges based on elevation and slope measurements (Goodwin et al. 2018, Farris et al. 2019, Goodwin & Mudd 2020). Goodwin and Mudd (2020) showed that airborne LiDAR data with a resolution of 1 m^2 can be used to adequately locate marsh margins in macrotidal settings. With repeated measures, detailed quantification of erosional processes such as those accomplished for other coastal shorelines (White & Wang 2003, Obu et al. 2017) are likely feasible for marsh edges. However, the utility of LiDAR-based topographic analysis of marsh edge morphology and retreat rates in microtidal systems remains to be verified.

Marsh Edge Processes

Marsh edge morphologies vary widely ranging from sharp cliff faces to gently sloping edges (Allen 2000, Tonelli et al. 2010, McLoughlin et al. 2015). The different morphologies are largely influenced by the local erosional processes taking place. These processes are dependent on tidal water level relative to platform elevation because it affects where and how tidal and wave energy is received. Elevation can dictate if breaking wave action or bottom shear stresses over adjacent tidal flats is more important in defining edge morphology (Tonelli et al. 2010, Francalanci et al. 2013). Three different erosional processes have been described in shaping marsh edge morphology in shallow coastal environments, including those found along the mid-Atlantic region of the USA (McLoughlin 2010, Priestas et al. 2015). The first process is undercutting and toppling. This occurs when sediment is more quickly eroded from the lower layers of substrate resulting in a platform overhang, which eventually bends and topples creating sharp, vertical scarps (Schwimmer 2001, Tonelli et al. 2010, Francalanci et al. 2013). This occurs most often where sediment is sandy and less cohesive. Secondly, root scalping occurs when waves break at elevations similar to the platform and weak areas in the vegetation mat detach, leaving the underlying sediment susceptible to erosion (Priestas et al. 2015). This can lead to a terrace or step-like marsh edge morphology. Lastly, bioerosion influences morphology where burrowing organisms are present in sufficient densities to weaken sediment causing cracks that widen and lead to block detachment (Schwimmer 2001) and sharp scarps. Marsh edges characterized by undercutting or crack formation are likely to be more prone to failure and rapid retreat, compared to terraced or gently sloping marsh edges where flow-generated bottom shear stresses entrain sediment at a slower rate (Francalanci et al. 2013).

Marsh Edge and Oyster Reef Coupling

Often found near marsh edges, oyster reefs are thought to behave as a coupled dynamical system with adjacent marshes (McGlathery et al. 2013). Therefore, the presence of oyster reefs, and the hard, stable substrate they form, may be a crucial component shaping marsh edge characteristics. Oysters reefs themselves can have different morphologies depending on the tidal-driven current and wave environment (Bahrs & Lanier 1981, Lenihan 1999), including those running either parallel or perpendicular to shorelines (fringe reefs) as wells as, irregular mounds found further from shore (patch reefs). These differences can be important because it is well established that oyster reefs can change the hydrodynamic energy in estuarine environments by increasing drag on the flow (Dame & Patten 1981, Whitman & Reidenbach 2012, Volaric et al. 2020) and attenuating wave energy (Chowdhury et al. 2019, Wiberg et al. 2019). Concurrently, oyster reefs also stabilize estuarine sediments by reducing resuspension and encouraging deposition of fine particles (Meyer et al. 1997, Reidenbach et al. 2013, Colden et al. 2016,). Combined, these environmental alterations suggest that oyster reefs can help mitigate marsh edge erosion. Erosion rates measured at marsh edges along the south and east coasts of the United States have shown that oyster reefs, especially in low wave energy environments, can have mitigative effects on erosion (Meyer et al. 1997, Piazza et al. 2005). Because oysters within Virginia's coastal bays are primarily intertidal (Hogan & Reidenbach 2019), the ability of oyster reefs to alter both the local mean flow (Volaric et al. 2018) and wave energy (Wiberg et al. 2019) varies as water depth changes due to tides. Wave dissipation is most effective when water depth over the reefs is relatively shallow (Chowdhury et al. 2019, Wiberg et al. 2019).

Study Objectives

The goal of this study is to first develop a general methodology using airborne LiDAR elevation data to accurately locate and characterize marsh edges bordering coastal bays in a microtidal environment using slope statistics. We then apply these methods to investigate if there are observable differences in marsh edge retreat and morphology at marshes both exposed to open water and those located behind natural and restored oyster reefs. To examine whether retreat is affected by oyster reef restoration, we build on a dataset of digitized shorelines from aerial imagery for mainland marshes from 2002 and 2009 (McLoughlin et al. 2013) and compare these to LiDAR collected in 2015 to analyze retreat for various marsh edges within Virginia, U.S.A. coastal bays. We quantify rate of retreat for reef-lined and control locations and rate of retreat before and after reef construction. Additionally, we compare marsh edge morphology for these same sites using the derived slope statistics. We then use the data to determine what relationships exist between marsh edge morphology and the physical environment to determine factors that can make marshes more vulnerable to retreat.

MATERIALS & METHODS

Study Site

The marshes and oyster reefs considered in this study are located within the Virginia Coast Reserve (VCR) on the eastern side of the Delmarva Peninsula, Virginia, USA. The VCR is a National Science Foundation Long-term Ecological Research (LTER) site encompassing over 100 km of coastline and coastal bays (Figure 3.1). The VCR contains many diverse coastal habitats including salt marshes, oyster reefs, and mudflats. Oysters in the VCR are of the species *Crassostrea virginica* and found largely in the intertidal zone. The coastal bays experience a mean tidal range of approximately 1.2 m with limited freshwater input (Marotti & Fagherazzi 2013). Narrow inlets through barrier islands connect the bays to the Atlantic Ocean and create a gradient of flushing and water residences times (Safak et al. 2015). Winds are dominantly from the north-northeast direction in winter and from the south in summer (Wiberg et al. 2019) and wave-driven erosion has been found to be the primary driver of marsh migration within these shallow coastal bays (Tonelli et al. 2010, Mariotti & Fagherazzi 2013, Leonardi et al. 2016b). Wave energy impacting the marsh edge depends on a combination of water depth, fetch distance, wind direction, and drag imposed along the seafloor (Fagherazzi & Wiberg 2009).

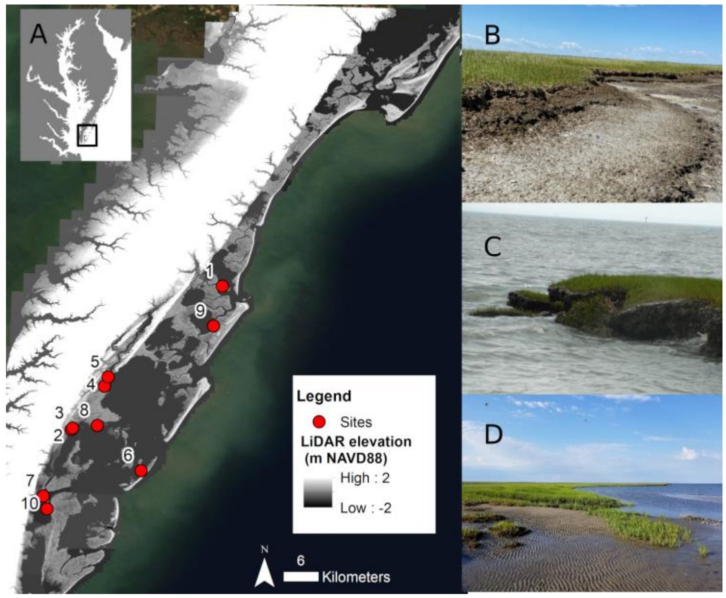

Figure 3.1. A) Marsh sites located in the Virginia Coast Reserve. At each site both a control and reef-lined marsh edge were located for analysis. On the right, examples of marshes with B) terraced, C) scarped, and D) ramped morphologies found in the VCR are shown. Photo credit for C & D: Qingguang Zhu, UVA

Method Development: LiDAR-Based Classification of Marsh Edges

A USGS airborne LiDAR dataset covering the extent of the VCR was collected in 2015 (Dewberry 2016) and was used to classify land area and locate marsh edges. The LiDAR elevation dataset was converted into a raster with pixel dimensions of 0.76 m x 0.76 m and projected in World Geodetic System 1982 (WGS84) Universal Transverse Mercator (UTM) Zone 18 and the North American Vertical Datum (NAVD88). It has 95% confidence values for vertical accuracy of 12.5 cm for non-vegetated and 17.7 cm for vegetated terrain (Dewberry

2016). Each surveying flight was conducted within two hours of low tide, however, some intertidal features were still underwater and were assigned (i.e., hydroflattened) to the level of the water surface elevation. From preliminary investigation of the LiDAR elevations, we found that the LiDAR survey captured the transition of many marsh platforms into surrounding mudflats, making identification of marsh edge location and morphology possible.

To determine if marsh edge morphology and retreat are affected by adjacency to oyster reefs, ten different marsh edges with fringing oyster reefs or adjacent to patch oyster reefs

Table 3.1. Metadata for the paired locations including site, marsh type (A = reef-lined, B = control), local reef name, edge length, type of restoration, shape, year restored, acres of reef (N/A ‘not applicable’ describes control sites where there are no reefs present, therefore no acreage), pixel count, the mean and standard deviation of slope extracted to each buffer area, and for reef-lined marshes the mean reef crest elevation relative to North American Vertical Datum (NAVD88) and local mean sea level (lmsl). For patch reefs surveyed 2008, the acreage represents the area of reefs within 40 m from the digitized edge.

Marsh Type	**Local reef name**	**Edge Length (m)**	**Type**	**Shape**	**Year**	**Acreage**	**Pixel Count**	**Mean**	**Std**	**Reef elevation (m NAVD88/m lmsl)**
A	Black Rock	175	shell	fringe	2010	0.88	5800	2.34	1.82	-1.0 /-0.91
B		175	control	control	N/A	N/A	5964	4.11	5.74	
A	Boxtree1	115	whelk	fringe	2012	0.55	2818	4.10	3.26	-0.98/-0.89
B		115	control	control	N/A	N/A	2998	5.25	3.15	
A	Boxtree2	120	whelk	fringe	2012	0.54	3388	3.90	3.02	-0.88/-0.77
B		120	control	control	N/A	N/A	3634	4.17	3.23	
A	Brownsville	180	shell	fringe	2010	0.73	5225	3.24	2.42	-0.53/-0.44
B		180	control	control	N/A	N/A	4892	3.76	3.41	
A	Cob	290	shell	fringe	2005	1.62	7500	1.64	0.97	-0.55/-0.44
B		290	control	control	N/A	N/a	9946	2.23	1.89	
A	Fowling Point	225	natural	patch	Before 2008	0.76	7607	2.23	1.82	-0.44/-0.34
B		225	control	control	N/A	N/A	7538	3.71	1.89	
A	Hillcrest	170	natural	patch	Before 2008	2.5	6109	2.31	1.69	-0.71/-0.67
B		170	control	control	N/A	N/A	6392	1.75	1.02	
A	Outlet	150	shell	patch	2008	0.78	6090	1.46	0.70	-0.46/-0.36
B		150	control	control	N/A	N/A	5356	3.37	3.25	
A	Paramore	175	shell	fringe	2008	1.04	6144	1.60	1.128	-0.91/-0.82
			shell	patch	2010	2.58				
B		175	control	control	N/A	N/A	4649	4.62	4.023	
A	Point of rocks	200	shell	patch	2010	0.97	7474	2.12	1.76	-0.47/-0.36
B		200	control	control	N/A	N/A	7484	3.81	3.56	

(within approximately 20 m of visible land) were chosen for investigation, referred to as reef-lined marshes (Table 3.1, Figure 3.1). For each site, we paired the reef-lined marsh with a nearby reference marsh, referred to as control, without an adjacent reef but having the same shoreline orientation. Edges varied in length between approximately 100 to 300 m. A point and shapefile dataset provided by The Nature Conservancy was used to locate areas of restored reefs with known build dates. The reefs include a combination of fringe and patch reefs restored using either deposited oyster or whelk shell. Build dates span from 2003 – 2019, forming 62 reefs covering a total of 51.8 acres. Two additional reef locations (Site 6 and Site 7, Table 3.1) from a 2008 NOAA funded survey of oyster reefs (Ross & Luckenbach 2009) were included to supplement the restored reef data. Patches within 40 m of a marsh edge were included in reef acreage for these two locations (Table 3.1). Many of these patch reefs are now considered ‘reference’ or ‘natural’ because of their decades old age, though all reefs in the region have been impacted by human activity and they were likely restored in some capacity through protective efforts. Additional details on edges and associated reefs are found in Table 3.1. Only reefs restored prior to 2015, when LiDAR elevation data was acquired, were included in this analysis. Restored reefs allowed us to place a date on the reefs and test for their ability to provide coastal protection. For each pair of edges, a marsh edge was first digitized where the scarp was visible on the elevation layer at resolution 1:1000. Approximately the same length of edge was digitized for both control and reef-lined marshes at each site, although length varied by site to conform to oyster coverage.

Marsh surface slope was calculated using the 3D Analyst Slope tool in ArcMap 10.5 after removal of hydroflattened elevations which were identified locally as pixels with a constant minimum low elevation extending to the bay. The tool employs the average maximum technique with 8 neighbors around a center cell to find the maximum rate of elevation change, where the expression:

$$\text{slope degrees} = \left(\tan^{-1}\sqrt{\frac{dz^2}{dx}+\frac{dz^2}{dy}}\right) * \frac{180}{\pi}$$

is used to calculate the degree of slope at each pixel using data from the 8 neighboring pixels.

At each marsh, we used the Linear Sampling toolbox added to ArcMap 10.5 to cast perpendicular transects 5 m apart extending 10 m in each direction from the digitized edge and extracted terrain slope data every meter along each transect. For each transect, we found the point of maximum slope, and used that as a proxy for the marsh edge in 2015 (Figure 3.2). The mean of these values was calculated to give an average edge slope for each marsh.

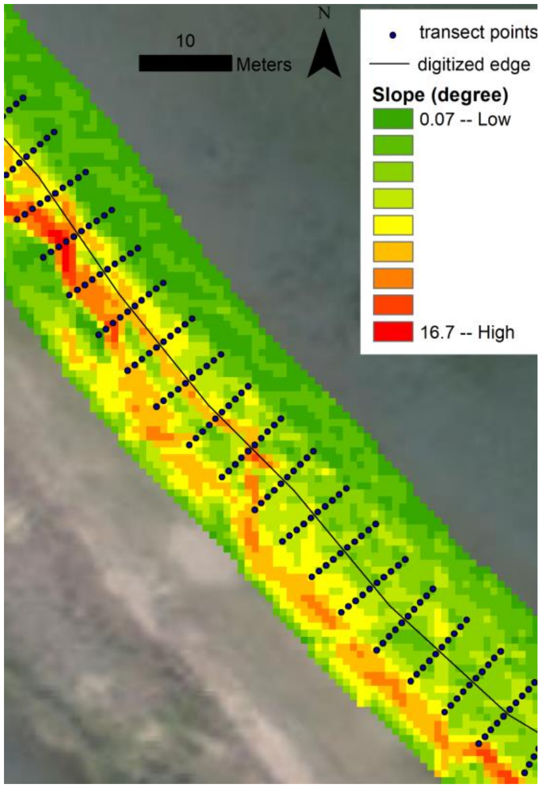

Figure 3.2. Slope data within the buffer area region for site 6B, a control marsh edge. Low to high values of slope (degree) and shown from green to red. The in-situ surveyed edge is shown in black, with perpendicular transects cast every 5 m with points every 1 m where slope data was extracted to locate the marsh edge.

Additionally, a 10 m buffer was created around each edge and slope data was extracted to determine the mean slope in the buffer area around the edge using the zonal statistics tool (Figure 3.2). Zonal statistics extract the data from each pixel within a given polygon to calculate statistics for an area. This can be useful to describe marsh edges that are more ramped, or terraced, and not well described by just a single edge location. It also allows for a repeatable method of determining slope at each marsh. These 10 m buffer locations are referred to as ‘buffer areas’.

To validate the utility of using airborne LiDAR for characterizing marsh edge morphology in a microtidal system, we compared remotely-sensed marsh elevation and edge descriptions with measured in-situ data obtained in 2010 (McLoughlin 2010). The in-situ edge surveys were obtained with a Trimble R8 GNSS System for 5 edges at 4 different marshes located within Hog Island Bay, Virginia. We recreated elevation profiles extending from the mudflat into the marsh platform for multiple transects at each marsh edge and compared the modeled and in-situ elevation profiles and morphologic descriptions with extracted slope statistics. Although there was a time difference of 5 years between datasets, the use of a stable marsh edge and marsh platforms allowed for comparisons to be made.

Quantifying Marsh Edge Retreat and Morphology Occurring at Reef-Lined and Control Marshes

Marsh site selection and physical environments

We compared the elevations between reef-lined marsh and control marsh locations at each site to determine if the two marshes were well paired and determine the drivers of retreat and morphology by extracting elevation to 10 m buffer areas (See Method development above). Elevations are reported in meters NAVD88. Platform elevation, taken to be the mean of the maximum point of elevation along transects spaced every 5 m along the digitized edge, and marsh edge elevation, the elevation at the point of maximum slope along transects, were analyzed (See Method development, Figure 3.2).

Wave exposure along the marsh edge was estimated using the local fetch distance. Fetch was previously modeled for the VCR in ArcMap 9.2 using scripts from USGS (Kremer & Reidenbach 2021). Mean fetch for summer 2015 was made into a raster grid of 30 x 30 m pixels, after being weighted by the proportion of time wind came from each direction. Direction was based on 10º increments and wind data came from the Wachapreague NOAA station (Kremer & Reidenbach 2021). Fetch data was extracted to each buffer area and the mean value was used to represent each location. Where the previously modeled fetch dataset did not cover the entire buffer area, the average of the partial data was used. In cases where there was no data present, the average of the 3 values nearest the approximate ends and midpoint of the digitized edge were averaged, each within 50 m of the digitized edge.

Marsh retreat

For the five mainland marsh sites (Sites 2, 3, 4, 6, & 7, Figure 3.1), we quantified changes in marsh edge position between the years 2002, 2009, and 2015. These dates were chosen because mainland marshes were previously digitized in the VCR for years 2002 and 2009 from aerial imagery (McLoughlin et al. 2015) and LiDAR was taken in 2015. To compute the marsh edge for 2015 we connected the points of maximum slope (See Method development) along transects at each marsh. The points were manually inspected and edited to account for edge effect discrepancies. To determine marsh retreat, shorelines and baselines edited in ArcGIS ArcMap 10.5 were imported to R. We used digitized shorelines for years 2002, 2009, and 2015. The Analyzing Boundary Movement Using R (AMBUR) package in R was used to assess marsh edge movement (Jackson et al. 2012). Transects were drawn every 5 m and filtered using a moving window of 5 transects along the length of each marsh (Jackson et al. 2012). The intersections of transects with shorelines were used to calculate and analyze end point rate (EPR m yr^{-1}), which is the rate of shoreline change between the youngest and oldest shorelines, and net change in shoreline movement (NC m) between the years 2002 and 2015. We used a 2-way ANOVA to explain the difference in mean retreat values from 2002 – 2015 with factors including type of marsh edge (reef-lined or control) and site ($\alpha = 0.05$). We also analyzed the rate of retreat before (2002-2009) and after (2009-2015) reef restoration using percent change in EPR and NC. The percent change analysis between time periods was completed where mainland adjacent reefs had known restoration dates after 2009 (Sites 2, 3, & 4). Again, two-way ANOVAs were used with percent change in EPR and NC as dependent variables and marsh type and site as independent variables.

Marsh edge morphology

We used the 10 m radius buffer at each marsh to capture the edge topography for all 10 sites. As previously described (Section Method development), slope statistics were calculated using zonal statistics. Using the transect method (described in Method development), the points representing the slope-defined edge were found and averaged to find the mean edge slope for each marsh. A 2-way ANOVA was used to determine if marsh edge morphology for the buffer area mean slope and mean edge slope were explained by type of marsh (reef-lined or control) and site. To validate the use of a 10 m radius buffer search area, the slope data was compared with results from a smaller, 5 m radius buffer region. We found that although values differed slightly, the same patterns for reef-lined and control marshes were observed for mean, standard deviation, and CV of slope for 5 m and 10 m buffer areas. We used the 10 m buffer areas for analysis because they offer a more complete picture of the marsh and mudflat system.

Drivers of marsh edge retreat and morphology

Spearman's rank correlations were used to examine possible relationships between EPR, NC, and physical (mean fetch, mean platform elevation, and mean edge elevation) and slope variables because of the non-normal distribution of the retreat data. We also analyzed whether mean edge slope and buffer area mean slope, our metrics for marsh edge morphology, were correlated with the physical variables for each location (n = 10). Pearson's correlation methods were used for the normally distributed, continuous variables with one mean value for each location (n = 20).

RESULTS

Method Development: LiDAR-Based Quantification of Marsh Edges

Remotely-sensed airborne LiDAR elevations were strongly correlated with in-situ GPS elevation data ($r^2 = 0.92$, n = 114, Figure 3.A1). Overall, we found that LiDAR and in-situ elevation profiles agreed for the stable marsh and marsh platforms (Figure 3.A2). The comparison of profiles from in-situ (2010) and LiDAR (2015) surveys captures the lateral retreat

Table 3.2. EPR (m yr^{-1}) and NC (m) and standard error (SE) for each marsh from 2002-2015 where marsh type A = reef-lined and B = control.

Site	Marsh Type	Local reef name	EPR (m yr^{-1}) 2002-2015	EPR (m yr^{-1}) SE	NC (m) 2002-2015	NC (m) SE
2	A	Boxtree1	-0.26	0.02	-3.27	0.25
2	B		-0.14	0.01	-1.74	0.17
3	A	Boxtree2	-0.26	0.03	-3.26	0.34
3	B		-0.22	0.04	-2.84	0.45
4	A	Brownsville	-0.74	0.07	-9.4	0.85
4	B		-0.79	0.07	-10.05	0.84
6	A	Fowling Point	-0.29	0.08	-3.58	1.03
6	B		-0.42	0.05	-5.35	0.64
7	A	Hillcrest	-0.28	0.03	-3.62	0.4
7	B		-0.24	0.05	-3.01	0.62

that occurred in 5 years' time. We found the highest buffer area mean slope and edge slopes at the scarped edge marshes and the lowest values at the ramped marsh (Table 3.A1, Figure 3.A3).

Marsh Retreat and Morphology Occurring at Reef-Lined and Control Marsh Edges

Marsh edge retreat

Results for shoreline movement suggested considerable variability in EPR (end point rate m yr^{-1}) and NC (net change m) across the sites for the period from 2002 to 2015 with values ranging from (mean ± se) -0.79 ± 0.07 to -0.14 ± 0.01 m yr^{-1} and -10.05 ± 0.84 to -1.74 ± 0.17 m, respectively (Table 3.2, Figure 3.3, Figure 3.4). The results of the 2-way ANOVAs suggested that there was no significant difference in retreat for reef-lined and control marsh edges for mean EPR (p = 0.91) and mean NC (p = 0.91) from 2002 – 2015 (Figure 3.4). However, there were significant differences in

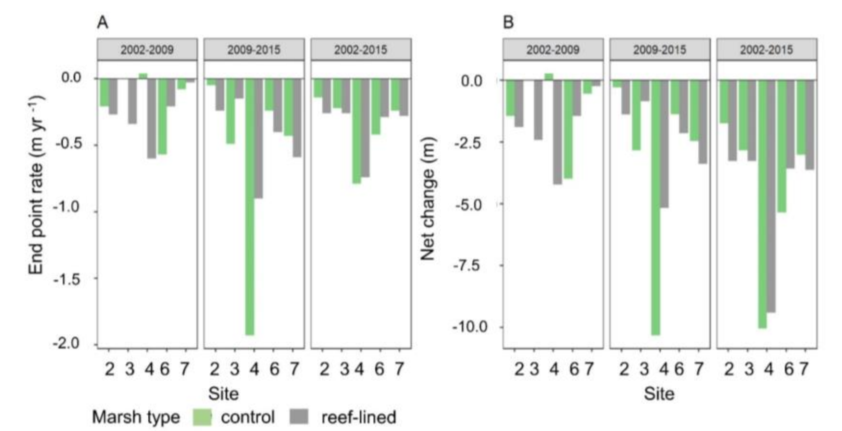

Figure 3.3. Mean EPR (A) and NC (B) at each location for each time period. Grey bars indicate reef-lined marshes and green bars indicate control marshes at each site.

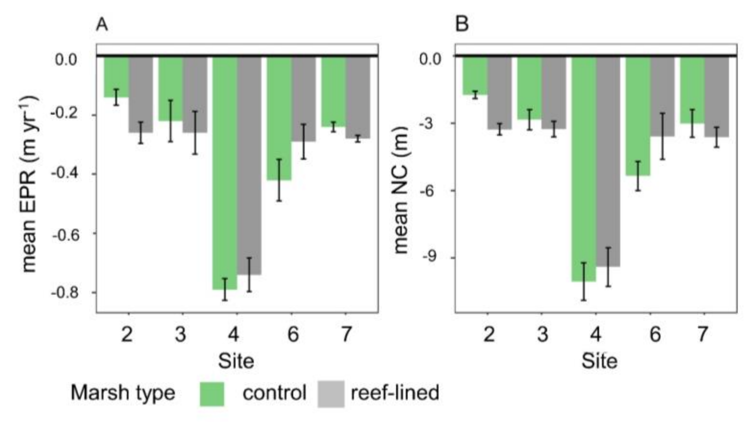

Figure 3.4. A) Mean EPR and B) NC with standard error bars for paired marshes at each site between 2002 – 2015. Grey bars indicate reef-lined marshes and green bars indicate control marshes at each site.

mean EPR ($p < 0.01$) and mean NC ($p < 0.01$) with site, where site 4, Brownsville, experienced significantly greater retreat compared to other sites.

There was no statistically significant difference in percent change of retreat variables for the time periods 2002-2009 and 2009-2015 with marsh type or site for both EPR (p = 0.7, p = 0.5) and NC (p = 0.7, p = 0.5) (Table 3.3). No clear patterns were found in change in retreat for reef-lined and control marshes at these sites. Contrary to our hypothesis, the greatest percent reduction in retreat rate (EPR) and movement (NC) was observed at a control marsh, Site 2B.

Table 3.3. Change and percent change from the periods 2002-2009 and 2009-2015 for end point rate (EPR m yr^{-1}) and net change (NC m) of movement. White fill indicates reduced shoreward movement, while grey indicates increased shoreward movement between the two time periods, where marsh type A = reef-lined and B = control.

Site	Marsh Type	Local Reef Name	EPR (m yr^{-1}) 2002-2009	EPR (m yr^{-1}) 2009-2015	EPR Δ	EPR % Δ	NC (m) 2002-2009	NC (m) 2009-2015	NC Δ	NC % Δ
2	A	Boxtree1	-0.27	-0.24	0.03	-12.5	-1.89	-1.38	0.51	-36.96
2	B		-0.21	-0.05	0.16	-320	-1.45	-0.29	1.16	-400
3	A	Boxtree2	-0.34	-0.15	0.19	-126.67	-2.41	-0.85	1.56	-183.53
3	B		0	-0.49	-0.49	100	0	-2.84	-2.84	100
4	A	Brownsville	-0.6	-0.9	-0.3	33.33	-4.22	-5.17	-0.95	18.38
4	B		0.04	-1.93	-1.97	102.07	0.28	-10.33	-10.61	102.71

Marsh edge morphology

Marsh edges without adjacent oyster reefs (control locations) had a greater buffer area mean slope (p = 0.005), indicating steeper topographies, compared to reef-lined marshes (Figure 3.5). The mean buffer area slope for reef-lined marshes was 2.5º, while that for control marshes was 3.7º. There was no significant difference in mean slope with site (p = 0.07). Similar results were found for edge slope, where control locations had significantly higher edge slope values (p=0.01), compared to reef-lined marsh locations (Figure 3.5), but no significant difference with site (p = 0.5). The mean edge slope for control marsh locations was 11.4º, while the mean for reef-lined marsh locations was 6.0º. The greatest difference, 15.6º, was observed at Site 1, and the smallest was less than 1º at Site 2. Slope statistics (Figure 3.5) largely correspond with marsh edge elevation data (Figure 3.6A), where control marshes have higher elevations and slope values, except for Site 7, where the pattern is reversed, and the higher reef-lined edge also has higher slope values.

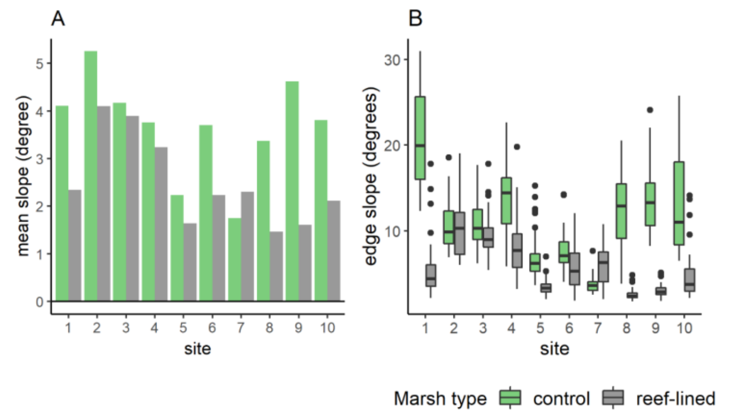

Figure 3.5. A) Mean buffer area slope and B) edge slope at each site for control and reef-lined marsh edges from transects. Grey bars indicate reef-lined marsh edges and green bars indicate control marsh edges at each site. Boxplot components: boxes indicate the interquartile range (IQR) with the interior line representing the median, whiskers the maximum and minimum (up to 1.5 times the IQR range), and dots represent outliers beyond the range.

Correlation analyses

The physical data extracted from each marsh edge, including buffer area elevation, edge elevation, platform elevation, and mean fetch, are shown in Figure 3.6. While there is variation between sites, the reef-lined and control edges at each site often have similar values. We also found that for reef-lined locations the marsh platform was found to be higher than the affronting reefs. Relative to NAVD88 mean platform elevation was 0.07 m, mean reef crest was -0.69 m, and the mean difference between the platform elevation and reef crests was 0.76 m. Correlation analyses between retreat and explanatory variables for the 5 sites (n = 10, marsh and control edges) suggest that marsh edge elevation was the only variable significantly correlated with retreat variables. There were strong significant negative correlations for

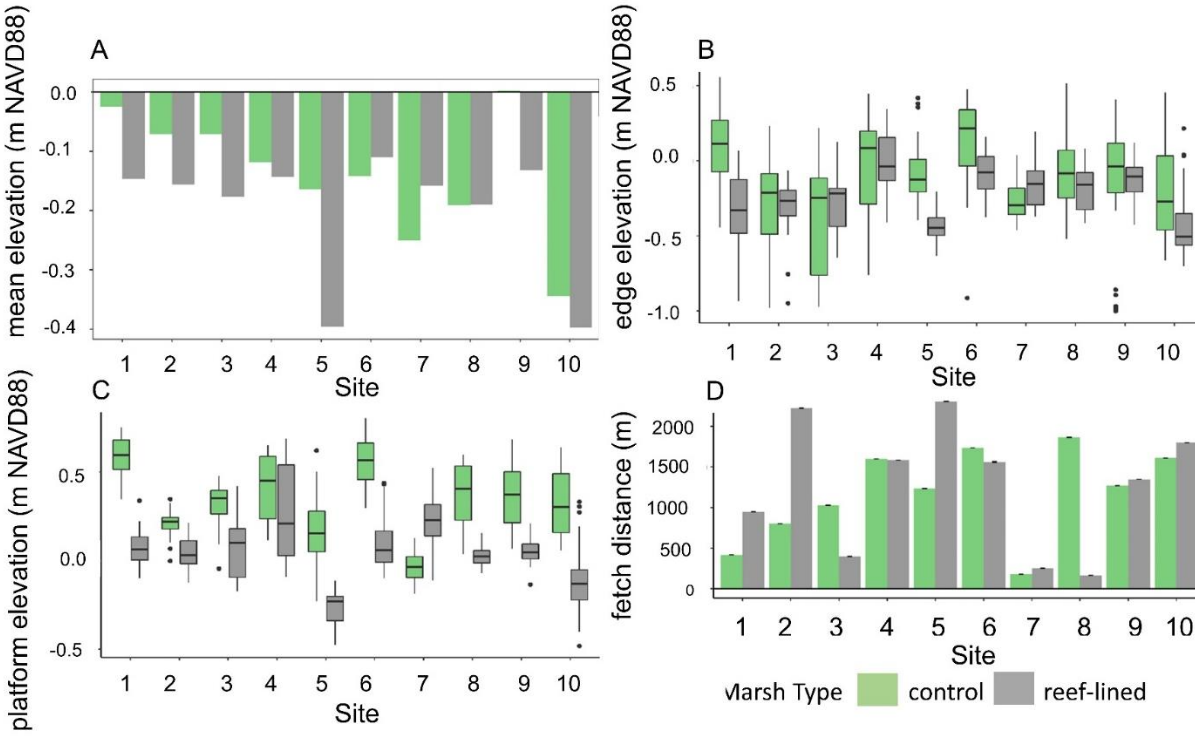

Figure 3.6. Physical characteristics for each marsh including: A) Mean elevation within the buffer areas at each marsh edge B) boxplot of edge elevations from transects at each site C) boxplot of platform elevations from transects at each site D) mean fetch distance (m). Elevations are measured in m NAVD88. Grey bars indicate reef-lined marshes and green bars indicate control marshes at each site. Boxplot components explained in Figure 3.5.

EPR (ρ = -0.90, p < 0.001) and NC (ρ = -0.88, p <0.01) with the elevation of the marsh edge (Table 3.4). The negative correlation corresponds to an increase in onshore movement of the marsh edge with increased marsh edge elevation. Mean fetch (EPR p =0.13, NC p = 0.14) and mean platform elevation (EPR p = 0.14, NC p = 0.13, Table 4) both showed negative, but not significant, relationships.

The only significant correlations between physical and slope variables were with platform elevation (Table 3.4). Buffer area mean slope showed a significant positive correlation with mean platform elevation (ρ = 0.65, p <0.01) and non-significant correlations with mean edge elevation (ρ = 0.12, p = 0.67), and mean fetch distance (ρ = 0.07, p= 0.77). Similar results were found for correlations with mean marsh edge slope. There was a significant positive correlation with mean platform elevation (ρ =0.76, p <0.001), a moderate though non-significant positive correlation with mean edge elevation (ρ =0.35, p = 0.13), and almost no correlation with mean fetch (ρ = 0.01, p=0.98). This indicates that marshes with more highly elevated platforms are more likely to have greater sloping edges.

For both EPR and NC, there was very low correlation to marsh edge slope (ρ = 0.07 and ρ = 0.05, respectively) and buffer area mean slope (ρ = 0.44 and ρ = 0.42).

Table 3.4. Correlation tests performed between retreat (EPR and NC) and marsh edge slope values with physical variables. Spearman's correlation tests were performed with non-normal retreat variables, and Pearson's correlations performed with marsh slope variables.

Retreat Variable	**Explanatory variable**	**Correlation estimate**	**P-value**
EPR	Fetch	-0.51	0.13
	Platform elevation	-0.50	0.14
	Edge elevation	-0.90	< 0.001
	Edge slope	0.07	0.84
	Mean slope	0.44	0.21
NC	Fetch	-0.50	0.14
	Platform elevation	-0.52	0.13
	Edge elevation	-0.88	< 0.01
	Edge slope	0.05	0.89
	Mean slope	0.42	0.23
Buffer area mean slope	Fetch	0.07	0.77
	Platform elevation	0.65	< 0.01
	Edge elevation	0.12	0.67
Edge slope	Fetch	0.01	0.98
	Platform elevation	0.76	< 0.001
	Edge elevation	0.35	0.13

DISCUSSION

Drivers of Morphology and Retreat

We developed and validated a technique using remotely-sensed elevation to quantify marsh edge morphology and retreat that can be used to monitor change with repeated measures. The LiDAR dataset used to characterize slope yielded a wide range of slope values, with edge slopes ranging from 2.6 ^{0} to 26.0^0 and buffer area mean slopes ranging from 1.5^0 to 11^0. A methodology using remotely-sensed elevation data can capture the morphology of large sections of the marsh edge more quickly and easily than in-situ measurements.

We found that higher marsh edges were correlated with greater rate of retreat (EPR) and net change (NC) and that marsh edges are likely to be more steeply sloping if they have high platforms. These correlations support that marsh edge erosion is driven by wave action and previous findings that highly elevated platforms are more likely to be undercut and experience greater edge erosion compared to more gently sloping morphologies (Schwimmer 2001, Moller & Spencer 2002, McLoughlin et al. 2015). The importance of platform elevation is also highlighted by studies that suggest marsh elevation and tide level can affect the energy driving erosion of the marsh edge since wave thrust is significantly decreased when a marsh is submerged, but otherwise increased as water becomes deeper owing to the larger waves that can develop (Tonelli et al. 2010, Wiberg et al. 2019).

While our findings support the important role of marsh edge and platform elevation on marsh retreat and edge morphology, the correlations were made with only 10 and 20 sections of marsh edge, for retreat and morphology, respectively. The majority of reefs fronting the reef-lined edges were restored reefs, which may reflect an effect of decision-making by managers to restore reefs in front of lower elevated marshes that may be less likely to erode, presenting a potential factor in reef placement. Oysters may also preferentially grow along low elevation edges, helping to explain why we found reef-lined edges at lower elevations with corresponding lower slope values, except at one site (Site 7). At that site, the reef-lined marsh was more highly elevated and had higher retreat values, consistent with marsh edge elevation being the most important predictor of marsh movement. These relationships among physical and retreat variables suggest that highly elevated marsh edges are most susceptible to retreat and should be targeted by coastal managers when trying to identify vulnerable shorelines. While there was not a significant relationship between retreat and marsh edge slope variables, this data was limited by the number of sites available from LiDAR data matched with restored reefs, and time between reef construction and data acquisition. Increasing the scale of the investigation with repeated LiDAR measurements and the addition of more sites may yield more clarifying results.

Morphology and Retreat Applied to Oyster Presence

Our results indicate that the presence of oyster reefs affects marsh edge morphology, with reef-lined marshes having more gently sloping edges compared to marsh edges lacking an adjacent reef. We did not find significant correlations between mean fetch distance and marsh morphology and retreat. Although there was no significant difference between reef-lined and control marshes for retreat variables, retreat rates ranged from 0.14 to 0.79 m yr^{-1} over the years 2002 – 2015 (Table 3.2) and were similar to past observations within Virginia's coastal bays and the Mid-Atlantic region (Schwimmer 2001, Taube 2013, McLoughlin et al. 2015). McLoughlin et al. (2015) and Taube (2013) both studied marshes within the VCR using shorelines from imagery from 1957 to 2009. McLoughlin et al. (2015) surveyed marshes at 4 sites bordering a large coastal bay; 3 of 4 had rates of erosion near or greater than 1 m yr^{-1} (0.98 – 1.63 m yr^{-1}). Taube (2013), who focused on mainland-bordering marshes, found 5 of 8 marshes to be retreating between 0.15 and 0.27 m yr^{-1}, one extreme location retreating at 1.58 m yr^{-1}, and 2 prograding marshes (0.46 and -0.0004 m yr^{-1}). Our rates of retreat more closely correspond to the findings from Taube (2013), who also observed marshes retreating both in the presence and absence of oyster reefs.

The marsh edges derived using the locations of maximum slope found from LiDAR data largely agreed with the edges digitized from aerial imagery for the years 2002 and 2009 (McLoughlin et al. 2013). Therefore, it is likely that the points of maximum slope are also closely defining the vegetation line at the marsh edge. This is also observed when manually inspecting the edges drawn from maximum slope locations. The data shows that the mean slope of the edge and buffer area slope are lower for reef-lined marshes, but no significant difference is found in retreat along the upper elevations of the marsh edge nearer the vegetation line and platform. We hypothesize that this is because erosion along the subtidal toe of the marsh edge, which is at an elevation similar to the reefs (Hogan & Reidenbach 2019), is reduced due to the presence of oyster reefs while the rate of retreat of the intertidal marsh edge is relatively unchanged by the presence of reefs. From this, we can hypothesize that reefs cause the marsh edges to elongate by stretching the marsh edge transition from the platform towards the lower intertidal zone, thereby causing the morphology to become less steep. Over time, oyster presence may begin to influence erosion rates along the upper marsh edge near the vegetation line due to increased frictional wave dissipation and/or other physical factors, such as advancing vegetation, along the elongated marsh edge. Our data are too limited to test this hypothesis and repeated LiDAR measurements over multiple years to decades may be necessary to capture these changes occurring at marsh edges due to the presence of oyster reefs.

Limitations of Data Extracted from LiDAR

The elevation and derived slope data used to compare morphology and create the marsh edges are dependent on the resolution and accuracy of the LiDAR measurements. While rasterized LiDAR elevation data on the order of 1 m^2 has been reported to satisfactorily describe edges (Goodwin & Mudd 2020), the resolution of the data limits the accuracy of derived calculations. Elevation data can be distorted over highly sloped terrain because values of elevation can change dramatically over short distances (Hodgson & Bresnahan 2004) and therefore more accurate estimates of slope, and often higher values, are found with reduced cell size (Grohmann 2015). The error associated with derived slope is also proportional to resolution and for high-resolution DEMs, error from slope algorithms is less important than error derived from the data (Zhou & Liu 2004). Determining error propagation is possible by using raw LiDAR data and plotting root mean square errors (RMSE), but also requires knowledge of spatial dependencies and autocorrelations (Hunter & Goodchild 1997).

Our analysis used slope data calculated using a pixel size of 0.76 m in each dimension and a moving kernel of 9 cells. The resulting slope values were therefore smoothed over this spatial dimension. Although, the agreement between the in-situ GPS and LiDAR data shows variability at the point level as is expected from the published vertical accuracy (12.5 and 17 cm for non-vegetated and vegetated terrain, respectively), the overall agreement was very high ($r^2 = 0.92$, Figure 3.A1) and we are confident in the quality of the elevation data used in the slope calculations. Since paired marshes are located close to one another, the accuracy in slope measurements is likely similar between paired sites, enabling us to understand how slope statistics compare between different locations, even if the slope values themselves are minorly affected by data and algorithm error.

Conclusions

In conclusion, the marsh edge morphology and retreat values we extracted from airborne LiDAR data supports that reef-lined marsh edges are more gently sloping compared to exposed marshes and the change in morphology is likely a precursor to measurable change in retreat. The elevation of the marsh edge was significantly correlated to retreat, while platform elevation was significantly correlated to marsh slope. The methods presented here can be utilized for monitoring future changes in marsh edge movement and morphology if repeated LiDAR surveys are conducted. Additionally, our findings can be used to locate areas vulnerable to change to aid in coastal management and conservation efforts. However, an integrated assessment of how vegetation dynamics (van de Koppel et al. 2005, Faegin et al. 2009, Feagin et al. 2009, Francalanci et al. 2013) and invertebrate behavior (Escapa et al. 2007, Davidson & Rivera 2010) affect marshes and marsh edge dynamics may be necessary to create a more holistic understanding of marsh retreat and morphology.

ACKNOWLEDGMENTS

In addition to support from within the Department of Environmental Sciences at the University of Virginia, we would like to thank the Nature Conservancy working within the Virginia Coast Reserve for sharing resources and local knowledge and researchers and staff at the Anheuser-Busch Coastal Research Center. This research was funded by the National Science Foundation grant DEB-1832221 to the Virginia Coast Reserve Long Term Ecological Research project. M. Reidenbach was supported by NSF grant OCE-1151314.

LITERATURE CITED

Allen JRL (2000) Morphodynamics of Holocene salt marshes: a review sketch from the Atlantic and Southern North Sea coasts of Europe. Quat Sci Rev, 19:1155-1231

Bahr LM, Lanier WP (1981) The ecology of intertidal oyster reefs of the South Atlantic coast: a community profile. FWS/OBS-81/15. US Fish and Wildlife Service, Office of Biological Services, Washington, DC

Blum LK, Christian RR, Wiberg PL, Cahoon DR (2021) Processes influencing marsh elevation in low and high-elevation zones in a temperature salt marsh. Estuar Coast doi.org/10.1007/s12237-020-00796-z

Chassereau JE, Bell JM, Torres R (2011) A comparison of GPS and lidar salt marsh DEMs. Earth Surf Process Landf 36:1770-1775

Chirol C, Haigh ID, Pontee N, Thompson CE, Gallop SL (2018) Parametrizing tidal creek morphology in mature saltmarshes using semi-automated extraction from lidar. Remote Sens Environ 209:291-311

Chowdhury MSN, Walles B, Sharifuzzman SM, Hossain MS, Ysebaert T, Smaal AC (2019) Oyster breakwater reefs promote adjacent mudflat stability and salt marsh growth in a monsoon dominated subtropical coast. Sci Rep 9,8549 https://doi.org/10.1038/s41598-019-44925-6

Colden A, Fall KA, Massey GM, Friedrichs C (2016) Sediment suspension and deposition across restored oyster reefs of varying orientation to flow: implications for restoration. Estuar Coast 39:1435-1448

Dame RF, Patten BC (1981) Analysis of energy flows in an intertidal oyster reef.
Mar Eco Prog Ser 5:115-124

Davidson NC (2014) How much wetland has the world lost? Long-term and recent trends in global wetland area. Mar Freshw Res 65:934-941

Davidson TM, Rivera CE (2010) Accelerated erosion of saltmarshes infested by the non-native burrowing crustacean *Sphaeroma quoianum*. Mar Eco Prog Ser 419:129-136

Day JW, Scarton F, Rismondo A, Are D (1998) Rapid deterioration of a salt marsh in Venice Lagoon, Italy. J Coast Res 14:583- 590

Dewberry (2016) Eastern shore Virginia QL2 LiDAR BAA. Report Produced for US Geological Survey. USGS Contract:G10PC00013. Task Order G15PD00284. https://coast.noaa.gov/htdata/lidar2_z/geoid18/data/8445/supplemental/va2015_usgs_eastern_shore_m8445_project_report.pdf

Duarte CM, Dennison WC, Orth RJW, Carruthers TJB (2008) The charisma of coastal ecosystems: addressing the imbalance. Estuar Coast: J CERF 31:233-238

Escapa M, Minkoff DR, Perillo GME, Iribarne O (2007) Direct and indirect effects of burrowing crab *Chasmagnathus granulatus* activities on erosion of southwest Atlantic *Sarcocornia*-dominated marshes. Limnol and Oceanogr 52:2340-2349F

Fagherazzi S, Wiberg, PL (2009) Importance of wind conditions, fetch, and water levels on wave-generated shear stresses in shallow intertidal basins. J Geophys Res 114:F03022

Farris AS, Defne Z, Ganju NK (2019) Identifying salt marsh shorelines from remotely sensed elevation data and imagery. Remote Sens 11:1795-1812

Feagin RA, Lozada-Bernard SM, Ravens TM, Moller I, Yeager KM, Baird AH (2009) Does vegetation prevent wave erosion of salt marsh edges? Proc Nat Acad of Sci 106:10109-10113

Francalanci S, Bendoni M, Rinaldi M, Solari L (2013) Ecomorphodynamic evolution of salt marshes: Experimental observations of bank retreat processes. Geomorphology 195:53-65

Glenn NF, Streutker DR, Chadwick DJ, Thackray GD, Dorsch SJ (2006) Analysis of LiDAR-derived topographic information for characterizing and differentiating landslide morphology and activity. Geomorphology 73:131-148

Goodwin, GCH, Mudd SM, Clubb FJ. 2018. Unsupervised detection of salt marsh platforms: a topographic method. Earth Surf Dynam 6:239-255

Goodwin CH, Mudd SM (2020) Detecting the morphology of prograding and retreating marsh margins- example of a mega-tidal bay. Remote Sens 12:13

Grohmann CH (2015) Effects of spatial resolution on slope and aspect derivation for regional-scale analysis. Comput Geosci 77: 111-117 DOI:10.1016/j.cageo.2015.02.003

Hladik C, Schalles J, Alber M (2013) Salt marsh elevation and habitat mapping using hyperspectral and LIDAR data. Remote Sens Environ 139:318-330

Hodgson ME, Bresnahan P (2004) Accuracy of airborne Lidar-derived elevation: empirical assessment and error budget. Photogramm Eng Remote Sensing 70:331-339

Hogan S, Reidenbach MA (2019) Quantifying and analyzing intertidal oyster reefs utilizing LiDAR-based remote sensing. Marine Ecol Prog Ser 630:83-99

Hunter GJ, Goodchild MF (1997) Modeling the uncertainty of slope and aspect derived from spatial databases. Geogr Anal 29:35-49

Jackson Jr. CW, Alexander CR, Bush DM (2012) Application of the AMBUR R package for spatio-temporal analysis of shoreline change: Jekyll Island, Georgia, USA. Comput Geosci 41:199-207

Kastler JA, Wiberg PL (1996) Sedimentation and boundary changes of Virginia salt marshes. Estuar Coast Shelf Sci 42:683-700

Kirwan ML, Guntenspergen GR, D'Alpaos A, Morris JT, Mudd SM, Temmerman S (2010) Limits on the adaptability of coastal marshes to rising sea level. Geophys Res Lett 37, L23401 doi:10.1029/2010GL045489

Kremer M, Reidenbach MA (2021) Modeled wind fetch for the bays of the Virginia Coast Reserve. Virginia Coast Reserve Long-Term Ecological Research Project Data Publication knb-lter-vcr.300.1 doi:10.6073/pasta/6e0e574063bf500ef5f2d855126697e6

Lenihan HS (1999) Physical-biological coupling on oyster reefs: how habitat structure influences individual performance. Ecol Monogr 69:251-275

Leonardi N, Defne Z, Ganju NK, Fagherazzi S (2016a) Salt marsh erosion rates and boundary features in a shallow bay. J Geophys Res Earth Surf 121:1861-1875

Leonardi N, Ganju NK, Fagherazzi S (2016b) A linear relationship between wave power and erosion determines salt-marsh resilience to violent storms and hurricanes. Pro Nat Acad Sci USA 113:64-8

Mariotti G, Fagherazzi S (2013) Critical width of tidal flats triggers marsh collapse in the absence of sea-level rise. Proc Nat Acad Sci USA 110:5353-5356

Mattheus CR, Rodriguez AB, McKee BA, Currin CA (2010) Impact of land-use change and hard structures on the evolution of fringing marsh shorelines. Estuar Coast Shelf Sci 88:365-376.

McGlathery KJ, Reidenbach MA, D'Odorico PAOLO, Fagherazzi S, Pace ML, Porter JH (2013) Nonlinear dynamics and alternative stable states in shallow coastal systems. Oceanogr 26:220-231

McLoughlin, SM (2010) Erosional processes along salt marshes edges on the Eastern Shore of Virginia. Master's thesis, University of Virginia, Charlottesville, VA

McLoughlin SM, McGlathery KJ, Wiberg PL (2013) Quantifying changes along mainland marshes in the Virginia Coast Reserve, 1957 – 2011: GIS data. Virginia Coast Reserve Long-Term Ecological Research Project Data Publication knb-lter-vcr.196.12 doi:10.6073/pasta/e2115c3f1fce44522b4c3ded4ae19a79

McLoughlin SM, Wiberg PL, Safak I, McGLathery KJ (2015) Rates and forcing of marsh edge erosion in a shallow coastal bay. Estuar and Coast 38:620-638

Medeiros S, Hagen S, Weishampel J, Angelo J (2015) Adjusting Lidar-derived digital terrain models in coastal models based on estimated aboveground biomass density. Remote Sensing 7:3507-3525

Meyer DL, Townsend EC, Thayer GW (1997) Stabilization and erosion control value of oyster cultch for intertidal marsh. Restor Ecol 5:93-99

Millette TL, Argow BA, Marcano E, Hayward C, Hopkinson CS, Valentine V (2010) Salt marsh geomorphological analyses via integration of multitemporal multispectral remote sensing with LiDAR and GIS. J Coast Res 26: 809 -816

Moller I, Spencer T (2002) Wave dissipation over macro-tidal saltmarshes: effects of marsh edge typology and vegetation change. J Coast Res SI 36:506-521

Morris JT, Porter D, Neet M, Nobel PA, Schmidt L (2005) Integrating LIDAR elevation data, multi-spectral imagery and neural network modelling for marsh characterization. Int J Remote Sens 26:5221-5234

Obu J, Lantuit H, Grosse G, Gunther F, Sachs T, Helm V, Fritz M (2017) Coastal erosion and mass wasting along the Canadian Beaufort Sea based on annual airborne LiDAR elevation data. Geomorphology DOI:10.1016/j.geomorph.2016.02.014

Piazza EP, Banks PD, La Peyre MK (2005) The potential for created oyster shell reefs as a sustainable shoreline protection strategy in Louisiana. Restor Ecol 13:499-506

Priestas AM, Mariotti G, Leonardi N, Fagherazzi S (2015) Coupled wave energy and erosion dynamics along a salt marsh boundary, Hog Island Bay, Virginia, USA. J Mar Sci Eng 3:1041-1065

Reidenbach MA, Berg P, Hume A, Hansen JCR, Whitman ER (2013) Hydrodynamics of intertidal oyster reefs: The influence of boundary layer flow processes on sediment and oxygen exchange. Limnol Oceanogr Fluids Environ 3:225 -239

Ross PG, Luckenbach MW (2009) Population assessment of eastern oysters (Crassostrea virginica*)* in the seaside coastal bays. Virginia Coastal Zone Management Program, Virginia Department of Environmental Quality, Richmond Virginia

Safak I, Wiberg PL, Kurum MO, Richardson DL (2015) Controls on residence time and exchange in a system of shallow coastal bays. Cont Shelf Res 97:7-20

Schenk T, Csatho B (2002) Fusion of LiDAR data and aerial imagery for a more complete surface description. Int Arch Photogramm Remote Sens 97:7- 20

Schmid KA, Hadley BC, Wijekoon N (2011) Vertical accuracy and use of topographic LiDAR data in coastal marshes. J Coast Res 27:116-132

Schwimmer, RA (2001) Rates and processes of marsh shoreline erosion in Rehoboth Bay, Delaware, USA. J Coast Res 17:672 -683

Stockdon HF, Sallenger Jr AH, List JH, Holman RA (2002) Estimation of shoreline position and change using airborne topographic Lidar data. J Coast Res 18:502-513

Taube SR (2013) Impacts of fringing oyster reefs on wave attenuation and marsh erosion rates. Master’s Thesis, University of Virginia, Charlottesville, VA

Tonelli M, Fagherazzi S, Petti M (2010) Modeling wave impact on salt marsh boundaries. J Geophs Res 115: C09028

Van de Koppel J, van der Wal D, Bakker JP, Herman PMJ (2005) Self-organization and vegetation collapse in salt marsh ecosystems. Am Nat 165(1): E1 – E12

Volaric MP, Berg P, Reidenbach MA (2018) Oxygen metabolism of intertidal oyster reefs measured by aquatic eddy covariance. Mar Ecol Prog Ser 599:75-91

Volaric MP, Berg P, Reidenbach MA (2020) Drivers of oyster reef ecosystem metabolism measured across multiple timescales. Estuar Coast 43:2034-2045

White SA, Wang Y (2003) Utilizing DEMs derived from LIDAR data to analyze morphologic change in the North Carolina coastline. Remote Sens Environ 85:39-47

Whitman ER, Reidenbach MA (2012) Benthic flow environments affect recruitment of *Crassostrea virginica* larvae to an intertidal oyster reef. Mar Eco Prog Ser 463: 117-191

Wiberg PL, Taube SR, Ferguson AE, Kremer MR, Reidenbach MA (2019) Wave attenuation by oyster reefs in shallow coastal bays. Estuar and Coast 42: 331-347

Zhao Y, Wang Q, Wang D, Wang YP (2017) Rapid formation of marsh-edge cliffs, Jiangsu coast, China. Mar Geol 385:260-273

Zhou Q, Liu X (2004) Analysis of errors of derived slope and aspect related to DEM data properties. Comput Geosci 30: 369-378

APPENDICES

Table 3.A1. Slope (degree) statistics from buffer areas around marsh edges from Fowling Point Marsh (FP), Chimney Pole Marsh (CP), Matulakin Marsh (MM), and 2 from Hog Island Marsh (HI) surveyed in-situ (McLoughlin 2010, McLoughlin et al. 2015).

Site	In-situ edge classification	Min	Max	Range	Mean	Std
CP	Terrace	0.01	29.7	29.6	7.4	5.5
FP	Ramp	0.1	20.9	20.8	4.3	2.8
MM	Scarp	0.1	33.4	33.4	11.0	6.0
HI_terrace	Terrace	0.04	35.9	35.9	5.6	5.9
HI_scarp	Scarp	0.1	40.3	40.2	8.1	9.3

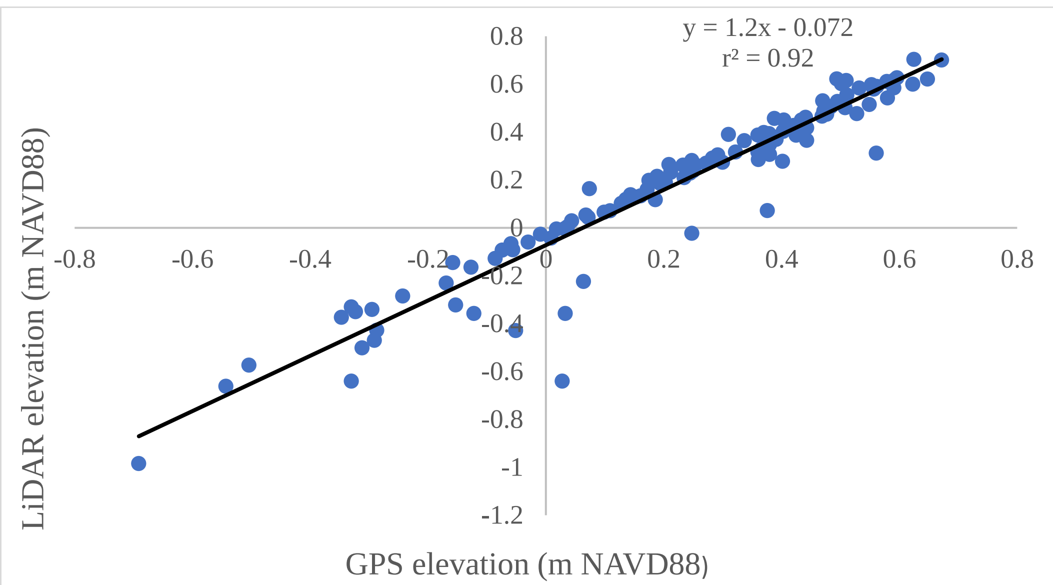

Figure 3.A1. Validation of LiDAR elevation data with in-situ GPS elevations, where LiDAR data was extracted to locations of in-situ data points at Fowling Point Marsh (n = 114).

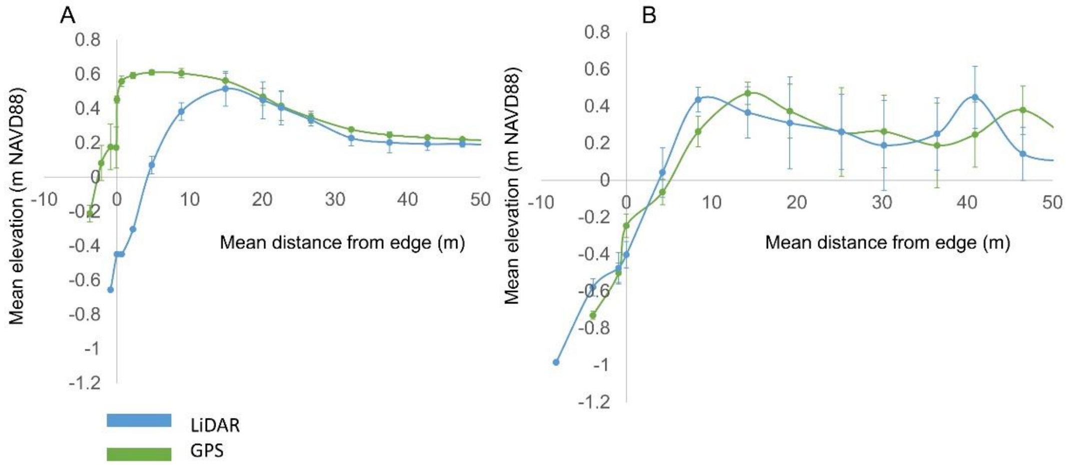

Figure 3.A2. Mean elevation profiles (± standard error from multiple transects) for A) an unstable marsh (CP) showing lateral retreat in the 5 years between surveys and and B) a stable marsh (FP). Distance from the edge is measured on the x-axis, where the edge is at 0 m and positive values are towards the platform.

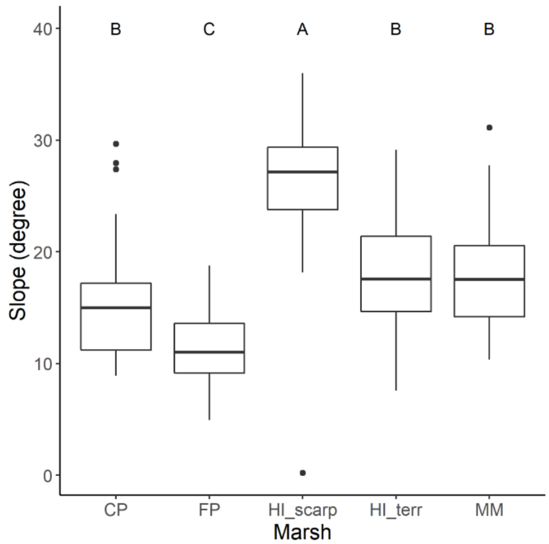

Figure 3.A3. Boxplots of edge slope values found along transects perpendicular to marsh edges. HI scarp had a significantly greater maximum slope than all other marshes, while FP had a maximum that was significantly lower. The maximum slope for CP, HI terrace (HI_terr), and MM, did not significantly differ from one another. For the boxplot: boxes indicate the interquartile range (IQR) with the interior line representing the median, whiskers are the maximum and minimum (up to 1.5. the IQR), and dots represent outliers beyond the range.

CHAPTER 4: Quantifying trade-offs in ecosystem services under various oyster reef restoration designs

This chapter in review at *Estuaries and Coasts* with MA Reidenbach as co-author.

ABSTRACT

Oyster populations within the coastal bays of Virginia have greatly declined, mainly due to overharvesting and disease, and past restoration efforts have largely focused on increasing their population. Current restoration goals have now expanded to simultaneously procure the wider ecosystem services oysters can offer, including shoreline protection and ecosystem diversification. However, trade-offs exist in designing artificial reefs because it is unlikely one design will optimize all services. This study compares the services provided by reef designs varying in elevation and width adjacent to an intertidal marsh within a coastal bay of Virginia, USA. We quantified wave attenuation to determine potential coastal protection of the adjacent marsh, and changes to sediment composition and infauna communities before and after reef construction for three years. After construction we also quantified oyster growth and population density to compare high and low elevation reef designs. High elevation reefs were more effective at attenuating waves (up to 21 % vs 0 % in year 3 post construction) and fostering oyster growth compared to low elevation reefs. Oysters atop high elevation reefs were on average approximately twice as dense and 20 % larger than those on low elevation designs. Reef width had a minimal effect on oyster population density. The presence of oyster reefs also increased infauna diversity and sediment organic matter. Our results indicate that artificial reef design can differentially affect the services provided through restoration and elevation is

especially important to consider when designing for oyster population enhancement and coastal protection.

Key words: oysters, restoration, ecosystem services, coastal protection, reef design

INTRODUCTION

Populations of the eastern oyster, *Crassostrea virginica*, across Virginia and the mid-Atlantic region of the United States were decimated by the beginning of the twentieth century due to a combination of overharvesting, poor water quality, and disease (Rothschild et al. 1994, Kemp et al. 2005). While original restoration efforts primarily focused on enhancing populations, restoration efforts have shifted to more ecosystem-based approaches due to the increased recognition of ecosystem services (Coen & Luckenbach 2000, Ehrenfeld 2000, Grabowski et al. 2012). Ecosystem services are described as the benefits provided by natural systems to human health and well-being extending from basic provisions including food and water, to cultural and recreational benefits (MEA 2005).

The ecosystem services provided by oyster reefs have been thoroughly summarized by Grabowski and Peterson (2007) and Coen et al. (2007). These include, in addition to oyster biomass production, the services of water filtration and pseudofeces production, carbon sequestration, shoreline and habitat stabilization, ecosystem diversification, and habitat provision. The benefits of these services range from increased biodiversity and productivity benefiting fisheries and ecological communities to reduction of greenhouse gases and mitigated effects of sea-level rise through oysters sequestering carbon in their shells and stabilizing shorelines, respectively. However, due to environmental or monetary constraints associated with restoration efforts, it is unlikely that all potential ecosystem services can be obtained and therefore trade-offs must often be made based on restoration goals (Nelson et al. 2009).

In practice, trade-offs made by focusing on restoring different services have been quantified in coastal landscapes. For example, Bilkovic & Mitchell (2013) found that hybrid stabilization of marsh shorelines could enhance water filtration by attracting epifauna and suspension feeders. However, they also observed localized declines in benthic productivity and nutrient cycling. Additionally, North et al. (2010) used ecological modeling to find that locations where oyster harvests are optimized may not also optimize spawning, with varying results largely influenced by local hydrodynamics. Strategies to enhance ecosystem services become more complicated when varied stressors are affecting a given species or habitat (Fulford et al. 2010). Quantification of these ecosystem services (Nelson et al. 2009, Grabowski et al. 2012) can provide metrics for weighing options and finding strategies that are most effective in reaching restoration goals.

Restoration to Enhance Population

The recruitment of larvae and oyster growth remains substrate limited within Virginia's coastal systems and generally across the U.S. Atlantic coastline (Mann & Powell 2007, Schulte et al. 2009). Therefore, the primary objective of oyster restoration along the Virginia coast has been to provide hard substrate for oyster larvae to land, attach, and grow to viable adults. These restoration efforts have primarily relied upon the natural transport and dispersion of larvae due to tidal currents and mixing (Fuchs & Reidenbach 2013, Hubbard & Reidenbach 2015) and the deposition of oyster and other bivalve shells along intertidal regions to create suitable benthic habitat for larval settlement and oyster growth (Whitman & Reidenbach 2012). More recent restoration projects have utilized 'oyster castles', which are concrete blocks that can interlock and be stacked, allowing for flexibility in design configuration. They have proven successful and to outperform other substrates at recruiting and retaining oysters (Theuerkauf et al. 2015). Oyster castle structures have also demonstrated the ability to promote both vertical accretion and horizontal expansion of oyster habitat (Theuerkauf et al. 2015). While vertical elevation has proven to have a positive effect on the success of oyster growth and recruitment (Bartol et al. 1999, Lenihan 1999, Schulte et al. 2009) there are environmental tradeoffs. At higher elevations oysters spend less time submerged and reduce their susceptibility to predation and sedimentation (Fodrie et al. 2014, Johnson & Smee 2014, Lenihan 1999). However, emergent time exposes oysters to greater stress through temperature, desiccation, and lowered food supply which can affect growth and survivability (Johnson & Smee 2014, Byers et al. 2015). Interstitial spacing, which can be incorporated in designs with oyster castles, can be beneficial for oyster growth in the presence of predators (Soniat et al. 2004, Hill & Wiessburg 2013), but may limit benefits to aquaculture.

Oyster Restoration for Coastal Protection

To protect shorelines from coastal erosion, past management efforts have relied heavily on shoreline armoring by using physical structures including seawalls, bulkheads, and breakwaters (Bulleri & Chapman 2009). The goal behind these techniques is to reduce the amount of energy received at the coast, because shoreline erosion is mainly attributed to incessant wave action and shear stresses that develop and suspend sediment (Fagherazzi & Wiberg 2009). However, these infrastructure techniques have ecological disadvantages including the loss of local biodiversity, and potential for enhanced transport of sediment (Bulleri & Chapman 2009).

Recent efforts have increasingly attempted to use constructed oyster reefs as natural habitat for coastal protection. These ‘living shorelines’ minimize the use of grey matter, concrete materials, and encourage the use of biologic materials such as oyster reefs and seagrass meadows to dampen wave action reaching coasts. Living shorelines have proven to be comparatively effective in mitigating coastal erosion while also enhancing local ecology (Davis et al. 2006). The dampening effects of wave energy created by the vertical obstruction caused by natural and artificial reefs, has been shown to decrease shoreline erosion and allow for increased sedimentation (Meyer et al. 1997, Piazza et al. 2005, Borsje et al. 2010, Wiberg et al. 2019). Oyster castles, which create vertical structure and interstices, can both promote oyster growth while increasing habitat complexity and enhancing local ecology (Soniat et al. 2004, Hill & Wiessburg 2013).

Ecosystem Changes in the Presence of Oyster Reefs

Oysters function as ‘ecosystem engineers’ because of their ability to influence community structure (Van der zee et al. 2012). By increasing benthic sediment stability, sediment organic matter content, and habitat heterogeneity, oyster reefs can enhance the biodiversity and trophic interactions of intertidal communities (Gutierrez et al. 2003, Van der Zee et al. 2012, Donadi et al. 2013). The increased protection and shelter from waves and predators provided by reefs can lead to increased infauna abundance and biomass in and around reefs and increased biodiversity after restoration (Castel et al. 1989, Langlois et al 2006, Van der zee et al. 2015).

As filter feeders, oysters take in nutrients by filtering the water column and removing suspended particles (Reidenbach et al. 2013), phytoplankton, and dissolved organic matter. This filtration process aids in nutrient cycling, whereby organic matter is assimilated within oysters and inorganic nutrients are excreted into the water column as particulates (Zhang et al. 2014). Oyster filtration can lead to some remineralization of nutrients and nutrient burial, increasing organic matter in sediments nearby reefs, as well as benthic respiration (Volaric et al. 2018). Changes in sediment characteristics before and after reef restoration projects have demonstrated these differences in sediment nutrients and particle size (Southwell et al. 2017), though in areas of established reefs, organic matter can vary due to local ecosystem interactions and primary producers that utilize the inorganic material (Smaal & Prins 1993, Smyth et al. 2016).

Study Objectives

Because artificial oyster reefs can alter a multitude of ecosystem services, including coastal protection and sediment transport, larval settlement, oyster growth, and local biodiversity, it is important to understand how variations in the design of these restored reefs alter the relative benefits of these services.

In this study, artificial oyster reefs in front of an elevated vegetated marsh platform within a coastal bay along the Eastern Shore of Virginia, U.S.A. were constructed in 2017. This site was monitored before (2017) and after construction for a three-year period (2018 – 2020). A total of eight reefs were constructed with four different reef designs differing in elevation and width. Each design was replicated twice. The questions this study addressed were:

1) How does elevation of the constructed oyster reef impact wave attenuation?
2) How does the elevation and shape of the constructed oyster reef impact larval settlement, oyster density, and growth?
3) How does the presence of constructed oyster reefs impact biomass and diversity of infauna within the surrounding sediment?
4) How does the presence of constructed oyster reefs impact sediment organic matter?

MATERIALS & METHODS

Study Site

Studies were performed within the Virginia Coast Reserve (VCR), a National Science Foundation (NSF) funded Long-term Ecological Research (LTER) site located on the Atlantic Ocean side of the Delmarva Peninsula, Virginia, USA (Figure 4.1). The VCR is located within the Volgenau Virginia Coast Reserve (VVCR) which covers over 100 km of coastline in Virginia and includes the largely undeveloped habitat encompassing upland forests, coastal bays, and barrier islands, connected to the open ocean through narrow inlets. The main driver of coastal erosion in the shallow bays, with a mean depth of 1-2 m, is wind (Mariotti & Fagherazzi 2013) and is dependent on water depth, wind direction, fetch distance, and drag on the seafloor (Fagherazzi & Wiberg 2009). In the VCR, coastal bays experience low freshwater input, a tidal range of 1.2 m, (Hansen & Reidenbach 2013), and a

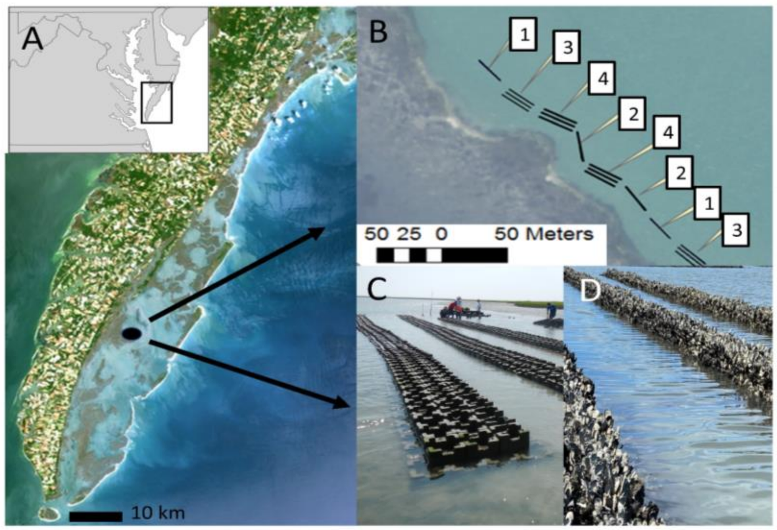

Figure 4.1 A) The VCR is located on the eastern side of the Delmarva Peninsula and the location of Short Prong Marsh located within the VCR is indicated by the black circle. The inset shows that VCR in context of the surrounding states. B) The random arrangement of the reef designs running parallel to the marsh edge is shown in the bottom image where reef designs are indicated as 1 = 1 row x 2 tiers, 2 = 1 row x 4 tiers, 3 = 3 row x 3 tiers, and 4 = 3 rows x 4 tiers. c) Oyster castles before settlement in 2017 and d) year 3 post construction (2020).

gradient of flushing created by exchange through the inlets (Safak et al. 2015). Winds are primarily from the south in the summer and north-northeast in the winter (Wiberg et al. 2019).

Oysters within the VCR are of the species *Crassostrea virginica* and found fringing on marshes and in patches on mudflats, predominantly in the intertidal zone (Hogan & Reidenbach 2019). Short Prong Marsh, within Hog Island Bay of the VCR, was selected to be a new long-term research site for oyster restoration. The Nature Conservancy (TNC), along with their network of community volunteers, constructed 8 oyster castle formations along the eroding marsh edge in summer 2017 (Figure 4.1). Each castle block weighs 30 pounds and measures one square foot by eight-inches high. Reef formations consisted of four different designs, each having 2 replicates, where elevation and width varied. The four designs included 1 row wide x 2 tiers high, 1 row x 4 tiers high, 3 rows x 2-tiers high, and 3 rows x 4 tiers high configurations. Rows were made approximately 1 m apart and 25 m long. Each design was made parallel to the marsh approximately 30 m from the edge and reefs were spaced 10 m apart. Those with 2 tiers are referred to as low elevation designs, and those with 4 tiers are referred to as high elevation designs. The dimensions of the oyster castles give the 2 tier, low elevation, reefs an approximate elevation of 40 cm off the seafloor and 4 tier, high elevation, reefs an approximate elevation of 80 cm. Mean water depth surrounding the constructed reefs is approximately 1 m deep, making the crests of the oyster castles for the low and high elevation designs approximately 0.6 m and 0.2 m below local mean sea level (lmsl), respectively.

Oyster Growth

Oyster density was measured in-situ using randomly placed 0.25 m x 0.25 m (0.0625 m^2) quadrats to count oysters greater than 1 cm in length. Sampling took place on one of each reef design. For each of the four reef designs, 3 replicates were randomly placed at the design's highest tier, giving a total of 12 replicates. For both high elevation reef designs (with either 1 or 3 rows), 3 additional replicates were also completed on the 2nd tier from the bottom (2nd of 4 stacked castles). Due to the stacked nature of the oyster castles, counts on the 2nd tiers of high elevation designs were quantified using 0.12 m x 0.25 m quadrats (6 additional quadrats). Sampling on this lower tier was completed to compare directly to the upmost tier of the low elevation designs, both at the same elevation above the seafloor. During year 3 post construction, oyster lengths were also measured to nearest 0.5 cm on the top (along the 4th tier) and mid-height (2nd tier) of the high elevation design, as well as on the top (2nd tier) of the low elevation oyster reef designs.

Wave Data

Water depth and significant wave height were analyzed through deployments of RBR TWR- 2050P wave gauges. Before construction, during the winter months (February- March) of 2017 pre-construction data were collected. Wave data were again collected during spring (April-May 2018) year 1 after construction and summer (July – August 2020) year 3 post construction. Wave gauges in year 1 and year 3 post construction were placed 10 m on either side, closer to the marsh or bay, of one high elevation (3 row x 4 tier) and one low elevation (1 row x 2 tier) design. Before reef construction, wave gauges were placed at similar distances from the marsh edge in the area where reefs were to be constructed. Deployments were approximately 4 weeks long and programmed to record waves averaged every 30 minutes with 1024 bursts taken at 4 Hz.

Water depths from wave gauges were corrected using atmospheric pressure data provided by NOAA. For each pair of wave gauges the data were matched by timestamp and sorted by corrected water depth, based on the shallower marsh-side measurements. We eliminated records from very shallow water so that each gauge was covered by at least 0.25 m of water. Data were then split into three categories based on depth as done by Wiberg et al. (2019) for shallow (< 0.75 m), intermediate (0.75 m – 1.0 m), and deep (> 1.0 m) water. These water depths bracket the tops of the different designs considering the low elevation reefs are approximately 0.4 m off the seafloor and high elevation reefs are approximately 0.8 m off the seafloor.

Infauna Collection and Analysis

Infauna were collected each summer for years pre-construction (2017) to year 3 post construction (2020). Sample collection occurred in June for all years, except in year 3 post construction where collection was delayed until late August 2020 due to Covid-restricted site access. Samples were collected by inserting a cylindrical 15 cm id PVC corer into the sediment 15 cm deep. For pre-construction infauna, 8 samples were taken randomly over the area where reefs were to be constructed. For the 3 years post construction, 8 samples were also taken, with 2 in proximity to each wave gauge on either side of the high and low elevation designs. Sediment was passed through a 1 mm sieve and living infauna were removed and placed in a jar with 70 % ethanol. Infauna abundance was recorded by classifying specimens into broad taxonomic classes including worms, small crustaceans (amphipods and isopods), large crustaceans (crabs), gastropods, and bivalves. For worms, all biomass was collected, but only those viewed under a microscope found with intact heads were added to the count, to avoid double counting broken individuals. Some decide only to count fully intact specimen due to frequent damage occurring during sieving (Gorska et al. 2019), however, with our limited number of samples each year we felt our methods were best. Biomass was analyzed one month after collection to standardize the procedure and reduce differences that preservation time may have on weight (Howmiller 1972, Wetzel et al. 2005). Biomass was estimated by measuring the ash free dry weight (AFDW) of each sample. Samples were dried in pre-weighed combusted tins, at 60 ºC for 48 h, weighed, and then placed in a muffle furnace at 500 ºC for 6 h (Rumohr 2009). Sample weight after time in the muffle furnace was subtracted from dry weight to obtain AFDW, the mass of the organic material in samples.

Sediment Collection and Analysis

A sediment core 3 cm id and 5 cm deep was also collected adjacent to each infauna core to quantify sediment organic matter each year post construction, while 10 cores were taken randomly over the mudflat pre-construction. After collection, sediment was placed in an oven at 60 ºC until dry. Sediment was powdered, and 2 g of each sample was placed in a pre-weighed and combusted tin. Samples were placed in a muffle furnace at 500 ºC for 6 h and weighed to obtain AFDW. The percent difference in sediment weight ((ash weight – dry weight/ dry weight) *100) represents the percent organic matter within each sample.

RESULTS

Oyster Density

The artificial reefs successfully fostered oyster growth on all the reef designs. All oyster counts were normalized to 0.0625 m^2, and density discussed refers to oyster counts in this area. The density on 2^{nd} tiers was found to be lower compared to that on 4th tiers of oyster castles for all years (Figure 4.2A, Table 4.1). Densities on

Table 4.1. Oyster density (per 0.0625 m^2) ± standard error (se) on high and low tiers completed years 1, 2, and 3 post construction and mean oyster length (cm ± se) for data collected in year 3 post construction. Mean length was calculated after 1 outlier was removed.

Year post construction	Tier	Mean Count (± se)	Mean length (cm ± se)
1	2	55.8 ± 5.1	--
	2 of 4	52.0 ± 10.0	--
	4	120.8 ± 4.4	--
2	2	31.0 ± 2.5	--
	2 of 4	46.0 ± 6.5	--
	4	73.5 ± 4.3	--
3	2	28.7 ± 1.4	6.1 ± 0.235
	2 of 4	46.0 ± 5.3	7.1 ± 0.15
	4	70.3 ± 4.5	7.4 ± 0.10

the high elevation 4th tiers averaged (± standard error) 120.8 ± 4.4, 73.5 ± 4.3, and 70.3 ± 4.5 oysters for years 1, 2, and 3 post construction, respectively. Low elevation 2nd tiers averaged 55.8 ± 5.1, 31.0 ± 2.5, and 28.7 ± 1.4 oysters for years 1, 2, and 3 post construction, while for high elevation 2nd tiers averaged 52.0 ± 10, 46.0 ± 6.5, and 46.0 ± 5.3 oysters (Table 4.1). Densities were highest 1 year after construction compared to subsequent years and the greatest standard error for density on the 2nd tier of high elevation designs.

Figure 4.2 A) Densities for years 1 – 3 post construction (2018 – 2020) computed from counts within 0.25 m x 0.25 m quadrats. Tier 2 is from the second tier of low elevation designs, while tiers 2 of 4 and 4 are from corresponding tiers of the high elevation designs. B) Lengths of oysters measured from various positions in year 3 (2020); one outlier was removed from the dataset.

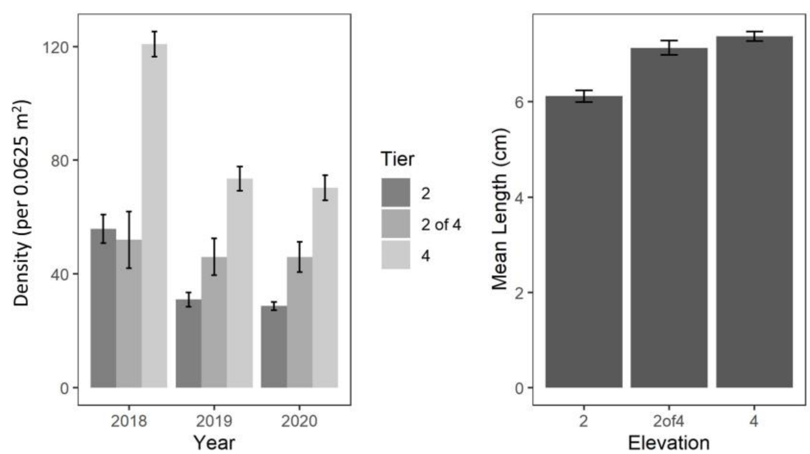

For density data we created a generalized linear model (glm) fit with a negative binomial distribution and the predictors of tier (2, 2nd of 4, 4), year as a continuous variable, and an interaction term between tier and year using the MASS package in R (Venables & Ripley 2002). The data were examined for autocorrelation among samples and residuals of each model were assessed for normality and heteroscedasticity. Each of the explanatory variables from the linear model explained oyster density including, tier ($\chi_{2,51}$=121.1, $p < 0.0001$), year ($\chi_{1,51}$= 32.7, $p < 0.0001$), and the interaction between the two variables ($\chi_{2,48}$= 8.5, $p = 0.01$). Interpretation of the interaction plot showed that while densities for tier 4 are greater than those on the 2nd tiers, the difference in density between the 2nd tiers on high and low elevation designs was also dependent on time since construction, where oyster densities on the 2nd tier samples from high elevation designs became more dense relative to 2nd tiers of low elevation designs with increasing age. We also fit 2 additional glms with negative binomial distributions for both low and high elevation designs to determine differences in density between the designs with 1 and 3 rows. Although differences were observed for density with year, as the previous analysis suggested, no difference in density between 1 and 3 row designs for low elevation reefs ($\chi_{1,16}$= 0.01 p = 0.93) or high elevation reefs when using combined samples from all tiers for total biomass ($\chi_{1,34}$= 3.52 p = 0.06) was found.

For year 3, oysters were greater in size along the high elevation reef designs (Table 4.1, Figure 4.2 B). For the high elevation design the mean length (± standard error) on the 4th tier was 7.4 ± 0.1 cm and the mean for the 2nd tier was 7.1 ± 0.15 cm. For the low elevation design the mean length for oysters on the 2nd tier was 6.1 ± 0.23 cm. These data show that by the year 3 post construction oysters were largely mature (about 7.5 cm or 3 inches [Lenihan 1999], Figure 2.2 B). A one-way ANOVA was used to determine differences in length and the ‘emmeans’ package in R was used for post-hoc analysis (Length 2020). Length differed with tier position ($F_{2,14}$ = 25.4, p < 0.0001) and oysters growing on low elevation designs were smaller than oysters growing on high elevation designs, when compared to either the high elevation 4th tier (t = -6.8, df = 14, p < 0.0001) or the lower 2nd tier (t = -5.5, df = 14, p < 0.001) samples. Length was similar on the tiers (4th and 2nd of 4) of the high elevation design (t = -1.4, df = 14, p = 0.4).

Wave Data

Mean water depths and offshore significant wave heights were similar for each deployment, before and after reef construction (Table 4.2). For year 1 and 3 post construction average water depths were 0.91 m and 1.03, respectively, nearing the top of the high elevation reefs. Wave height comparison between offshore and onshore before reef construction (2017) found little attenuation over the approximate 25 m distance between the gauges. Wave heights during years 1 and 3 post construction (2018 and 2020) are shown in Figure 4.3 and wave attenuation statistics are included in Table 4.3. The approximately month-long sampling in years 1 and 3 indicated no wave attenuation over the low elevation design. The high elevation design fostered 13 % attenuation in year 1 and 21 % attenuation in year 3 when averaged across all wave conditions and water depths. Since reef construction was completed in 2017 after the

Table 4.2. Mean and maximum values for water depth and significant wave height (Hs) from combined marsh and bay- side wave gauges for each of the sampling periods including pre-construction (2017) and year 1 (2018) and 3 (2020) post construction. Values were calculated from data collected when the marsh-side gauges was in at least 0.25 m of water.

	Location	Depth (mean ±se /max) m	Hs (mean ± se/max) m
Pre-construction	Bay	1.34 ±0.01/2.07	0.06± 0.003/0.37
	Marsh	0.63± 0.01/1.38	0.06± 0.003/0.38
Year 1	Bay	0.99 ±0.006/ 2.05	0.09± 0.001/0.40
	Marsh	0.83 ±0.006/1.98	0.09± 0.001/0.36
Year 3	Bay	1.19± 0.01/2.47	0.06± 0.001/0.49
	Marsh	0.87 ±0.01/1.87	0.06± 0.001/0.44

Table 4.3. Percent attenuation from trendlines and R^2 values for scatterplots made comparing marsh and bay-side significant wave heights for all data and each water depth (shallow (< 0.75 m), intermediate (0.75 – 1.0 m), and deep (> 1.0 m)) for each deployment, including pre-construction (2017) and years 1 (2018) and 3 (2020) post construction.

	Water Depth	Pre-construction	Year 1		Year 3	
Bay vs marsh		No reefs	Low	High	Low	High
Attenuation	All	2 %	1 %	13 %	0 %	21 %
R^2		0.98	0.98	0.95	0.98	0.93
Attenuation	Shallow		1 %	5 %	0 %	40 %
R^2			0.98	0.85	0.98	0.91
Attenuation	Intermediate		1 %	14 %	0 %	25 %
R^2			0.98	0.98	0.98	0.95
Attenuation	Deep		0 %	15 %	0 %	13 %
R^2			0.99	0.99	0.98	0.95

spawning season, the year 1 data collected before the next spawning event indicate wave attenuation was caused primarily by the oyster castles, not due to the presence of oysters. The reef structure increased attenuation with increase in water depth during year 1 with no oyster growth, 5%, 14%, and 15 %, respectively for shallow, intermediate, and deep water. In year 3, after considerable oyster growth, wave attenuation was measured to be 40 %, 25 %, and 13 % for shallow, intermediate, and deep water, respectively (Figure 4.3, Table 4.3), which indicates increasing wave attenuation with decreasing water depth. Therefore, with additional oyster growth, the high elevation design is much more effective at attenuating waves than having either no reef (pre-construction) or solely the oyster castle structure (year 1 post construction), especially in shallow water (ranging from 0.25 m to 0.75 m).

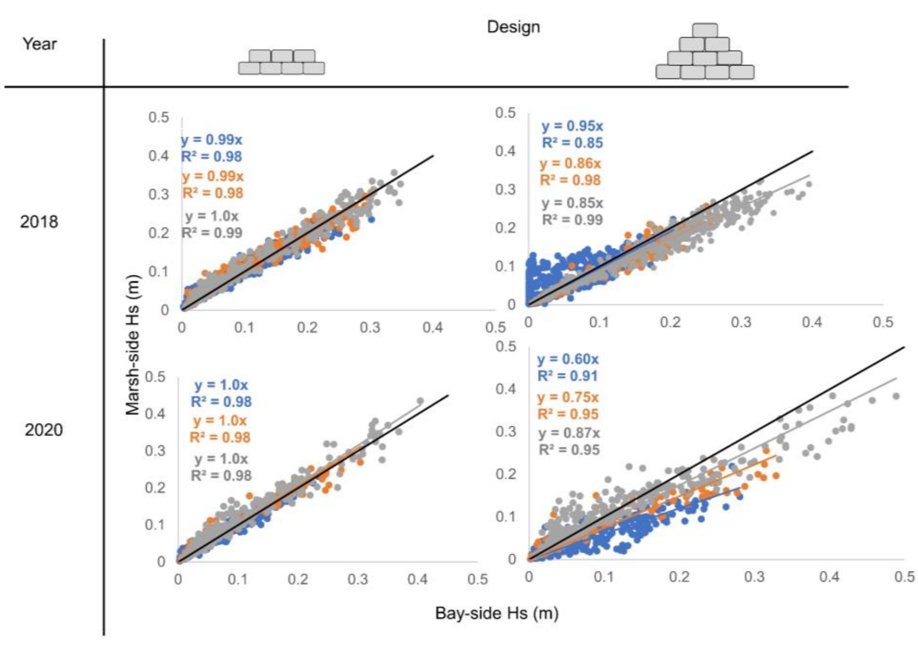

Figure 4.3. The scatter plots show the attenuation for the low (1 row x 2 tiers; left panel) and high (3 rows x 4 tiers; right pannel) elevation designs for years 1 (2018) and 3 (2020) post construction with attenuation analyzed for shallow (< 0.75 m, blue), intermediate (0.75 – 1.0 m, orange), and deep (> 1.0 m grey) water. Trendlines and R^2 values for each water depth range are displayed. Attenuation is estimated as the relative reduction in wave height as waves propagate across the reef, measured as 1 minus the slope of the trendline, with the intercept at 0. A 1:1 line (black) was added for comparison and its slope of 1 would indicate that bay and marsh wave heights were the same.

Infauna Community

Total infauna abundance, with data combined from 8 cores, was highest before reefs were constructed (Figure 4.4). We observed that in year 1 post construction samples the total infauna abundance was lowest, followed by a rebound in year 2, though still lower than the initial total, followed by a slight decrease in year 3 (Table 4.4, Figure 4.4). A one-way ANOVA comparing abundance found differences between years ($F_{3,28}$= 3.6, p = 0.03), and the post-hoc analysis found that pre-construction infauna were more abundant than in year 1 post construction (t = 2.97, df = 28, p = 0.03). After construction, different taxa, other than worms, begin to compose a larger percent of the overall specimen collected.

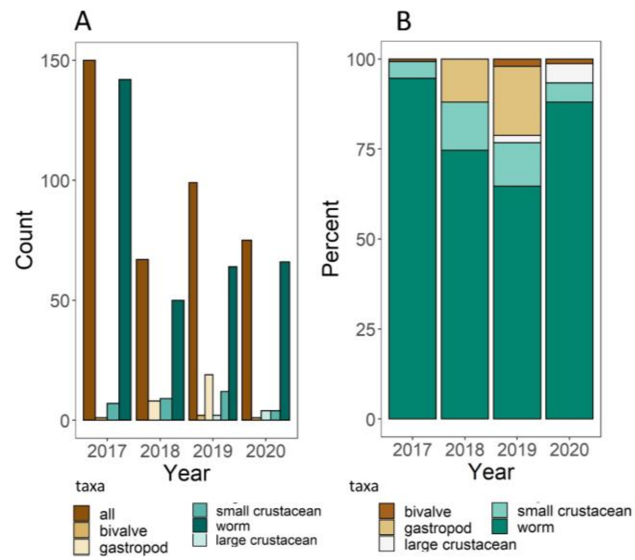

Figure 4.4. Infauna abundance (count) for A) each taxon from combined 8 samples each year and B) the proportion of each taxon from the combined data.

Total biomass (g AFDW) was also highest pre-construction compared to the 3 years post construction. Similar to abundance, biomass was also lowest in year 1, followed by an increasing biomass in year 2, and a slight decline in year 3 post construction (Table 4.4, Figure 4.5). However, the biomass pre-

Table 4.4. Mean infauna abundance, biomass (g AFDW), and sediment organic matter (%) ± standard error (se) for samples collected pre-construction (2017) through year 3 (2020) post construction.

Year	Abundance (count ± se)	AFDW (g ± se)	OM (% ± se)
Pre-construction	18.8 ± 2.9	0.11 ± 0.02	2.05 ± 0.11
1	8.4 ± 1.8	0.12 ± 0.02	1.77 ± 0.28
2	12.5 ±1.8	0.18±0.03	2.15 ± 0.34
3	9.4 ±3.1	0.17 ± 0.05	2.52 ± 0.13

construction is heavily skewed by 1 large bivalve. This is apparent when comparing Figures 4.4 and 4.5 for abundance and AFDW. Without this single specimen the total biomass, pre-construction is similar to that in year 1, but is less than that observed in years 2 and 3 post construction. Overall, no difference in the biomass between years ($F_{3,28}$ =1.04, p = 0.39) was found. In years 2 and 3 post construction, crustaceans also take up larger proportions of the total biomass. The larger variation in sample biomass in year 3 post construction may be explained by the increased presence of larger fauna, with a greater proportion of crustaceans collected.

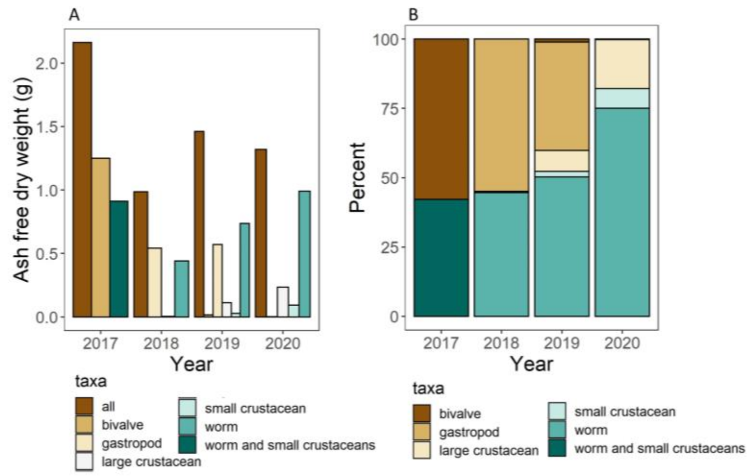

Figure 4.5 Infauna AFDW (ash free dry weight) for A) each taxon for combined 8 samples each year and B) the percent of AFDW for each taxon for combined samples. In pre-construction data (2017) the outlying single bivalve (1.251 g was removed) when analyzing differences in sample abundance between years in the one-way ANOVA.

We also added the relative abundance and biomass for each taxon to determine an importance value. High importance values indicate that a given taxon composes a larger part of the community, whether it be through abundance, biomass or size, or a combination of both. The importance of gastropods (snails) declined through time after construction, while the importance of worms remained high throughout all years (Figure 4.6). The importance of small crustaceans was very high the year after construction and then fell, while the importance of large crustaceans (crabs) increased throughout the years after oyster reef construction.

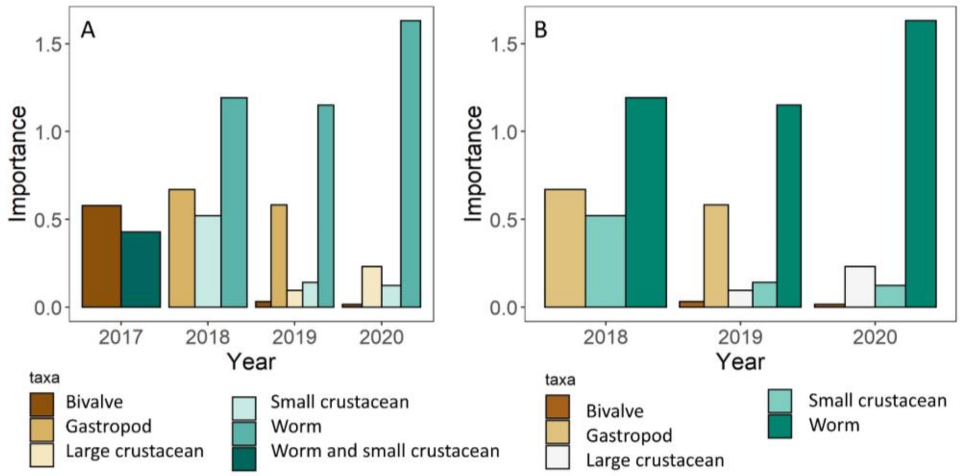

Figure 4.6 A) Importance value for each taxon found in each year's samples. Importance value was calculated by adding together the proportion of each taxa's abundance and biomass in the combined 8 samples collected each year. For pre-construction samples (2017), the importance value was only calculated for 1 bivalve, because AFDW was combined for worms and small crustaceans that year. B) The years after restoration (2018 – 2020, right) emphasize the increasing importance of large and small crustaceans.

Sediment Composition

Sediment organic matter increased after construction of the oyster reefs (Table 4.4). Values ranged from 1.8 % (year 1 post construction) to 2.5 % (year 3 post construction). Despite the increasing trend after construction, analysis found the percent organic matter was not different between years ($F_{3,30}$= 1.9, p = 0.15).

DISCUSSION

Oyster Population

Oyster growth on the high elevation reef design was higher than growth on the low elevation designs. This effect of elevation was also found by other studies where higher elevations contributed to more successful recruitment and growth (Bartol et al. 1999, Lenihan

1999, Schulte et al. 2009). This has been attributed to greater flow rates occurring over more elevated reefs as well as less susceptibility to sedimentation (Lenihan 1999, O'Beirn et al. 1999). The interaction between oyster density on different tiers and year since construction makes interpretation of elevation less clear. Data from year 1 post construction of the reefs indicated clear differences between densities on low and high elevation reef designs, while densities in later years were more similar overall. However, large differences between tiers at the same elevation (tier 2 of the low elevation, and tier 2nd of 4 on the high elevation reef) were shown to exist 3 years post construction. These results emphasize that time, as the reef develops, is important to consider when monitoring overall success of reef designs. The results also indicate that the effect of sheltering provided by higher tiers may become more important as oyster grow and become more susceptible to predation and other physical factors (Bartol et al. 1999, O'Beirn et al. 2000, Whitman & Reidenbach 2012). Additionally, we found some indication that multiple rows may impact oyster densities on high elevation designs, the differences were slight and our data show that density is more dependent on reef elevation than reef width.

Coastal Protection Potential

Observed wave data were captured pre-construction, after construction with little growth (year 1), and after construction with mature oysters (year 3). While minimal changes in significant wave height from bay to marsh occurred over the low elevation oyster reef, attenuation continued to increase over time for the high elevation reef design. Because the data from year 1 come from a time when there was minimal oyster growth on the reefs, the difference between the year 1 and year 3 post construction data show the difference in wave attenuation between the structure itself and with the addition of oysters. Therefore, not only are the structures acting to reduce wave height, and consequent energy from reaching the marsh, but oysters themselves are adding to this service of coastal protection. It should also be noted that for the high elevation reef designs, we observed a greater amount of attenuation in shallower water compared to deeper water. Similar findings were found within the VCR at different locations (Wiberg et al. 2019) and this is likely due to the increased ability of oysters to interact with wave orbitals in shallow water, causing greater frictional resistance, as well as initiate wave breaking before reaching the marsh edge. Little variation in attenuation was observed at the low elevation reef design under intermediate (0.75 m to 1 m water depth) and deep water (> 1 m depth), likely because at these water levels minimal reduction in wave orbitals and interaction with the reef structure occurred.

Infauna Community Responses

The infauna community and sediment composition experienced change as the oyster reefs matured. While worms dominated the infauna community both before and after restoration, larger infauna began to compose greater proportions of biomass and abundance as time since post construction increased. The increase in large crustaceans (such as crabs) near the reefs is likely due to increased habitat and shelter or reefs may act as a predation location (Harwell et al. 2011, Hill & Weissburg 2013). Increases in higher order species can alter community dynamics can be altered, influencing populations of fish and other higher order transient species (Rodney & Paynter 2006, Gregalis et al. 2009). The first summer of sampling after restoration also saw the lowest abundance of infauna, indicating ta disturbance effect observed in year 1 post construction. Sampling in year 3 also occurred the last week of August 2020, rather than early June as the previous 3 years due to lab accessibility due to Covid-restrictions. Therefore, some patterns observed in year 3 may be affected by seasonality and variability of infauna within coastal estuaries (Harwell et al. 2011).

While some oyster restoration studies report rapid responses in infauna communities after oyster restoration (Davis et al. 2006), others found a lag between the growth of oysters and enhancement of infauna communities (Liu et al. 2018). Infauna communities are also subject to great variability both spatially and temporally (Grabowski et al. 2005, Ziegler et al. 2017). Habitats with muddy sediments can take longer time to recover biotic communities compared to cleaner sands (Dernie et al. 2003). This could explain the general increase in infauna abundance and biomass in the years after restoration observed (Figures 4.4 and 4.5). Similarly, change in sediment composition is also likely to be a more gradual process taking place over longer periods of time, especially within our samples using cores taken 5 cm deep. Our findings therefore support previous literature that suggests different services are likely to respond at different timescales (La Peyre et al. 2014, Volaric et al. 2020), with oyster growth and wave attenuation observed more quickly than the responses observed in infauna and sediment composition. This emphasizes the need for long-term monitoring. While the high elevation design in our study worked best to promote multiple ecosystem services, managers should examine reef design for relative elevation compared to marsh elevation and water depth.

Study Limitations

Although we found greater oyster densities and oyster lengths with higher reef elevations, presumably a maximum height exists above which oyster densities and growth rate will decrease, due to decreases in submergence time and increased exposure to atmospheric conditions. An analysis of existing oyster reef elevation throughout the VCR (Hogan & Reidenbach 2019) found that the oyster reef crests ranged from -0.7 to 0.1 m lmsl, reiterating that healthy reefs need to be submerged a portion of the tidal cycle (Ridge et al. 2015). Considering the mean water depth in year 1 post construction was 0.91 m and 1.03 m in year 3, at 80 cm above the seafloor the high elevation reefs were found to be approximately -0.1 to -0.2 m below the msl calculated from wave gauges, placing them about 0.2 m below this maximum elevation range. Future studies could construct reefs both above and below this elevation to test limits on oyster growth. Still, these data indicate that perhaps elevation in addition to tier position are both important in determining oyster growth and survivability. Although there may be some change in elevation due to structure settlement, there is a need to continuously monitor reef elevation because oyster growth adds to the elevation with time. This also highlights an advantage that green nature-based solutions have over traditional solutions, where green solutions can adapt and grow to meet changes such as rising sea levels, continuously buffering coasts, while traditional built structures are made to adjust and fit an environment for only a snapshot in time.

Other biological factors could also affect the outcome of oyster restoration success. We observed the appearance of algal cover on top of tiers and between rows of different designs. Although differences in algal cover were not quantified in this study, algal cover presents another factor that can affect oyster growth and benthic processes not reflected in our data (Thomsen & McGlathery 2006, Volaric et al. 2019). Density was higher year 1 compared to year 2 and 3 post construction, which reported similar oyster densities. This could be due to a growth response, where there is a greater amount of recruitment and development of juveniles early on, but density is reduced as fewer oysters successfully reach maturity (Gosselin & Qian 1997), even though overall biomass may have increased with fewer, larger oysters. Although we did not take length measurements year 1 post construction, it is likely that the oysters were not mature at this time, and therefore although densities were greater, biomass was likely less at this time based upon oyster shell length to biomass ratios reported in the literature (Southworth et al. 2010).

Conclusion

Our study provides evidence that oyster reef design differentially affects ecosystem services provided by oyster restoration. Specifically, higher elevation reefs had more dense oysters with greater lengths on upper tiers compared to lower tiers and wave attenuation was also greatest over the higher elevation design. Wave attenuation increased as the reef matured. Together this data indicate that the higher elevation reef design at Short Prong Marsh works best to foster both oyster growth and coastal protection. The width of the reef (1 row vs. 3 rows) had minimal effect on oyster densities. The presence of restored oyster reefs increased the incidence of higher trophic level species, with crustaceans composing larger proportions and having greater importance of total infauna collected as oyster reefs matured. Additionally, we observed an increasing trend in organic matter with time following restoration. While our results agree with literature that higher elevation reefs better foster oyster growth and wave attenuation, the data also emphasize the need for continued monitoring over long periods of time as reefs mature and accrete vertically.

ACKNLOWLEDGEMENTS

We thank The Nature Conservancy at the Virginia Coast Reserve for constructing the oyster restoration site and partnering with us on this restoration study. We would also like to the thank the staff at the Anheuser-Busch Coastal Research Center for assistance in field studies. This research was funded by the National Science Foundation grant 1832221 to the Virginia Coast Reserve Long Term Ecological Research project. M. Reidenbach was supported by the National Science Foundation grant OCE-1151314.

LITERATURE CITED

Bartol IK, Mann R, Luckenbach M (1999) Growth and mortality of oysters (Crassostrea virginica) on constructed intertidal reefs: effects of tidal height and substrate level. J Exp Mar Biol Ecol 237:157-184

Bilkovic DM, Mitchell MM (2013) Ecological tradeoffs of stabilized salt marshes as a shoreline protection strategy: effects of artificial structures on microbenthic assemblages. Ecol Eng 61:469-481

Borsje BW, van Wesenbeeck BK, Dekker F, Paalvast P, Bouma TJ, van Katwijk MM, De Vries MB (2010) How ecological engineering can serve in coastal protection. Ecol Eng 37:113-122

Bulleri F, Chapman MG (2009) The introduction of coastal infrastructure as a driver of change in marine environments. J Appl Ecol 47:26-35

Byers JE, Grabowski JH, Piehler MF, Hughes AR, Weiskel HW, Malek JC, Kimbro DL (2015) Geographic variation in intertidal oyster reef properties and the influence of tidal prism. Limnol Oceanogr 60:1051-1063

Castel J, Labourg PJ, Escaravage V, Auby I, Garcia ME (1989) Influence of seagrass beds and oyster parks on the abundance and biomass patterns of meio- and macrobenthos in tidal flats. Estuar Coast Shelf Sci 28:71-85

Coen LD, Luckenbach MW (2000) Developing success criteria and goals for evaluating oyster reef restoration: ecological function or resource exploitation? Ecol Eng 15:323-343

Coen LD, Brumbaugh RD, Bushek D, Grizzle R, Luckenbach MW, Posey MH, Powers SP, Tolley G (2007) Ecosystem services related to oyster restoration. Mar Ecol Prog Ser 341:303-307

Davis JLD, Takacs RL, Schnabel R (2006) Evaluating ecological impacts of living shorelines and shoreline habitat elements: an example from the upper western Chesapeake Bay, p. 55-61. In: Erdle SY, Davis JLD, Sellner KG (eds.) Management, policy, science, and engineering of nonstructural erosional control in the Chesapeake Bay, CRC Publ. No. 08 – 164, Chesapeake Bay.

Dernie KM, Kaiser MJ, Warwick RM (2003) Recovery rates of benthic communities following physical disturbance. J Anim Ecol 72:1043-1056

Donadi S, Westra J, Weerman EJ, Van der Heide T, Van der Zee EM, Van de Koppel J, Olff H, Piersma T, Van der Veer HW, Eriksson BK (2013) Nontrophic interactions control benthic producers on intertidal flats. Ecosystems 16:1325-1335

Ehrenfeld JG (2000) Defining the limits of restoration: the need for realistic goals. Restor Ecol 8:2-9

Fagherazzi S, Wiberg PL (2009) Importance of wind conditions, fetch, and water levels on wave-generated shear stresses in shallow intertidal basins. J Geophys Res 114 F03022, doi:10.1029/2008JF001139

Fodrie FJ, Rodriguez AB, Baillie CJ, Brodeur MC, Coleman SE, Gittman RK, Keller DA, Kenworthy MD, Poray AK, Ridge JT, Theuerkauf EJ, Lindquist NL (2014) Classic paradigms in a novel environment: inserting food web and productivity lessons from rocky shores and saltmarshes into biogenic reef restoration. J Appl Ecol 51:1314-1325

Fuchs HL, Reidenbach MA (2013) Biophysical constraints on optimal patch lengths for settlement of a reef-building bivalve. PLOS ONE 8: e71506

Fulford RS, Breitburg DL, Luckenbach M, Newell REI (2010) Evaluating ecosystem response to oyster restoration and nutrient load reduction with a multispecies bioenergetics model. Ecol Appl 20:915-934

Grabowski JH, Hughes AR, Kimbro DL, Dolan MA (2005) How habitat setting influences restored oyster reef communities. Ecology 86:1926-1935

Grabowski JH, Peterson CH (2007) Restoring oyster reefs to recover ecosystem services. In: Cuddington K, Byers JE, Wilson WG, Hastings A (eds) Ecosystem engineers: concepts, theory and applications 281-298. Amsterdam: Elsevier-Academics Press.

Grabowski JH, Brumbaugh RD, Conrad RF, Keeler AG, Opaluch JJ, Peterson CH, Piehler MF, Powers SP, Smyth AR (2012) Economic valuation of ecosystem services provided by oyster reefs. BioScience 621: 900-909

Gregalis KC, Johnson MW, Powers SP (2009) Restored oyster reef location and design affect responses of resident and transient fish, crab, and shellfish species in Mobile Bay, Alabama. Trans Am Fish Soc 138:314-327

Gorska B, Gromisz S, Wlodarska-Kowalczuk M (2019) Size assessment in polychaete worms – application of morphometric correlations for common North Atlantic taxa. Limnol Oceanogr Methods 17:254-265

Gosselin LA, Qian P (1997) Juvenile mortality in benthic marine invertebrates. Mar Ecol Prog Ser 146:265-282

Gutierrez JL, Jones CG, Strayer DL, Iribarne OO (2003) Mollusks as ecosystem engineers: the role of shell production in aquatic habitats. Oikos 101:79-90

Hansen JC, Reidenbach MA (2013) Seasonal growth and senescence of a Zostera marina seagrass meadow alters wave-dominated flow and sediment suspension within a coastal bay. Estuar Coast 36: 1099-1114

Harwell HD, Posey MH, Alphic TD (2011) Landscape aspects of oyster reefs: effects of fragmentation on habitat utilization. J Exp Mar Biol Ecol 409:30-41

Hill JM, Weissburg MJ (2013) Habitat complexity and predator size mediate interactions between intraguild blue crab predators and mud crab prey in oyster reefs. Mar Ecol Prog Ser 488:209 -219

Hogan S, Reidenbach MA (2019) Quantifying and mapping intertidal oyster reefs utilizing LiDAR-based remote sensing. Mar Ecol Prog Ser 630:83-99

Howmiller RP (1972) Effects of preservatives on weights of some common microbenthic invertebrates. Trans Am Fish Soc 4:743-746

Hubbard AB, Reidenbach MA (2015) Effects of larval swimming behavior on the dispersal and settlement of the eastern oyster Crassostrea virginica. Mar Ecol Prog Ser 535: 161-176

Johnson KD, Smee D (2014) Predators influence the tidal distribution of oyster (Crassostrea virginica). Mar Biol 161:1557-1564

Kemp WM, Boynton WR, Adolf JE, Boesch DF, Boicourt WC, Brush G, Cornwell JC, Fisher TR, Glibert PM, Hagy JD, Harding LW, Houde ED, Kimmel DG, Miller WD, Newell RIE, Roman MR, Smith EM, Stevenson JC (2005) Eutrophication of Chesapeake Bay: historical trends and ecological interactions. Mar Ecol Prog Ser 303:1-29

La Peyre MK, Humphries AT, Casas SM, La Peyre JF (2014) Temporal variation in development of ecosystem services from oyster reef restoration. Ecol Eng 64:34-44

Langlois TJ, Anderson MJ, Babcock RC (2006) Inconsistent effects of reefs on different size classes of macrofauna in adjacent sand habitats. J Exp Mar Biol Ecol 334:269-282

Lenihan HS (1999) Physical-biological coupling on oyster reefs: how habitat structure influences individual performance. Ecol Monogr 69:251-275

Length RV (2020) emmeans: Estimated Marginal Means, aka Least-Squares Means. R package version 1.5.3. https://CRAN.R-project.org/package=emmeans.

Liu ZQ, Yu P, Chen M, Cai M, Fan B, Lv W, Youhui H, Li Y, Zhao Y (2018) Macrobenthic community characteristics and ecological health of a constructed intertidal oyster reef in the Yangtze Estuary, China. Mar Pollut Bull 135: 95-104 doi: 10.1016/j.marpolbul.2018.07.019.

Mann R, Powell EN (2007) Why oyster restoration goals in the Chesapeake Bay are not and probably cannot be achieved. J Shellfish Res 26:905-917

Mariotti G, Fagherazzi S (2013) Critical width of tidal flats triggers marsh collapse in the absence of sea-level rise. Proc Natl Acad Sci USA 110:5353-5336

Meyer DL, Townsend EC, Thayer GW (1997) Stabilization and erosion control value of oyster clutch for intertidal marsh. Restor Ecol 5:93-99

Millennium Ecosystem Assessment (MEA) Ecosystems and Human Well-Being: Synthesis (2005) Washington DC: Island Press

Nelson E, Mendoza G, Regetz J, Polasky S, Tallis H, Cameron DR, Chan KMA, Daily GC, Goldstein J, Kareiva PM, Lonsdorf E, Naidoo R, Ricketts TH, Shaw MR (2009) Modeling multiple ecosystem services, biodiversity conservation, and tradeoffs at landscape scales. Front Ecol Environ 7: 4-11

North EW, King DM, Xu J, Hood RR, Newell REI, Paynter K, Kellog ML, Liddel MK, Boesch DF (2010) Linking optimization and ecological models in a decision support tool for oyster restoration and management. Ecol Appl 23:851-866, doi.org/10.1890/08-1733.1

O'Beirn FX, Luckenbach M, Mann RL, Harding J, Nestlerode J (1999) Ecological functions of constructed oyster reefs along an environmental gradient in Chesapeake. Final Report, Aquatic Reef Habitat Program, Chesapeake Bay Program, Annapolis, MD

O'Beirn FX, Luckenbach M, Nestlerode JA, Coates GM (2000) Toward designing criteria in constructed oyster reefs: oyster recruitment as a function of substrate type and tidal height. J Shellfish Res 19: 387-395

Piazza BP, Banks PD, La Peyre MK (2005) The potential for created oyster shell reefs as a sustainable shoreline protection strategy in Louisiana. Restor Ecol 13:499-506

Reidenbach MA, Berg P, Hume A, Hansen JC, Whitman ER (2013) Hydrodynamics of intertidal oyster reefs: The influence of boundary layer flow processes on sediment and oxygen exchange. Limnol Oceanogr Fluids Environ 3:225-239

Ridge JT, Rodriguez AB, Fodrie FJ, Lindquist NL, Brodeur MC, Coleman SE, Grabowski JH, Theuerkauf EJ (2015) Maximizing oyster-reef growth supports green infrastructure with accelerating sea-level rise. Sci Rep 5:14785 doi.org/10.1038/srep14785

Rodney WS, Paynter KT (2006) Comparisons of macrofaunal assemblages on restored and non-restored oyster reefs in mesohaline regions of the Chesapeake Bay in Maryland. J Exp Mar Biol Ecol 335:39-51

Rumohr H (2009) Soft-bottom macrofaunal: Collection, treatment, and quality assurance of samples. ICES Techniques in marine environmental Sciences 43, doi: http://dx.doi.org/10.25607/OBP-238

Rothschild BJ, Ault JS, Goulletquer P, Jensen WP, Heral M (1994) Decline of the Chesapeake Bay oyster population: a century of habitat destruction and overfishing. Mar Ecol Prog Ser 111:29-39

Safak I, Wiberg PL, Richardson DL, Kurum MO (2015) Controls on residence time and exchange in a system of shallow coastal bays. Cont Shelf Res 97:7-20

Schulte DM, Burke RP, Lipcius RN (2009) Unprecedented restoration of a native oyster metapopulation. Science 325:1124-1128

Smaal AC, Prins TC (1993) The uptake of organic matter and release of inorganic nutrients by bivalve suspension feeder beds. In: Dame RF (ed) Bivalve filter feeders in estuarine and coastal ecosystem processes 271-298. Berlin: Springer-Verlag.

Smyth AR, Geraldi NR, Thompson SP, Piehler MF (2016) Biological activity exceeds biogenic structure in influencing sediment nitrogen cycling in experimental oyster reefs. Mar Ecol Prog Ser 560: 173-183

Soniat TM, Finelli CM, Ruiz JT (2004) Vertical structure and predator refuge mediate oyster reef development and community dynamics. J Exp Mar Biol Ecol 310:163-182

Southwell MW, Veenstra JJ, Adams CD, Scarlett EV, Payne KB (2017) Changes in sediment characteristics upon oyster reef restoration, NE Florida, USA. J Coast Zone Manag 20:442 doi: 10.4172/2473-3350.1000442

Southworth M, Harding JM, Wesson JA, Mann R (2010) Oyster (Crassostrea virginica, Gmelin 1791) population dynamics on public reefs in the Great Wicomico River, Virginia, USA. J Shellfish Res 29:271-290

Theuerkauf SJ, Burke RP, Lipcius RN (2015) Settlement, growth, and survival of eastern oysters on alternative reef substrates. J Shellfish Res 34:241-250

Thomsen MS, McGlathery K (2006) Effects of accumulations of sediments and drift algae on recruitment of sessile organisms associated with oyster reefs. J Exp Mar Biol Ecol 328:22-34

Van der Zee EM, Van der Heide T, Donadi S, Eklof JS, Eriksson BK, Olff H, Van der Veer HW, Piersma T (2012) Spatially extended habitat modification by intertidal reef-building bivalves has implications for consumer-resource interactions. Ecosystems 15: 664-673

Van der Zee EM, Tielens E, Holthuijsen S, Donadi S, Eriksson BK, Van der Veer HW, Piersma T, Olff H, Van der Heide T (2015) Habitat modification drives benthic trophic diversity in an intertidal soft-bottom ecosystem. J Exp Mar Biol Ecol 465:41-48

Venables WN, Ripley BD (2002) Modern Applied Statistics with S. 4th ed. New York: Springer

Volaric MP, Berg P, Reidenbach MA (2018) Oxygen metabolism of intertidal oyster reefs measured by aquatic eddy covariance. Mar Ecol Prog Ser 599:75-91

Volaric MP, Berg P, Reidenbach MA (2019) An invasive macroalga alters ecosystem metabolism and hydrodynamics on a tidal flat. Mar Ecol Prog Ser 628:1-16

Volaric MP, Berg P, Reidenbach MA (2020) Drivers of Oyster Reef Ecosystem Metabolism Measured Across Multiple Timescales. Estuar Coast 43:2034–2045

Wetzel MA, Leuchs H, Koop JHE (2005) Preservation effects on wet weight, dry weight, and ash-free dry weight biomass estimates of four common estuarine macro-invertebrates: no difference between ethanol and formalin. Helgol Mar Res 59:206-213

Whitman ER, Reidenbach MA (2012) Benthic flow environments affect recruitment of *Crassostrea virginica* larvae to an intertidal oyster reef. Mar Ecol Prog Ser 463:177-191

Wiberg P, Taube SR, Ferguson AE, Kremer MR, Reidenbach MA (2019) Wave attenuation by oyster reefs in shallow coastal bays. Estuar Coast 42:331-347

Zhang S, Liu Y, Yang H (2014). Biologically induced deposition of fine suspended particles by filter-feeding bivalves in land-based industrial marine aquaculture wastewater. PLOS ONE 9(9): e107798, https://doi.org/10.1371/journal.pone.0107798

Ziegler SL, Grabowski JH, Baillie CJ, Fodrie FJ (2017) Effects of landscape setting on oyster reef structure and function largely persist more than a decade post-restoration. Restor Ecol 26: 933 – 942

CHAPTER 5: Quantifying the influence of oyster reefs on infauna and sediment distributions within intertidal mudflats

This chapter has been submitted to *Marine Ecology Progress Series* with Elizabeth AK Murphy, Martin P Volaric, Max CN Castorani, Peter Berg, and Matthew A Reidenbach as co-authors

ABSTRACT

Oysters are described as estuarine ecosystem engineers because their reef structures provide habitat for a variety of flora and fauna, alter hydrodynamics, and can affect sediment composition. Benthic infauna living within the reef and in adjacent sediments are directly influenced by these alterations. However, to what spatial extent oyster reefs can influence sediment composition and infauna distributions surrounding the oyster reefs remains uncertain. We sampled sediment and infauna across eight intertidal mudflats, with distances up to 100 m from oyster reefs within coastal bays of Virginia, USA, to determine if distance from reefs and physical site characteristics (elevation and hydrodynamics) explain the spatial distributions of infauna and sediment. We found that taxa diversity and total infauna density increased with distance from reefs, however, the opposite was observed for large crustaceans (crabs). The probability of observation increased for gastropods and bivalves and decreased for large crustaceans by 2.5 times within ~40 m from oyster reefs. Water residence time, used to quantify the movement of water, was found to have the strongest correlation to both organic matter and grain size, indicating local water velocities, not proximity to reefs, primarily drives the spatial distribution of sediment composition within the surrounding intertidal mudflat. This study emphasizes the complex nature of bio-physical couplings and the spatial extent to which oyster reefs can engineer intertidal communities.

Key words: ecosystem engineers, oyster reefs, infauna, sediment, distributions

INTRODUCTION

Ecosystem engineers are organisms that affect communities directly and indirectly by influencing resource availability via the creation or modification of physical structures (Jones et al. 1994, Angelini et al. 2011). Common examples of ecosystem engineers include animals, such as beavers that create dams (Jones et al. 1994, Wright & Jones 2002) and plants, such as trees (Jones et al. 1997), that alter flows of nutrients, chemical cycling, and habitat provisioning. However, the spatial scale over which ecosystem engineers affect communities and ecosystems is often difficult to define and is largely dependent on the species and alteration or process examined (Wright & Jones 2004, Hastings et al. 2007). Small-scale effects may go undocumented because they are more difficult to detect or measure. For example, large physical habitat modifications, such as beaver dams and tree canopies are easily observable, while smaller scale processes such as changes to soil biogeochemistry require more careful analysis over specified spatial and temporal scales (Jones et al. 1997, Wright & Jones 2004, Hastings et al. 2007). Therefore, careful consideration for the engineering species and processes quantified are necessary in determining scales of influence.

Given their abilities to impact environments, ecosystem engineers are often incorporated into landscapes as part of restoration efforts (Byers et al. 2006). Thus, to help guide the siting and design of restoration projects, determining the spatial extent over which ecosystem engineers impact their environment is important. Managers of estuarine ecosystems often incorporate ecosystem engineers as a part of nature-based solutions to improve ecosystem functions such as coastal protection, biodiversity, and water quality (Davis et al. 2006, Currin et al. 2010). One of these marine ecosystem engineers is the oyster. Oysters are hard-bodied organisms that build solid, fixed structures in otherwise unstable soft-sediment systems and alter the abiotic environment in three major ways. First, physical reef structures provide habitat and refuge to fauna including polychaetes, crustaceans, and fish (Posey et al. 1999, Lenihan et al. 2001, Grabowski et al. 2005). Second, they change hydrodynamic patterns by virtue of this physical structure. The rough surface of oyster reefs increases drag and turbulence, altering flow patterns and locally increasing sediment resuspension and transport from the reef crest, while also trapping fine sediments adjacent to the reef (Lenihan 1999, Whitman & Reidenbach 2012, Reidenbach et al. 2013, Colden et al. 2016). Oyster reefs can attenuate wave energy and in some cases reduce shoreline erosion (Piazza et al. 2005, Wiberg et al. 2019). Third, oysters can change sediment composition by altering grain size, organic matter content, and sediment biogeochemistry through direct inputs of pseudofeces deposited from filter feeding and the indirect facilitation of benthic microalgae productivity (Newell et al. 2002, Kellogg et al. 2013, Southwell et al. 2017). The fine particles, which are likely to be trapped, also hold nutrients in organic rich sediments more readily (Nedwell 1999).

Burrowing organisms (infauna) dominate muddy intertidal habitats and are considered ecosystem engineers due to their bioturbation (Aller 1993, Meysman et al. 2006) which can oxygenate sediment and increase available habitat for themselves and other infauna (Solan et al. 2004, Byers & Grabowski 2014, Murphy & Reidenbach 2016). Infauna community structure is dependent on many factors, including sediment and water characteristics such as grain size, temperature, pH, and oxygenation (Paterson et al. 2009, Widdicombe et al. 2009, Dauvin et al. 2017, Veiga et al. 2017). Sediment grain size, which is influenced by oyster reefs, can affect infauna's ability to burrow, consume oxygen, and feed (Wilson 1990, Janssen et al. 2005, Dorgan et al. 2016). A shift to finer sediments, which compact more easily, can limit the advection and diffusion of water and dissolved gases through interstitial porewaters resulting in thinner oxic layers and flatter topography relative to areas with coarser grained sediments and less compaction (Byers & Grabowski 2014, Nybakken & Bertness 2005). Therefore, oyster mediated changes to sediments and hydrodynamics may have cascading effects on estuarine ecosystem function, affecting biodiversity, sediment stability (Dashtgard et al. 2008), and biogeochemical processes.

Relevant to restoration efforts, burrowers help prevent negative impacts of disturbances in linked systems, such as the top layer of sediment and the water above, whereby diverse infauna populations can increase nutrient transfers, lessen the impact of species loss, and stabilize trophic interactions (Austen et al. 2002). Benthic diversity can also have positive effects on the overall health of estuarine environments by increasing water column nutrient availability (Ieno et al. 2006) and increasing nutrient cycling (Covich et al. 2004). Infauna are also important prey for mobile invertebrates, birds, and fish, helping to shape community structure (Van der Zee et al. 2012).

Studies of the effects of bivalves and rocky reefs on adjacent infauna communities are mixed and have largely focused on in subtidal environments (Table 5.A1). Researchers have found, depending upon the composition of infauna, benthic communities in proximity to reefs can either be enhanced (Ambrose and Anderson 1990, Dahlgren et al. 1999, Barros et al. 2001, Barros et al. 2004, Langlois et al. 2005, Zalmon et al. 2014), or decreased (Posey & Ambrose 1994, Ambrose & Anderson 1990, Barros et al. 2001, Langlois et al. 2005, Reeds et a. 2018) with respect to abundance, density, and/or richness. Reeds et al. (2018) identified that the ecological footprint of a single constructed reef may be up to 15 times the area of the reef. However, most studies found that patterns varied among species and with organism size (Davis et al. 1982, Ambrose & Anderson 1990, Fabi et al. 2002, Langlois et al. 2006), demonstrating that taxa-specific behaviors and tolerances are important to consider in understanding reef-infauna relationships.

To determine how oysters' impact the spatial distribution of infauna and sediment composition through ecosystem engineering, we sampled eight intertidal mudflats adjacent to oyster reefs in coastal Virginia, USA, to quantify how distance to oyster reefs can explain infauna and sediment distributions. Together this work describes how local site characteristics, including distance to oysters, elevation, and hydrodynamics, work to influence community structure.

MATERIALS & MEHTODS

Study Site

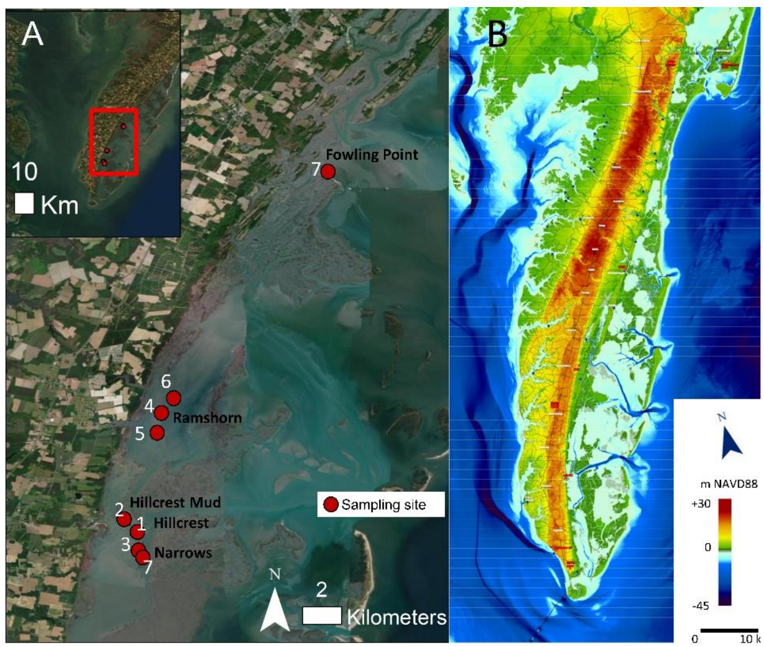

Figure 5.1. A) Locations of the 8 intertidal mudflats situated near oyster reefs that were sampled, labeled according to sites in Table 1. The inset shows the extent of the Virginia Coast Reserve (VCR), found on the eastern side of the Delmarva Peninsula. B) Bathymetry for the region with elevation and depth (meters) relative to the North American Vertical Datum of 1988 (NAVD88) zero (Richardson et al. 2018)

We studied intertidal mudflats located within the Virginia Coast Reserve (VCR). The VCR is within the Volgenau Virgina Coast Reserve (VVCR), a system of barrier islands, coastal bays, and upland marshes extending across more than 100 km of coastline along the Atlantic Ocean of the Delmarva Peninsula in Virginia, USA (Figure 5.1). The VCR is also a National Science Foundation funded Long-term Ecological Research (LTER) site. The tidal range is approximately 1.2 m (Hansen &

Reidenbach 2013) and within the intertidal mudflats, numerous oyster reefs exist primarily as patch reefs of the Eastern oyster, *Crassostrea virginica.* In this system, the majority of oyster reefs have been heavily influenced by human activity and have largely been restored starting in the mid to late 1900s (Luckenbach et al. 2005, Kennedy et al. 2011). The oysters are predominately intertidal and restoration has relied on providing hard substrate to provide elevated structure suitable for oyster larval settlement and growth (Whitman & Reidenbach 2012). Previous work in the VCR has shown that oysters affect resident flora and fauna (Thomsen & McGlathery 2006) and alter benthic metabolism (Volaric et al. 2018).

Data Collection

We sampled eight intertidal mudflat sites in proximity to oyster reefs (Figure 5.1 and 5.2) during the summers of 2016 and 2019. In 2016, we collected infauna and sediment samples at 4 sites (sites 1-4, Table 5.1) along 100 m transects (2-4 transects per site) starting from oyster reefs. Site 2 was largely a control with oyster patches interspersed and transects did not start at a particular reef. Infauna cores (25 cm diameter, 10 cm deep) were collected every 0, 28, 56, and 98 m and sediment cores (3 cm diameter, 5 cm deep) were taken every 14 m along each transect (n = 4 samples per transect for infauna, n = 8 samples per transect for sediment), except for one transect where infauna samples were taken at 0, 12.5, 50, and 87.5 m and sediment cores taken every 12.5). In 2019, we sampled infauna and sediment at 4 additional sites (5-8, Table 5.1), using a gridded sampling design to ensure varied

Table 5.1. Sampling site metadata including mudflat local name, year sampled, and the number of cores collected.

Site number	Local name	Year	Infauna cores	Sediment cores
1	Hillcrest	2016	16	32
2	Hillcrest Mud	2016	12	24
3	Narrows	2016	8	16
4	Ramshorn C	2016	8	16
5	Ramshorn A	2019	16	28
6	Ramshorn B	2019	16	28
7	Narrows A	2019	16	28
8	Fowling Point	2019	16	28

distances from reefs. At each site, we sampled along four, 75 m transects spaced 25 m apart and arranged parallel to reefs where they were continuous or the edge of the mudflat where reefs were patchy (Figure 5.2). At each transect, we collected infauna cores (15 cm diameter, 15 cm deep) every 25 m (n = 4 per transect, 16 per site) and sediment cores (3 cm diameter, 5 cm deep) every 12.5 m (n = 7 per transect, n = 28 per site). Sediment samples for organic matter and grain size analysis were kept frozen and refrigerated, respectively, until processed, while infauna samples were processed immediately following collection.

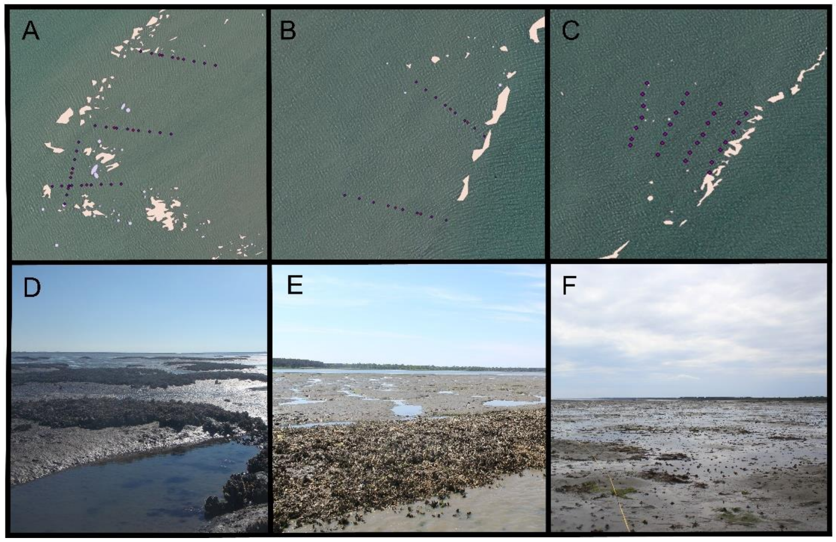

Figure 5.2. Infauna and sediment sampling locations along transects at site 1 (A), site 4 (B), and site 6 (C) and ground views of the oyster reefs at site 1 (D) and site 4 (E). Site 1 (A & D) illustrates a patchy oyster reef complex, where site 4 (B & E) illustrates a more continuous reef. Panel F shows a ground view of a sampling transect directed away from a reef.

Infauna cores were wet sieved (1mm mesh) and living fauna were identified to five broad taxonomic levels: polychaetes, bivalves, gastropods (dominated by snails), small crustaceans (amphipods, isopods, shrimp), and large crustaceans (crabs). Though dominated by burrowers, the epifaunic gastropods where also included in the benthic infauna analysis. In 2016, polychaetes were identified to the family level to determine the diversity of polychaetes, with a list of taxa and total counts given in Table 5.A2. Rarely, nemerteans and acorn worms (*Enteropneusta*) were identified. These organisms were included in the polychaete taxon for analysis. Abundance for each taxon and total biomass for each sample (ash free dry weight, AFDW) were recorded. Infauna were dried for 48 h at 60º C to measure dry weight and combusted for 6 h at 500º C for AFDW. Sediment organic matter was estimated using the same procedure for AFDW. In 2016, sediment grain size was estimated using a Beckman Coulter LS I3 320 laser diffraction particle size analyzer, following treatment with hydrogen peroxide to remove organic matter. Sediment was also sampled for porosity in 2016, but data were found to be highly correlated to grain size and was not included as a separate parameter in the analysis. Linear distance to the nearest oyster reef greater than 5 m^2 was determined using GIS software (ArcMap 10.5) with an existing oyster reef polygon map based on LiDAR elevation (Hogan & Reidenbach 2020). Reefs not included in that dataset were added using the same methods (Hogan & Reidenbach 2019).

Data Analysis

Interpolated surfaces

To determine how infauna communities and sediment composition change with distance to oyster reefs, geospatially-interpolated prediction surfaces for total infauna, sediment organic matter, and sediment grain size distributions at each sampling site were created using the Geostatistical Analyst extension in ArcMap (10.5). Geostatistical interpolation has the advantage of modeling data between known data points. We used Empirical Bayesian Kriging (EBK) to create a distribution of prediction surface responses based on spatial autocorrelation, semivariogram estimation, and associated errors. EBK predictions are ideal for non-stationary and less spatially dense data because predictions are based on the probability of likelihoods from many semivariograms parameters estimated using restricted maximum likelihood rather compared to other kriging methods using only one semivariogram with estimation using weighted least squares (Krivoruchko 2012, ESRI 2016). The Exploratory Spatial Data Analysis

(ESDA) package was used to help examine distributions and normality to meet assumptions for best modeling, showing if transformations would likely lead to the best fitting semivariograms. Semivariogram model, transformation type, and search neighborhood type (standard circular or smoothed circular with minimum 10 neighbors) were chosen from all possible combinations based on that with the lowest root-mean-square-error (RMSE; Gunarathna et al. 2016, Gupta et al. 2017).

Geostatistical layers for total infauna specimen were created for 6 of the 8 sites (sites 1,2, and 5-8). We were unable to create interpolated rasters for sites 3 and 4 because we collected only 8 infauna cores from these sites. Sediment organic matter was modeled for all 8 sites and grain size for the 4 sites from 2016 (sites 1-4).

Statistical Analyses

To determine the spatial extent to which oyster reefs affect the composition of infauna and sediment surrounding the reefs, we examined sediment organic matter and infauna variables (biomass, density, and presence/absence for taxon groups and the total community) as a function of distance to the reef, elevation, and site water residence time (as a proxy for local flow). Elevation was determined at each sample location using a 2015 USGS LiDAR elevation raster layer (Dewberry 2016). Water residence time (WRT) was estimated using an empirically validated regional hydrodynamic model (Safak et al. 2015). A low WRT suggests the active flushing of water masses, typically associated with higher mean flow rates.

Correlation analysis

Data analysis showed highly non-normal distributions. Therefore, we used non-parametric Spearman's rank correlation (Hauke & Kossowski 2011, Zar 2014), to quantify pairwise associations between infauna variables (including total community AFDW, and density for the broad categories of taxa polychaetes, bivalves, gastropods, small crustaceans, and large crustaceans) and site characteristics (distance, elevation, and WRT). Because sampling cores for infauna differed in size between the two sampling years, we converted the abundances and AFDW measurements in 2016 and 2019 to density m^{-3}. Previous studies have explained taxa specific relationships with distance to reefs (Ambrose & Anderson 1990, Davis et al. 1982, Fabi et al. 2002, Langlois et al. 2006), we therefore investigated trends in densities of each taxon group and the total infauna community. We removed three observations where AFDW estimates were less than 0, likely due to minimal AFDW that were below the accuracy of our measurements.

For sediment variables, we fit Spearman's rank correlations between percent organic matter with distance, elevation, and WRT. Grain size was only sampled for 2016 (samples n = 88, sites = 4). For grain size, the same variables of distance, elevation, and WRT were used in correlations. We also examined the correlation between organic matter and grain size.

We used the rcorr function in the "Hmisc" package (Harrell 2021) in R 4.0.3 (R Core Team 2020) to obtain correlation coefficients and p-values.

Multiple Regression Analysis

Because infauna density was largely driven by polychaetes (present in all but 2 samples), we used binomial multiple regression analyses to explain variation in the presence or absence of bivalves, gastropods, small crustaceans, and large crustaceans. We also analyzed the total number of taxa (including polychaetes) present, our metric for richness, as a continuous independent variable.

For bivalves, gastropods, small crustaceans, and large crustaceans, we used generalized linear mixed models (GLMM) to model the presence or absence of individual taxa (with logit link function) as a function of elevation and distance. Taxa richness was modeled using a Poison GLMM (log link function). To control for heterogeneity among sites and collection dates, we specified site and year as random intercept terms for all GLMMs.

We fit a linear mixed-model to predict sediment grain as a function of distance, elevation, and WRT with a random intercept for site.

Mixed models were fit in R using ‘lme4’ 1.1.25 (Bates et al. 2015) and were validated by examining simulated residuals using ‘DHARMa” package in R (Hartig 2020). Data for sediment organic matter were unable to meet the assumptions tested by DHARMa; thus, we analyzed these data using Spearman’s rank correlations only.

RESULTS

Geostatistical Interpolations

For total infauna, there is a trend of increasing abundance away from oyster patches, however, some of the sites with patchier oyster reefs show less overall variability as a function of distance (Figure 5.3A). Meanwhile, sediment organic matter tended to be higher closer to reefs (Figure 5.3B). Similarly, the data from sites with patchier oyster reefs, show less variability. This pattern

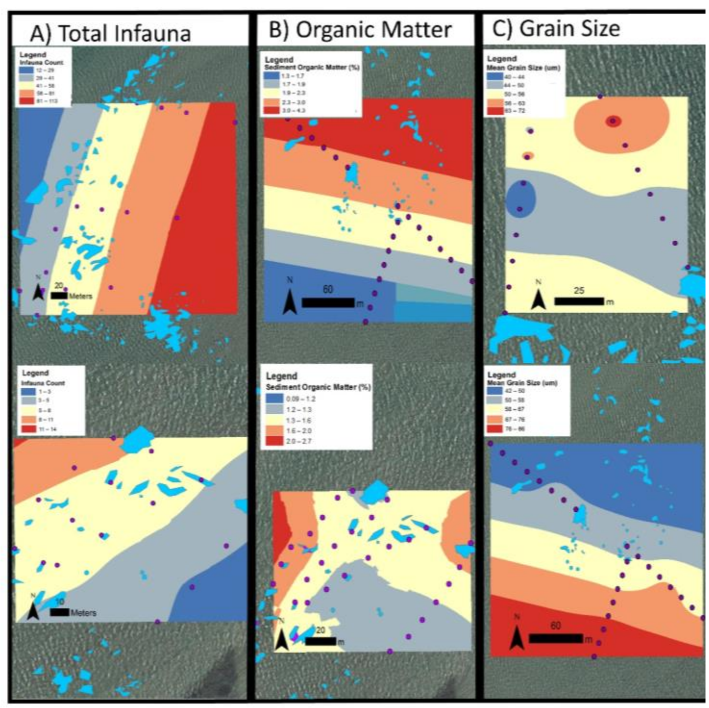

Figure 5.3. Examples of interpolated surfaces for A) total infauna count (sites 1 and 7, top and bottom panels) B) sediment organic matter (sites and 2 and 7) and C) sediment grain size (sites 3 and 2). Two sampling sites for each variable are displayed. High to low values are colored along a red – blue gradient, though the scale changes between site and for each variable. Digitized oyster reef polygons are seen overlaid the surfaces in light blue. Purple points indicate the location of infauna or sediment cores at each site.

also applied to the grain size distributions (Figure 5.3C), but with a pattern of smaller gain size nearer reefs. Only at one of the sites (site 4) was the spatial pattern reversed.

Table 5.2. Spearman's rank correlation coefficients (ρ) and p-values (ρ /p-value) for taxa density (per m^{-3}), biomass (per m^{-3}), and site variables (distance, elevation, and WRT). Red text indicates significant correlations.

	DISTANCE	ELEVATION	WRT
DISTANCE	1/ --	-0.05 /0.63	-0.02/0.87
TOTAL INFAUNA	0.26/0.01	-0.29/0.00	-0.38/0.00
TOTAL AFDW	-0.02/0.87	0.02/0.81	-0.22/0.02
POLYCHAETE	0.24/0.02	-0.43/0.00	-0.32/0.00
BIVALVES	0.25/0.01	-0.22/0.03	-0.39/0.00
GASTROPODS	0.39/0.00	-0.22/0.02	-0.43/0.00
SMALL CRUSTACEANS	0.16/0.10	-0.17/0.08	-0.24/0.01
LARGE CRUSTACEANS	-0.27/0.00	0.30/0.00	-0.06/0.55

Correlation Analyses

Spearman's rank correlations found correlations between infauna variables and at least one site characteristic, including distance, elevation, and WRT (See Table 5.2 for all test statistics). Distance from oyster reefs was not correlated to elevation or WRT. Bivalves and gastropods were correlated with all site variables, with densities increasing farther from reefs, at

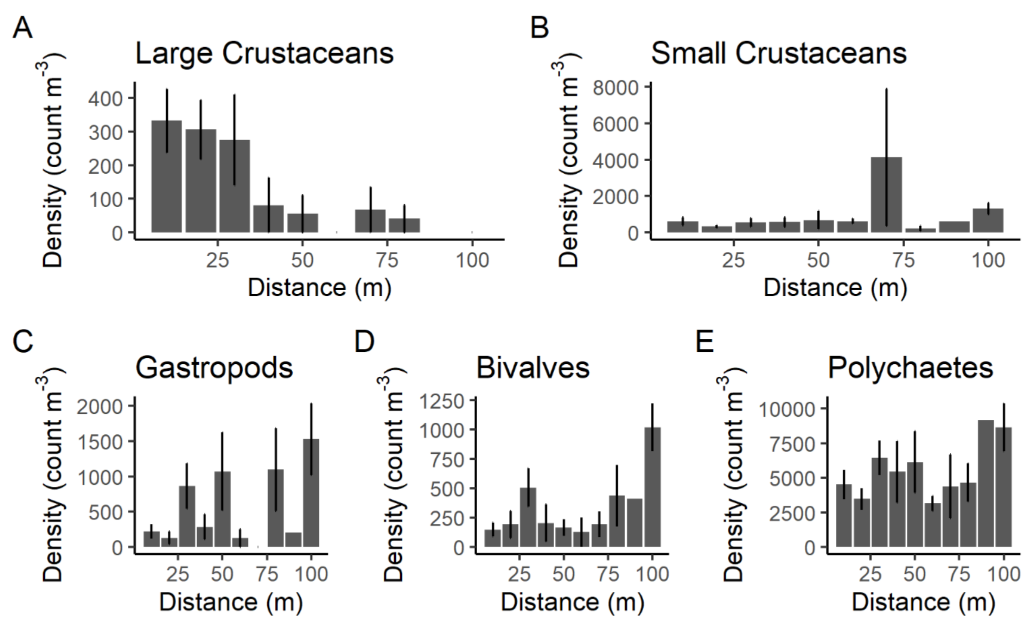

Figure 5.4. Bar plots for taxa densities at sampled at different distances from oyster reefs. Bars (± standard error) represent the mean density (count m^{-3}) from binned data from every 10 m from oyster reefs for A) large crustaceans, B) small crustaceans, C) gastropods, D) bivalves, and E) polychaetes

lower elevations, and in faster flows (lower WRT). By contrast, large crustaceans were denser closer to reefs and at higher elevations (Figure 5.4 and 5.5). Small crustaceans did not vary with distance from reefs or elevation but were more abundant in faster flows (lower WRT). Polychaete density increased with distance from reefs, at lower elevations, and with faster flows. Total infauna density increased further from reefs and at lower elevations, while total biomass was only increased with low WRT values (faster flows).

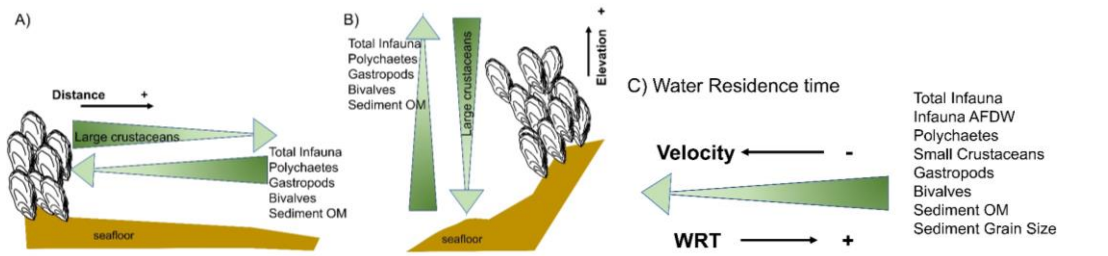

Figure 5.5. Conceptual diagrams for significant correlations for infauna and sediment variables with A) distance B) elevation C) WRT. For infauna and sediment variables the direction of the green arrow indicates a decreasing magnitude of the variable. The magnitude of the site variables is indicted by +/- signs.

For sediment, organic matter was decreased further from oyster reefs and at higher elevations (Table 5.3, Figure 5.5 and 5.6). Organic matter also increased with slower water velocities. Grain size decreased with WRT values and sediment organic matter (Table 5.3, Figures 5.5 and 5.6). This indicates that finer sediment particles are associated with high organic matter and slower moving flows. The analyses for organic matter and grain size agree since organic matter is negatively related to grain size, and with slower flows there should be increased organic matter and reduced grain size.

Table 5.3. Spearman's rank correlation coefficients (ρ) and p-values for sediment grain size and percent organic matter with site variables (distance, elevation, WRT, and each other).

Site Variable	Percent OM		Grain size	
	ρ	p-value	ρ	p-value
Distance	-0.25	0.001	-0.08	0.47
WRT	0.48	0.00	-0.27	0.01
elevation	-0.28	0.00	0.02	0.84
OM	---	---	-0.87	0.00

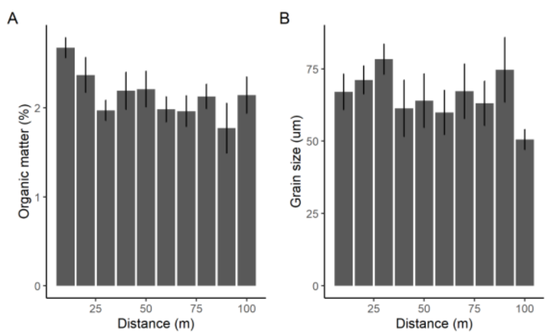

Fig. 5.6. Bar plots of A) organic matter (%) and B) grain size (μm) at varied distances from oyster reefs. Bars (± standard error) represent the mean from binned data from every 10 m from oyster reefs.

Regression Analyses

The occurrence of individual taxa was affected differently depending upon reef site characteristics (See Table 5.4 for all test statistics). The occurrence of bivalves and gastropods increased with distance from oyster reefs and lower elevations, while large crustaceans decreased with distance and lower elevations (Table 5.4, Figure 5.7). Occurrence of small crustaceans was the only response variable that was not affected by site variables (Figure 5.7B). Predicted values suggest that bivalves and gastropods were 2.5 times more likely to occur at distances 40 m and 30 m from reefs, respectively, while occurrence of large crustaceans decreased by 2.5 times 40 m away from oyster reefs (Figure 5.7A and 5.7C). Small crustacean occurrence varied little over the spatial extent examined, with a less than 25 % change in occurrence over a distance greater

Table 5.4. Results (estimated coefficients (β), standard errors (SE), z-values, and p-values) of the regression analyses predicting the presence of taxa and richness using distance and elevation. Number of observations = 108.

Taxa (P/A)	Distance				Elevation			
	β	SE	z-value	P-value	β	SE	z-value	P-value
Bivalves	0.04	0.01	2.74	0.01	-5.88	2.37	-2.48	0.01
Gastropods	0.04	0.014	3.07	0.002	-5.55	2.73	-2.04	0.04
Sm Crustaceans	0.01	0.01	0.98	0.33	-1.79	-1.83	-0.98	0.33
L Crustaceans	-0.03	0.01	-2.17	0.03	3.38	1.70	1.98	0.047
Richness	0.003	0.002	1.09	0.27	-0.16	0.38	-0.43	0.67

than 90 m (Figure 5.7B). The richness (number of broad taxa represented) was not affected by distance (p = 0.27) or elevation (p = 0.67).

Additionally, sediment grain size, was unaffected by distance (p = 0.13), elevation (p = 0.21), or WRT (p = 0.26).

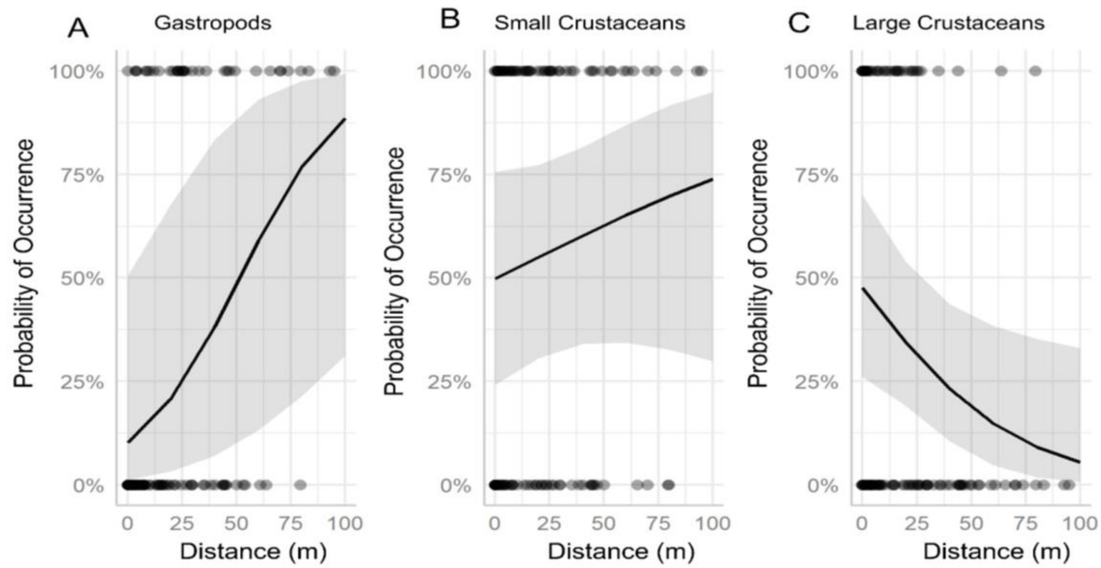

Figure 5.7. Distance effects plots for A) gastropods, B) small crustaceans, and C) large crustaceans. The plots indicate that the probabilities of observing gastropods and large crustaceans are strongly affected by distance from reefs, though in opposite directions, where likelihood of observing gastropods increases further from reefs but decreases for crustaceans. Distance does not strongly affect the likelihood of observing small crustaceans. The shaded area shows the 95% confidence intervals using the "ggeffects" package (Lüdecke 2018) and raw data are represented as filled circles.

DISCUSSION

Infauna and Sediment Distributions

The interpolated surfaces generated in this study show that patterns for infauna and sediment distributions relative to distance to reefs can vary between sites. For sediment, we organic matter was higher closer to oyster reefs (Figure 5.3). However, while spatial patterns were evident for sediment with respect to distance from the reef, the range of grain size and organic matter for many sites is very narrow, evidence that sediment distributions vary locally and are likely influenced by more than just distance from oysters. Grain size for all samples across the 8 sites ranged from 39.8 μm to 127.2 μm, while at the individual site level the range was typically much smaller, where for example grain size ranged from 40.0 μm to 61.3 μm at site 4. Total abundance also varies with distance to reefs and is often species dependent. This agrees with previous findings (Ambrose & Anderson 1990, Fabi et al. 2002, Langlois et al. 2006) and highlights the importance of examining individual taxa in correlation and regression analyses.

An interesting, yet somewhat expected finding from the interpolated surfaces is that gradients in infauna and sediment distributions are less distinct when oysters are patchy throughout the region, compared to regions composed of one single or a few large intact oyster reefs (Figure 5.2). This result provides evidence that distance can indeed alter the distributions of sediment and infauna because patchier regions can increase effects of both biological and physical interactions with multiple patch reefs. This adds to previous findings within the VCR that found strong relationships between water residence time and sediment characteristics (Wiberg et al. 2015). Taken together, the results indicate that infauna and sediment characteristics are influenced by numerous environmental variables including variability in elevation and wave environments, in addition to distance from reefs.

Sediment Analyses

While previous studies found that oyster reefs can trap fine sediment (Colden et al. 2016) and promote increased sediment organic matter (Southwell et al. 2017), other environmental factors such as wave and/or tidally-driven current velocities may be the dominant drivers of sediment distribution (Wiberg et al. 2015), especially in high energy environments (Reidenbach et al. 2013, Byers & Grabowski 2014). Sediment organic matter was correlated with distance, but also with water residence time and elevation, indicating a combination of variables is responsible for affecting sediment organic matter. Additionally, while the regression analyses found none of the site variables explained grain size distribution, there were correlations found with water residence time and organic matter, emphasizing the importance of the local flow in altering sediment characteristics and agrees with studies that indicate finer sediments hold more nutrients (Nedwell 1999).

Infauna Analyses

For infauna data, we used correlation analyses to examine if distance and site variables were related to taxa densities and regression analyses to explain presence/absence of taxa because some taxa were less populous. Significant site variables were similar in both analyses. Correlation analyses show that distance, elevation, and water residence time were related to the majority of taxa, where each was correlated with a similar number of infauna variables. In the regression analyses, all individual taxa were explained by distance and elevation, with the exception of small crustaceans.

Bivalves and gastropods were more likely to be present further from reefs, agreeing with previous literature that 'halos' exist around oysters (Posey & Ambrose 1994, Reeds et al. 2018) and that distributions of infauna differ depending on species and size (Davis et al. 1982, Ambrose & Anderson 1990, Fabi et al. 2002, Langlois et al. 2006). A study by Reeds et al. (2018), found an abundance 'halo' of 30m around artificial reef. Because this study investigated one reef, with radial sampling, they were able to estimate an area of influence 15x that of the reef area. Our sites consisted of mudflats with patchy reefs of different sizes and were unable to estimate an accurate footprint. However, our results found that bivalves and gastropods were 2.5 times more likely to occur at distances 40 m and 30 m from reefs, respectively, while large crustaceans decreased by 2.5 times 40 m away from oyster reefs (Figure 5.7A and 5.7C). These changes in taxa presence within a similar distance found by Reeds et al. (2018) could suggest the area of influence (15x reef area) is similar for oyster reefs in our study.

Previous studies on predator-prey interactions have found that not only crabs, but also birds and fish, utilize bivalve reefs for habitat and to feed upon infauna (Lenihan et al. 2001, Kulp et al. 2011, Van der Zee et al. 2012). These interactions help explain why large crustacean density and likelihood of observation increased closer to reefs and at higher elevations, while all other individual taxa and richness showed opposite trends. Due to the nature of predating crabs and other transient predators such as fish or birds (Van der zee et al. 2012, Reeds et al. 2018), other taxa may seek refuge in sediment more distant from reefs. Therefore, the observed trends of higher relative densities of other taxa away from reefs may also be due to predation, rather than a behavioral response. Reefs are generally higher in elevation compared to their surrounding sediment (Hogan & Reidenbach 2019), and if infauna predators are more likely found on reefs, they will also be found at higher elevations. Large crustaceans were also the only taxon where WRT data were not correlated to its density. This could be because crabs are more transient and mobile, spending less time in and dependent upon sediment and more resilient to environmental conditions, compared to other taxa such as polychaetes or bivalves (Davis et al. 1982, Langlois et al. 2006).

We were unable to find a variable to explain small crustacean presence through the regression analysis, and density was only correlated with WRT. These organisms may be more susceptible to predation, drift, or ecological variables (behavioral and trophic) not investigated in this study. Although it was not used in the regression analyses, flow and tidal current can cause patchy distributions in small crustaceans, limiting densities (Grant 1980). Local hydrodynamics can also create microtopographic features (such as sediment ripples) affecting distributions of infauna (Barros et al. 2004).

Higher flow rates, having low water residence times, can indirectly affect infauna abundance by increasing predation and disturbance by increasing transport (Palmer 1988) and dictating the success of passive and choice settlement (Butman et al. 1988, Snelgrove et al. 1998). All infauna correlation coefficients with WRT were negative, indicating slower flows increased infauna abundances, richness, and biomass, evidence that water residence time represents an important variable in species distributions.

Conclusions

Future efforts to understand how infauna and sediment are affected by oyster reefs would benefit from repeated measures at these mudflats to see if the spatial distributions we found are representative, and possibly identify year-to-year variations. In addition, sampling to address seasonality could be informative. While each of the sampling events in 2016 and 2019 were completed during the summer months, there could be variation within and between seasons (Zajac & Whitlatch 1982, Harwell et al. 2011). The 10 to 15 cm depth to which cores were sampled may affect taxa presence, abundance, and biomass in samples, although macrofauna become less abundant below 15 cm (Hines & Comtois 1985), resulting in the recommended depth range of 10 - 15 cm (Raz-Guzman & Grizzle 2001). We were also unable to address the size and age of oysters needed to affect communities due to patchy areas with multiple reefs of unknown age in proximity to samples. The nearness of reefs to one another could explain some of the effects we observed, as other studies have found isolation from artificial reefs affects infauna and sediment observations (Zalmon et al. 2014). Knowing how these variables affect infauna and sediment distributions could be informative in designing future oyster restoration projects to maximize biodiversity and overall ecosystem function.

In summary, this study clearly shows that oyster reefs affect their surroundings by significantly altering distributions of infauna and sediment surrounding oyster reefs on intertidal mudflats. Distance to oyster reefs affects infauna distributions, especially when taxa are examined independently. Oyster reefs also likely provide habitat to large crustaceans and increase sediment organic matter and decrease grain size. This study found that oyster reefs impact both sediment and infauna characteristics up to 100 m away from the reefs with changes in occurrence of 2.5x for most taxa within 40 m. The findings also highlight the importance of local variation, how distributions are likely to differ between mudflats, and the role of other physical variables such as site elevation and water residence time in altering infauna and sediment characteristics. As large-scale oyster restoration projects continue to address a wider range of ecosystem services consideration should be made to the spatial extent of reef effects on infauna and sediment. The management of intertidal mudflat communities will become increasingly challenging with sea-level rise and damaging storms under climate change, and benthic communities will be directly challenged with changing tide levels, temperature, salinity limiting suitable habitat and altering community structures (Fujii 2012). Therefore, understanding how systems are connected, such as oysters, infauna and sediment, can help create management strategies in a changing world.

ACKNOWLEDGEMENTS

We would like to the thank the staff at the Anheuser-Busch Coastal Research Center for assistance in field campaigns in 2016 and 2019. This research was funded by the National Science Foundation grant 1832221 to the Virginia Coast Reserve Long Term Ecological

Research project. EAK Murphy was funded by the National Science Foundation Graduate Research Fellowships Program. M Reidenbach was supported by the National Science Foundation grant OCE-1151314.

LITERATURE CITED

Aller RC (1994) Bioturbation and remineralization of sedimentary organic matter: effects of redox oscillation. Chem Geol 114:331-45

Ambrose RF, Anderson TW (1990) Influence of an artificial reef on the surrounding infaunal community. Mar Biol 107: 41-52

Angelini C, Altieri AH, Silliman BR, Bertness MD (2011) Interactions among foundation species and their consequences for community organization, biodiversity, and conservation. BioScience 61:782-789

Austen MC, Lambshead PJD, Hutchings PA, Boucher G, Snelgrove PVR, Heip C, King G, Koike I, Smith C (2002) Biodiversity links above and below the marine sediment-water interface that may influence community stability. Biodiv Conserv 11:113-136

Barros F, Underwood AJ, Lindegarth M (2001) The influence of rocky reefs on structure of benthic macrofauna in nearby soft-sediments. Estuar Coast Shelf Sci 52: 191-199.

Barros, F, Underwood, AJ, Archambault P (2004) The influence of troughs and crests of ripple marks on the structure of subtidal benthic assemblages around rocky reefs. Estuar Coast Shelf Sci 60:781-790

Bartholomew A (2001) Polychaete Key for Chesapeake Bay and Coastal Virginia. https://www.vims.edu/research/units/legacy/benthic_ecology/_docs/polychaete_key.pdf

Bates D, Machler M, Bolker B, Walker S (2015) Fitting linear mixed-effects models using lme4. Journal of Statistical Software. 67: 1-48. doi: 10.18637/jss.v067.i01

Butman CA, Grassle JP, and Webb CM (1988) Substrate choices made by marine larvae settling in still water and in a flume flow. Nature 333: 771-773

Byers JE, Cuddington K, Jones CG, Talley TS, Hastings A, Lambrinos JG, Crooks JA, and Wilson WG (2006) Using ecosystem engineers to restore ecological systems. Trends Ecol Evol 21: 493-500

Byers JE, Grabowski JH (2014) Soft-sediment communities. In: Bertness MD, Bruno JF, Silliman BR, Stachowicz JJ (eds) Marine Community Ecology and Conservation. Sinauer Associates, Sunderland, CA, 227 - 249

Colden AM, Fall KA, Cartwright GM, and Friedrichs CT. (2016) Sediment suspension and deposition across restored oyster reefs of varying orientation to flow: implications for restoration. Estuar Coast 39: 1435 – 1448

Covich AP, Austen MC, Barlocher F, Chauvet E, Cardinale BJ, Biles CL, Inchausti P, Dangles O, Solan M, Gessner MO, Statzner B, Moss B (2004) The role of biodiversity in the functioning of freshwater and marine benthic ecosystems. Bioscience 54: 767-775

Currin CA, Chappel WS, Deaton A (2010) Developing alternative shoreline armoring strategies: The living shoreline approach in North Carolina, in Shipman, H, MN Gelfenbaum, KL Fresh, and RS Dinicola, eds., Puget Sound Shorelines and the Impacts of Armoring-Proceedings of a State of the Science Workshop, May 2009: *U.S*. Geologic Survey Scientific Investigations Report 2010, 5254: 91-102

Dahlgren CP, Posey MH, Hulbert AW (1999) The effects of bioturbation on the infaunal community adjacent to an offshore hardbottom reef. Bull Mar Sci.64: 21-34

Dashtgard, SE, Gingas MK, Pemberton SG. (2008) Grain-size controls on the occurrence of bioturbation. Palaeogeogr Palaeoclimatol Palaeoecol 257: 224-243

Dauvin JC, Lucas S, Navon M, Lesourd S, Mear Y, Poizot E, Alizier S (2017) Does the hydrodynamic, morphometric and sedimentary environment explain the structure of soft-bottom benthic assemblages in the Eastern Bay of Siene (English Channel)? Estuar Coast Shelf Sci 189: 156-172

Davis N, VanBlaricom GR, Dayton PK (1982) Man-made structures on marine sediments: effects on adjacent benthic communities. Mar Biol 70: 295-304

Davis JLD, Takacs RL, Schnabel R (2006) Evaluating ecological impacts of living shorelines and shoreline habitat elements: an example from the upper western Chesapeake Bay. Management, policy, science, and engineering of nonstructural control in the Chesapeake Bay, 55

Dewberry (2016) Eastern shore Virginia QL2 LiDAR BAA. USGS task order G15PD00284

Dorgan KM, D'Amelio CD, Lindsay SM (2016) Strategies of burrowing in soft muddy sediments by diverse polychaetes. Invertebr Biol 135: 287-301

ESRI (2016) "What is Empirical Bayesian kriging?" Kriging in Geostatistical Analyst. https://desktop.arcgis.com/en/arcmap/10.3/guide-books/extensions/geostatistical-analyst/what-is-empirical-bayesian-kriging-.htm (accessed Jan 2020)

Fabi G, Luccarini F, Panfili M, Solusstri C, Spagnolo A (2002) Effects of an artificial reef on the surrounding soft-bottom community (central Adriatic Sea). ICES J Mar Sci 59: S343-S349

Fujii T (2012) Climate change, sea-level rise and implications for coastal and estuarine shoreline management with particular reference to the ecology of intertidal benthic macrofauna in NW Europe. Biology 1:597-616

Grabowski JH, Hughes AR, Kimbro DL, Dolan MA (2005) How habitat setting influences restored oyster reef communities. Ecology 86:1926-1935

Gunarathna MHJP, Kumari MKN, Nirmanee KGS (2016) Evaluation of interpolation methods for mapping pH of groundwater. International Journal of Latest Technology in Engineering, Management & Applied Science 3: 1-15

Gupta A, Kamble T, Machiwal D (2017) Comparison of ordinary and Bayesian kriging techniques in depicting rainfall variability in arid and semi-arid regions of north-west India. Environ Earth Sci 76: 512

Hansen, J.C., and M.A. Reidenbach. 2013. Seasonal growth and senescence of a Zostera marina seagrass meadow alters wave-dominated flow and sediment suspension within a coastal bay. Estuar Coast 36:1099-1114

Harrell Jr FE (2021) Hmisc: Harrell miscellaneous. R package version 4.5-0. https://CRAN.R-project.org/package=Hmisc

Hastings A, Byers JE, Crooks JA, Jones CG, Lambrinos JG, Talley TS, Wilson WG. (2007) Ecosystem engineering in space and time. Ecol Lett 10: 153 – 164. doi: 10.1111/j.1461-0248.2006.00997.x

Hartig F (2020). DHARMa: Residual diagnostics for hierarchical (Multi-Level/Mixed) regression models. R package version 0.3.3.0 https://CRAN.R-project.org/package=DHARMa

Harwell HD, Posey MH, Alphic TD. (2011) Landscape aspects of oyster reefs: effects of fragmentation on habitat utilization. J Exp Mar Biol Ecol 409: 30 -41

Hauke J, Kossowaski T (2011) Comparison of values of Pearson’s and Spearman’s correlation coefficients on the same sets of data. Quaestiones Geographicae 30: 87 -93

Hines AH, Comtois KL (1985) Vertical distribution of infauna in sediments of a subestuary of Central Chesapeake Bay. Estuaries 8(3): 296-304

Hogan S, Reidenbach MA (2019) Quantifying and mapping intertidal oyster reefs utilizing LiDAR-based remote sensing. Mar Ecol Prog Ser 630: 83-99

Hogan S, Reidenbach MA (2020) Oyster patches within 16 different 0.25 km2 regions throughout the Virginia Coast Reserve, 2015 ver 1. Environmental Data Initiative. https://doi.org/10.6073/pasta/fd4e88047d5a7e19838d1c20ae7be38a

Ieno EN, Solan M, Batty P, Pierce GJ (2006) How biodiversity affects ecosystem functioning roles of infaunal species richness, identity and density in the marine benthos. Mar Eco Prog Ser 311: 263-271

Janssen F, Huettel M, Witte U (2005) Pore-water advection and solute fluxes in permeable marine sediments (II): benthic respiration at three sandy sites with different permeabilities (German Bright, North Sea). Limnol Oceanogr 50: 779-792

Jones CG, Lawton JH, Shachak M (1994) Organisms as ecosystem engineers. In: Ecosystem Management. Springer, New York, NY. https://doi.org/10.1007/978-1-4612-4018-1_14

Jones CG, Lawton JH, Shachak M (1997) Positive and negative effects of organisms as physical ecosystem engineers. Ecology 78: 1946 -1957

Kennedy VS, Breitburg DL, Christman MC, Luckenbach MW, Paynter K, Kramer J, Sellner KG, Dew-Baxter J, Keller C, Mann R (2011) Lessons learned from efforts to restore oyster populations in Maryland and Virginia 1990 – 2007. J Shellfish Res 30: 719-731

Kellogg ML, Cornwell JC, Owens MS, Kennedy PT (2013) Denitrification and nutrient assimilation on a restored oyster reef. Mar Eco Prog Ser 480:1-19

Krivoruchko, K (2012) Empirical Bayesian Kriging implemented in ArcGIS Geostatistical Analyst. ESRI, Redlands, CA, USA <http://www.esri.com/news/arcuser/1012/empirical-byesian-kriging.html> (accessed Jan 2020)

Kulp RE, Politano V, Lane HA, Lombardi SA, Paynter KT (2011) Predation of juvenile *Crassostrea virginica* by two species of mud crabs found in the Chesapeake Bay. J Shellfish Res 30: 261-266

Langlois, TJ, Anderson AJ, Babcock RC (2005) Reef associated predators influence adjacent soft-sediment communities Ecology 89: 1508-1519

Langlois TJ, Anderson MJ, Babcock RC (2006) Inconsistent effects of reefs on different size classes of macrofauna in adjacent sand habitats. J Exp Mar Biol 334(2): 269-282

Lenihan HS (1999) Physical-biological coupling on oyster reefs: how habitat structure influences individual performance. Ecol Monogr 69:251-275

Lenihan HS, Peterson CH, Byers JE, Grabowshil GW, Colby DR (2001) Cascading of habitat degradation: oyster reefs invaded by refugee fishes escaping stress. Ecol Appl 11: 764-782

Luckenbach MW, Coen LD, Ross PG, Stephen JA (2005) Oyster reef habitat restoration: relationships between oyster abundance and community development based on two studies in Virginia and South Carolina. J Coast Res SI 40: 64-78

Lüdecke D (2018) ggeffects: Tidy Data Frames of marginal effects from regression models. Journal of Open Source Software 3:72. doi:10.21105/joss.00772

Meysman FJ, Middelburg JJ, Heip CH (2006) Bioturbation: a fresh look at Darwin's last idea. Trends Ecol Evol 21:688-95

Murphy EA, and Reidenbach MA (2016) Oxygen transport in periodically ventilated polychaete burrows. Mar Biol 163, 208 doi:10.1007/s00227-016-2983-y

Nedwell DB, Jickells TD, Trimmer M, Sanders R (1999) Nutrients in estuaries. Adv Ecol Res 29:43-92

Newell RIE, Cornwell JC, Owens MS (2002) Influence of simulated bivalve biodeposition and microphytobenthos on sediment nitrogen dynamics: A laboratory study. Limnol Oceanogr 47: https://doi.org/10.4319/lo.2002.47.5.1367

Nybakken JW, Bertness MD (2005) Marine Biology an Ecological Approach. Pearson Education Inc. as Benjamin Cummings, San Francisco, CA

Palmer MA (1988) Epibenthic and marine meiofauna: separating predation, disturbance, and hydrodynamic effects. Ecology 69: 1251-1259

Paterson DM, Aspden RJ, Black KS (2009) Intertidal flats: ecosystem functioning of soft sediment system. In: Perillo GME, Wolanski E, Cahoon DR, Brinson MM (eds) Coastal Wetlands an Integrated Ecosystem Approach. Oxford, UK, 317 – 373

Piazza BP, Banks PD, La Peyre MK (2005) The potential for created oyster shell reefs as a sustainable shoreline protection strategy in Louisiana. Restor Ecol 13(3): 499–506

Posey MH, Ambrose WG (1994) Effects of proximity to an offshore hard-bottom reef on infaunal abundances. Mar Biol 118:745-753

Posey MH, Alphin TD, Powell CM (1999) Use of oyster reefs as habitat for epibenthic fish decapods. In: Luckenbach MW, Mann R, Wesson JA (1999) Oyster reef habitat restoration: a synopsis and synthesis of approaches; proceedings from the symposium, Williamsburg, Virginia, April 1995. Virginia Institute of Marine Science, College of William and Mary. http://doi.org/10.21220/V5NK51 pp 229-237

Raz-Guzman A, and Grizzle RE (2001) Techniques for quantitative sampling of infauna and small epifauna in seagrass. In Short FT, Coles RG (eds) Global Seagrass Research Methods. Amsterdam: Elsevier Science 237–253. doi: 10.1016/B978-044450891-1/50013-X

Reeds KA, Smith JA, Suthers IM, Johnston EL (2018) An ecological halo surrounding a large offshore artificial reef: Sediments, infauna, and fish foraging. Mar Environ Res 141:30-38

Reidenbach MA, Berg P, Hume A, Hansen JCR, Whitman ER (2013) Hydrodynamics of intertidal oyster reefs: the influence of boundary layer flow processes on sediment and oxygen exchange. Limnol Oceanogr Fluids Environ 3: 225-239

Richardson D, Porter J, Oertel G, Zimmerman R, Carlson C, Overman K, Carlson C (2018) Integrated topography and bathymetry for the Eastern Shore of Virginia ver 10. Environmental Data Initiative. https://doi.org/10.6073/pasta/63a22558d6650fae8232b6a8814a90d5 (Accessed 2021-07-15).

Safak I, Wiberg PL, Kurum MO, Richardson DL (2015) Controls on residence time and exchange in a system of shallow coastal bays. Cont Shelf Res 97: 7-20

Snelgrove PVR, Grassle JP, Butman CA (1998) Sediment choice by settling larvae of the bivalve, *Spinsula solidissima* (Dillwyn), in flow and still water. J Exp Mar Biol Ecol 231(2): 171 – 190

Solan M, Cardinale BJ, Downing AL, Engelhardt KAM, Ruesink JL, Srivastava DS (2004) Extinction and ecosystem function in the marine benthos. Science 306: 1177-1180

Southwell MW, Veenstra JJ, Adams CD, Scarlett EV, Payne KB (2017) Changes in sediment characteristics upon oyster reef restoration, NE Florida, USA. Journal of Coastal Zone Management. 20(1) DOI: 10.4172/2473-3350.1000442

Thomsen MS, McGlathery K (2006) Effects of accumulations of sediments and drift algae on recruitment of sessile organisms associated with oyster reefs. J Exp Mar Biol Ecol 328:22-34

Van der Zee EM, van der Heide T, Donadi S, Eklof JS, Eriksson BK, Olff H, van der Veer HW, Piersma T (2012) Spatially extended habitat modification by intertidal reef-building bivalves has implications for consumer-resource interactions. Ecosystems 15: 664-673

Van der Zee EM, Tielens E, Holthuijsen S, Donadi S, Eriksson BK, Van der Veer HW, Piersma T, Olff H, van der Heide T (2015) Habitat modification drives benthic trophic diversity in an intertidal soft-bottom ecosystem. J Exp Mar Biol and Ecol 465:41-48

Veiga WR, Sousa-Pinto, I, Rubal M (2017) Relationship between structure of microbenthic assemblages and environmental variables in shallow sublittoral soft bottoms. Marine Environmental Research 129: 396 – 407

Volaric MP, Berg P, Reidenbach MA (2018) Oxygen metabolism of intertidal oyster reefs measured by aquatic eddy covariance. Mar Ecol Prog Ser 599:75-91

Whitman ER, Reidenbach MA (2012) Benthic flow environments affect recruitment of *Crassostrea virginica* larvae to an intertidal oyster reef. Mar Ecol Prog Ser 463:177-191

Wiberg PL, Carr JA, Safak I, Anutaliya A (2015) Quantifying the distribution and influence of non-uniform bed properties in shallow coastal bays. Limnol Oceanogr Methods 13:746 – 762

Wiberg PL, Taube SR, Ferguson AE, Kremer MR, Reidenbach MA (2019) Wave attenuation by oyster reefs in shallow coastal bays. Estuar Coast 42:331-347 https://doi.org/10.1007/s12237-018-0463-y

Widdicombe S, Dashfield SL, McNeill CL, Needham HR, Beesley A, McEvoy A, Oxnevad S, Clarke KR, Berge JA (2009) Effects of CO2 induced seawater acidification on infaunal diversity and sediment nutrient fluxes. Mar Ecol Prog Ser 379: 59 -75

Wilson WH (1990) Competition and predation in marine soft-sediment communities. Ann Rev Ecol S 21: 221-241

Wright JP, Jones CG (2002) An ecosystem engineer, the beaver, increases species richness at the landscape scale. Oecologia 132: 96 – 101

Wright JP, Jones CG (2004) Predicting effects of ecosystem engineers on patch-scale species richness from primary productivity. Ecology 85(8): 2071 – 2081

Zajac R, Whitlatch R (1982) Responses of estuarine infauna to disturbance. I. Spatial and temporal variation of initial recolonization. Mar Ecol Prog Ser 10:1-14

Zalmon IR, Saleme de Sa F, Neto EJD, de Rezende CE, Mota PM, de Almeida TCM (2014) Impacts of artificial reef spatial configuration on infaunal community structure – Southeastern Brazil. J Exp Mar Biol Ecol 454: 9-17

Zar JH (2014) Biostatistical Analysis. Fifth edition. Pearson India Education Services Pvt. Ltd.

APPENDICES

Table 5.A1. Modified from Langlois et al. (2006) with sediment analysis and additional sources added. Summary of part studies on the effects of infauna and sediment with distance to hard structured reefs. Arrows indicate the magnitude of change for the variables listed

Study	Location	Sampling zone	Scale	Distance & small infauna	Distance & large infauna	Distance & grain size	Correlation: Infauna & GS	Correlation: Infauna & OM
Langlois et al. 2006	NE, New Zealand	Shallow ~10m, open coast	2m – 30 m	No	NA	No	Weak	NA
Langlois et al. 2005	NE, New Zealand	Shallow ~10m, open coast	2m – 30 m	NA	Yes Crabs ↑ distance↓ Urchin, bivalve ↓, distance ↑	No	Abundance↑, GS ↓	NA
Davis et al. 1982	SW, USA	Shallow ~ 13 m, open coast	Transects 4 – 100 m	No	Yes Polychaetes ↑, distance↓ Sea pen ↓, distance ↓	Yes GS ↑, distance↓	Yes	No
Ambrose & Anderson 1990	SW, USA	Shallow ~ 13 m, open coast	Transects 10s m	Yes, Differed per species	NA	Yes GS ↑, distance↓	Yes	
Barros et al. 2004	SE, Australia	Rocky subtidal	Close vs far 4 m vs 15 m	0.5 mm sieve Taxa ↑, distance ↓ Polychaetes ↑, distance ↓	NA	GS ↑, distance ↓	Yes	NA
Barros et al. 2001	SE, Australia	Shallow rocky reefs	1, 5, 10 m		NA	GS ↑, distance ↓	Weak	NA
Dahlgren et al. 1999	NC, USA	50 km offshore	10 – 75 m transects	NA	1.5 cm 1 species ↓, distance	NA	NA	NA
Posey & Ambrose 1994	NC, USA	~ 32 m, deep offshore	10s m Up to 75m transects	0.5 mm sieve Total infauna, polychaete, bivalve, isopod, amphipod, abundance ↑ with distance ↑	NA	NA	Yes	NA
Van der Zee et al. 2012	Netherlands, Wadden Sea	Intertidal	100 m grids	Species abundance ↑ distance ↓	NA	Yes	Yes	Yes
Zalmon et al. 2014	Brazil	9 m deep	0-15 m	0.5 mm sieve Different functional groups respond differently with distance	NA	GS ↓, distance ↑ not significant	Yes	NA
Fabi et al. 2002	Adriatic Coast	1.2 NM offshore, 11 m deep	10s of m, up to 50 m	0.5 mm sieve Densities in/out of reef similar Diversity ↑, distance ↓	N/A	GS ↓, distance ↓	Yes	NA

Table 5.A2. Polychaete families collected during 2016 sampling, total number in each family over 44 cores (25 cm diameter). Polychaete identifications were made using Polychaete Key for Chesapeake Bay and Coastal Virginia (Bartholomew 2001).

Polychaete family	Total from 2016
Lumbrineridae	422
Capitellidae	322
Nereidae	256
Spionidae	164
Glyceridae	128
Maldanidae	111
Oenonidae	63
Eunicidae	54
Hesionidae	42
Cirratulidae	40
Orbiniidae	38
Paraonidae	35
Phyllodocidae	16
Ampharetidae	11
Arabellidae	5
Arenicolidae	2
Pectinariidae	2
Phyllodocidae	2
Terebellidae	2
Nephtyidae	1

CHAPTER 6: Conclusions

The work for this dissertation was guided by the need to understand where and under what physical conditions oysters exist and to quantify the ecosystem services oysters provide. The findings provide valuable data on oyster distributions and validate oysters' use as a nature-based solution. The new methods to quantify oyster distributions and their influence on local and broad scales presented in this work offers recommendations for successful management in the restoration and community enhancement of vulnerable coastal ecosystems.

In Chapter 2, LiDAR elevation was validated as a successful tool to map intertidal oyster populations and data extracted to mapped oyster patches indicate they are found within less a 1 m range of elevation. The data were used to locate potentially suitable habitat for oysters in terms of elevation and wave environments and shows there is ample area within Virginia's coastal bays likely to promote successful oyster growth. While other studies have shown that elevation affects oyster growth and recruitment (Bartol et al. 1999, Lenihan 1999, Schulte et al. 2009), this study provided evidence of a specific elevation range in which oysters exist on a bay-wide scale. The data also show that compared to wave variables, suitable elevation is more limited and critical to defining habitat. In Chapter 3 the utility of LiDAR was further examined in intertidal systems and was successfully used to quantify marsh morphology in terms of slope, after validation with in-situ profiles and morphological descriptions. The data were applied to determine the role of oysters in buffering marsh edges from wave energy by analyzing the morphology and retreat for control and reef-lined marshes. The findings indicate that morphologies of reef-lined marsh edges are more gently sloping, which are more likely to experience slower rates of volumetric erosion and retreat compared to sharply scarped edges (Schwimmer 2001, Francalanci et al. 2013, McLoughin et al. 2015).

The dissertation then turned to in-situ observations of an oyster restoration project to quantify the ecosystem services between constructed reef designs varying in elevation and width. While width had minimal effect on services, the data again emphasize the importance of elevation in oyster restoration. Chapter 4 found that constructed reefs higher in elevation foster greater oyster growth and wave attenuation, providing greater coastal protection. Data before and after restoration show trends of increased infauna diversity and sediment organic matter, agreeing with other bivalve restoration studies (Castel et al. 1989, Van der Zee 2015, Southwell et al. 2017). While Chapter 4 examined changes to infauna and sediment locally, to further understand the spatial extent that oysters can influence their surrounding communities, Chapter 5 examined how infauna and sediment composition changed with distance to oyster reefs using large scale sampling over 8 intertidal mudflats. The work successfully combined visual analysis using geostatistically-interpolated surfaces and statistical modeling, describing distribution patterns visually and statistically. Because previous works have cited variation in patterns with species (Davis et al. 1982, Langlois et al. 2006), infauna were statistically analyzed in classes of broad taxa and findings suggest that distance, examined over the scale of 100 m, explained the density and presence of infauna. For sediment distributions, the wave environment likely plays a more dominate role compared to proximity to reefs.

Overall, this work highlights the importance of physical variables, including elevation and wave environments, in determining the success of oyster restoration and the ecosystems services they provide. The methods and findings can be used to target future restoration sites for greater success in achieving goals specific to oyster growth, coastal protection, and/or biodiversity. The work also emphasizes the importance of long-term data collection to monitor for changes taking place in dynamic estuarine environments. While some ecosystem changes may be made on short timescales (such as oyster growth), other services require long-term monitoring for a full understanding of the processes taking place (La Peyre et al. 2014, Volaric et al. 2020).

This work was also successful in demonstrating the power of combining remotely-sensed and field data to address questions of restoration over different spatial scales and understand the dynamic, complex nature of coastal environments. With continued acquisitions of high-resolution LiDAR data, the techniques presented here can be used to further monitor intertidal habitats and benefit long-term analyses. For example, extending the work from Chapter 3, as has been done in previous studies, to monitor shoreline change (White & Wang 2003, Obu et al. 2017) and repeated mapping of oysters to measure changes in elevation and areal coverage (Chapter 2). As remotely-sensed products make it more manageable to track oyster coverage and marsh edges, lags in datasets can be avoided.

With the health and stability of susceptible coastal systems, facing increasing pressures under climate change, at stake (Lotze et al. 2006, Duarte et al. 2008), this work provides innovative methods and findings to help monitor change and mitigate damaging alterations. The findings provide evidence that oysters are critical to the broader intertidal community, and not only are oyster populations enhanced through restoration, but also the ecosystem services they provide. These studies bolster the support for oyster reefs as a nature-based solution that should be incorporated into coastal management strategies to enhance and protect both the ecological and built communities along coasts.

Literature Cited

Bartol IK, Mann R, Luckenbach M (1999) Growth and mortality of oysters (Crassostrea virginica) on constructed intertidal reefs: effects of tidal height and substrate level. J Exp Mar Biol Ecol 237:157-184

Castel J, Labourg PJ, Escaravage V, Auby I, Garcia ME (1989) Influence of seagrass beds and oyster parks on the abundance and biomass patterns of meio- and macrobenthos in tidal flats. Estuar Coast Shelf Sci 28:71-85

Duarte CM, Dennison WC, Orth RJW, Carruthers TJB (2008) The charisma of coastal ecosystems: addressing the imbalance. Estuar Coast J CERF 31:233-238

Francalanci S, Bendoni M, Rinaldi M, Solari L (2013) Ecomorphodynamic evolution of salt marshes: Experimental observations of bank retreat processes. Geomorphology 195:53-65

La Peyre MK, Humphries AT, Casas SM, La Peyre JF (2014) Temporal variation in development of ecosystem services from oyster reef restoration. Ecol Eng 64:34-44

Langlois TJ, Anderson MJ, Babcock RC (2006) Inconsistent effects of reefs on different size classes of macrofauna in adjacent sand habitats. J Exp Mar Biol Ecol 334:269-282

Lenihan HS (1999) Physical-biological coupling on oyster reefs: how habitat structure influences individual performance. Ecol Monogr 69:251-275

Lotze HK, Lenihan HS, Bourque BJ, Bradbury RH, Cooke RG, Kay MC, Kidwell SM, Kirby MX, Peterson CH, and Jackson JB (2006) Depletion, degradation, and recovery potential of estuaries and coastal seas. Science 312:1806-1809

McLoughlin SM, Wiberg PL, Safak I, McGLathery KJ (2015) Rates and forcing of marsh edge erosion in a shallow coastal bay. Estuar and Coast 38:620-638

Obu J, Lantuit H, Grosse G, Gunther F, Sachs T, Helm V, Fritz M (2017) Coastal erosion and mass wasting along the Canadian Beaufort Sea based on annual airborne LiDAR elevation data. Geomorphology DOI:10.1016/j.geomorph.2016.02.014

Schulte DM, Burke RP, Lipcius RN (2009) Unprecedented restoration of a native oyster metapopulation. Science 325:1124-1128

Schwimmer, RA (2001) Rates and processes of marsh shoreline erosion in Rehoboth Bay, Delaware, USA. J Coast Res 17:672 -683

Southwell MW, Veenstra JJ, Adams CD, Scarlett EV, Payne KB (2017) Changes in sediment characteristics upon oyster reef restoration, NE Florida, USA. J Coast Zone Manag 20 DOI: 10.4172/2473-3350.1000442

Van der Zee EM, Tielens E, Holthuijsen S, Donadi S, Eriksson BK, Van der Veer HW, Piersma T, Olff H, Van der Heide T (2015) Habitat modification drives benthic trophic diversity in an intertidal soft-bottom ecosystem. J Exp Mar Biol Ecol 465:41-48

Volaric MP, Berg P, Reidenbach MA (2020) Drivers of oyster reef ecosystem metabolism measured across multiple timescales. Estuar Coast 43:2034-2045

White SA, Wang Y (2003) Utilizing DEMs derived from LIDAR data to analyze morphologic change in the North Carolina coastline. Remote Sens Environ 85:39- 47

Zalmon IR, Saleme de Sa F, Neto EJD, de Rezende CE, Mota PM, de Almeida TCM (2014) Impacts of artificial reef spatial configuration on infaunal community structure – Southeastern Brazil. J Exp Mar Biol Ecol 454:9-17